STRUCTURAL PERFORMANCE OF HYBRID TIMBER CONNECTIONS WITH VARYING BOLT PATTERNS AT AMBIENT AND ELEVATED TEMPERATURES

By

Aba A. Owusu

A thesis submitted to
The Faculty of Graduate and Postdoctoral Affairs
In partial fulfillment of the requirements for the degree of

Master of Applied Science

In

Civil Engineering

Department of Civil and Environmental Engineering
Carleton University

Ottawa, Ontario

Abstract

The research project presented in this study aimed to study the effect of bolt numbers and patterns on protected and unprotected concealed steel-glulam hybrid connections. Fifteen full-scale concealed (wood-steel-wood) connections were experimentally examined: five ambient and ten fire resistance experiments. Four and six steel bolts in two different patterns were arranged to form four different connection configurations that were experimentally examined. Also, each connection configuration was tested with and without fire protection of the steel components using wood plugs. Ambient specimens were tested under gradually increased monotonic loads until failure; whereas the other specimens were subjected to elevated temperatures that followed CAN/ULC-S101 standard fire, while being loaded to 100% of the ultimate design load capacity of the weakest connection configuration.

The experimental results revealed that, although the protected connection configuration had slightly less moment-resisting capacity than that of the unprotected configuration at ambient temperature, it had an increased failure time of about 20 minutes at elevated temperatures. Also, increasing the bolt number from four to six, improved the connection' moment capacity by about 66%. However, increasing the number of bolts from four to six bolt in the connections tested at elevated temperature mainly affected the connection's failure mode. Furthermore, raising the bottom row of bolts to the mid-height of the beam section increased the maximum moment capacity of the connection by about 90% compared to that of the similar connection but with the bottom row close to the bottom side of the beam section. Similar to the bolt number, the bolt pattern mainly affected the failure mode of the connections subjected to fire.

Acknowledgements

I am grateful to Jehovah God for granting me the wisdom that has helped me through this Masters' program.

I want to extend my gratitude to my supervisor, Prof. George Hadjisophocleous, for this great opportunity and for his motivation, support and guidance throughout my program in Fire Safety Engineering. My gratitude also goes to my co-supervisor, Dr. Sam Salem for always pushing me to do better and for welcoming me at Lakehead University Fire Testing and Research Laboratory (LUFTRL).

I am also very thankful to Cory Hubbard and Oluwamuyiwa Okunrounmu for their support in helping set up all the tests we ran for this research.

To my family in Ghana, I say thank you for the support and encouragements throughout this stage of my life. My appreciation also goes to Prof. Abass Braimah, Hannah Keelson, Oluwadamilola Okunrounmu and King Ankobea-Ansah, for their contributions toward the successful completion of this program.

Table of Contents

List of Tables

List of Figures

1 INTRODUCTION

1.1 Background

The use of wood in building construction around the world has considerably increased in the last few years due to its renewability and sustainability. There are mainly two types of construction associated with wood: light frame construction and heavy timber construction. In Canada, timber construction is considered heavy when the dimensions of beams and columns exceed 150 mm and 50 mm for decks, whereas light frame construction involves beams and columns and decks with a dimension less than 150 mm and 50 mm, respectively. Light frame construction is highly used in residential buildings of one to four storeys. Due to the smaller size, this type of construction is usually protected with gypsum board to improve their fire resistance [1]. The type of wood usually used in heavy timber construction is Glued-laminated timber (glulam). Glulam is an engineered-wood product that is composed of pieces of dimensioned timber end jointed by being placed in horizontal layers and held together by an adhesive agent to form a final product with a greater length and cross-sectional dimensions, and with better mechanical properties than the individual lamina.

In heavy timber construction, structural members are joined together using connections some of which use steel plates and bolts that can be configured in different forms such as exposed, concealed and seated. Unlike light wood frame constructions, the bulky sizes of heavy timber structures make them more resistive to fire thereby making their charring rate relatively slower. The resulting char formed on the surface prevents heat from reaching the unburnt wood beneath the surface.

Design requirements for fire safety in Canada are enshrined in Division B, Part 3 of the Fire Protection, Occupant Safety and Accessibility of the National Building Code of Canada (NBCC) [2]. Provisions included in the code are mainly based on extensive fire testing, engineering calculations and practical experiences acquired over decades, but recent times have seen a rise in

the use of performance-based design approach where systems are designed with fire safety engineering principles and validated with known acceptance criteria in the code. The code prescribes a 45 min or 1-hour fire resistance rating for combustible construction up to certain height. [2]

The province of Ontario restricted the height of wood frame buildings to four storeys, but recently a height of six storeys is allowed in the current version of the OBC. This depicts the increasing trust for wood in constructing mid-rise buildings in Canada to meet the needs of the growing population and to facilitate the use of environmentally friendly construction materials.

A study conducted by Ali and Hadjisophocleous shows that steel bolts play a major role in the charring rate and the fire resistance time of timber connections [3]. In their study, glulam connections were modelled using finite element software, and the model predictions were compared against full-scale tests' results. It was observed from both, the experimental and numerical outcomes that the rate of degradation of the connection's strength was determined by the relative exposure of the steel components, e.g., bolts and plates, to fire. The cross-sectional dimensions reduction due to wood charring initiated brittle failure, such as wood splitting, which eventually led to failure of the assembly. In another study, conducted by Petrycki and Salem [4], the fire performance of concealed wood-steel-wood glulam connections using two and three rows of bolts, each of two bolts, was experimentally investigated. In addition to the number of bolt rows, the effect of bolt's end distance on the fire resistance of the connections was investigated. Experimental results revealed that, increasing the number of bolt rows, from two to three rows, increased the fire resistance time of the glulam beam-to-column connection by a greater increment than that observed by increasing the bolt's end distance from four- to five-times the bolt diameter.

Many researchers put emphasis on axially loaded connections [5] under either compressive or tensile loading parallel to wood grain [6], or perpendicular to wood grain [7]. However, in framed timber structures, beam-to-column connections may exert certain degree of moment resistance, mainly due to the large cross-sectional dimensions of timber elements as well as the existence of several steel connecting components, such as steel plates, bolts, etc. Research on the mechanical behavior of dowelled steel-to-timber moment-resisting connections was conducted by Xu, Bouchaïr and Racher. In their study, a model was also proposed for simulating the behavior of timber joints, such as the bending moment-carrying capacity, the global moment-rotation response and the failure modes [8]. In another study, an analytical model to study the forces acting on the different components of timber-steel hybrid connections along with the prediction of the connection's moment-resisting capacity and its failure modes was developed. From this research, numerical models to determine the bending moment capacity and failure mode of timber-steel hybrid moment-resisting connections was developed. [9]

1.2 Problem Statement

Recent research on the fire performance of concealed (wood-steel-wood), hybrid timber connections has shown that these connections do not perform as well as exposed (steel-wood-steel) and seated connections. This is mainly due to the presence of the steel connecting components, such as plates and bolts, both of which transfer heat to the interior of the wood section and increase the charring rate. Also, in concealed wood-steel-wood connections, the timber beam cross-sectional dimensions are considerably reduced due to the slotted cuts that are necessary to insert the connecting steel plate. Despite their relatively poor performance in fire, concealed connections are popular because of their aesthetic appearance.

The research presented in this thesis focused on studying the structural behavior of concealed glulam bolted connections at both, ambient and elevated temperatures. All test specimen presented in this study were connected to form a semi-rigid connection due to the need to investigate the structural fire performance of moment-resisting timber connections to better understand laterally loaded timber structures which can develop bending moments at the beam-to-column connections. In order to improve the fire performance of concealed timber connection, a relatively larger section was used to account for the effect of reduced cross section due to charring, also steel components, e.g., steel bolts and plates, were fully protected with wood plugs, to cater for the transfer of heat from the steel components to the inner core of the wood section which negatively affects the connection's failure time in fire.

1.3 Objectives

- Investigate structural performance of moment-resisting concealed connections at ambient and elevated temperatures.
- Study the effects of the number of bolts and their patterns on the structural performance of concealed connections at ambient and elevated temperatures.
- Study the performance of fully protected concealed connections when subjected to fire.

2 LITERATURE REVIEW

This chapter provide a brief introduction to fire resistance and the various codes and standards as well as the properties of wood and steel at ambient and elevated temperature. It also includes a review of literatures dealing with research on the behavior of hybrid connections in both ambient and elevated temperatures.

2.1 Fire Resistance

Fire resistance rating is the length of time a structural member can support its load before collapsing. The main aim of designing fire resistance for structural members is to ensure that the member will support their load during fire to prevent collapse of the building. Whereas the fire resistance for separation is needed to ensure that the fire will be contained in the room of fire origin and will not spread through the building. The fire resistance ratings of structural and non-structural building element are determined in a furnace as per the applicable standards. The Europeans use the International Standard ISO 834 [10] and British Standards BS 476 [11] while in North America ASTM E-119 [12] and CAN/ULC-S101-14 [4] are used.

Fire severity is a measure of the destructive impact of a fire. Although it is usually measured in units of time [1]; it also can be measured in terms of time, temperature, or strength.

From a structural perspective, building codes require that structural elements have enough fire resistance to maintain stability and prevent collapse. In other words, the fire resistance of a building should be greater than the severity of the fire [2].

The Canadian standard for fire resistance CAN ULC S-101-14 [13] provides detailed procedures

be used for the standard fire test. The Canadian standard is similar to the standard time-temperature curve ASTM E-119 [12] as shown in Figure 2.1.

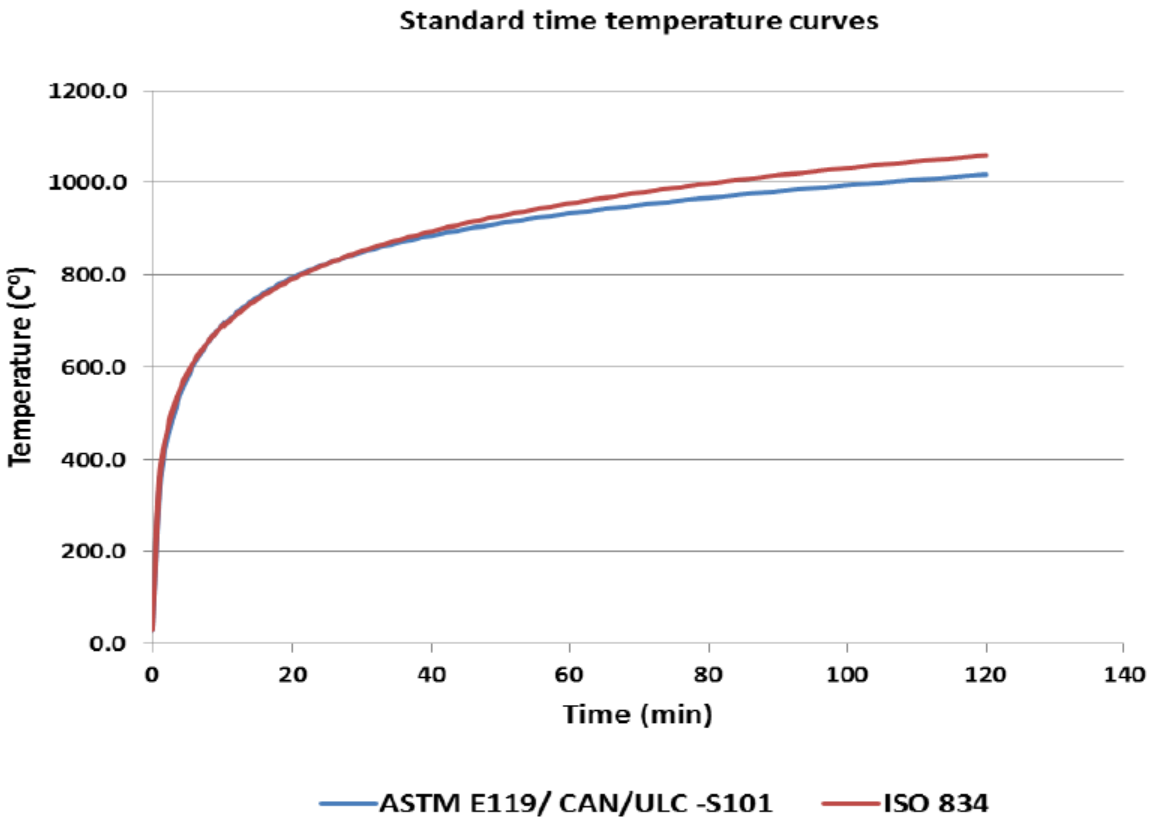

Figure 2.1. Standard fire time-temperature curves [adopted from 3]

2.2 Wood and Steel Properties

The main materials used in this research are wood and steel. Therefore, this section focuses on the behavior of each material when exposed to both ambient and elevated temperatures.

2.2.1 Timber at ambient temperature

Wood is an organic cellulose material widely used in construction in most parts of the world. Wood is a non-isotropic material, as its properties depend on the direction in which they are measured, for example, longitudinal, tangential and radial directions, as shown in Figure 2.2.

Timber is very strong when compressed in the longitudinal direction and flexible under bending loads. Wood exhibits great strength in tension and compression when loaded parallel to grain rather than perpendicular to grain. In terms of tensile strength, wood has higher longitudinal strength as compared to the tangential and radial strength [14].

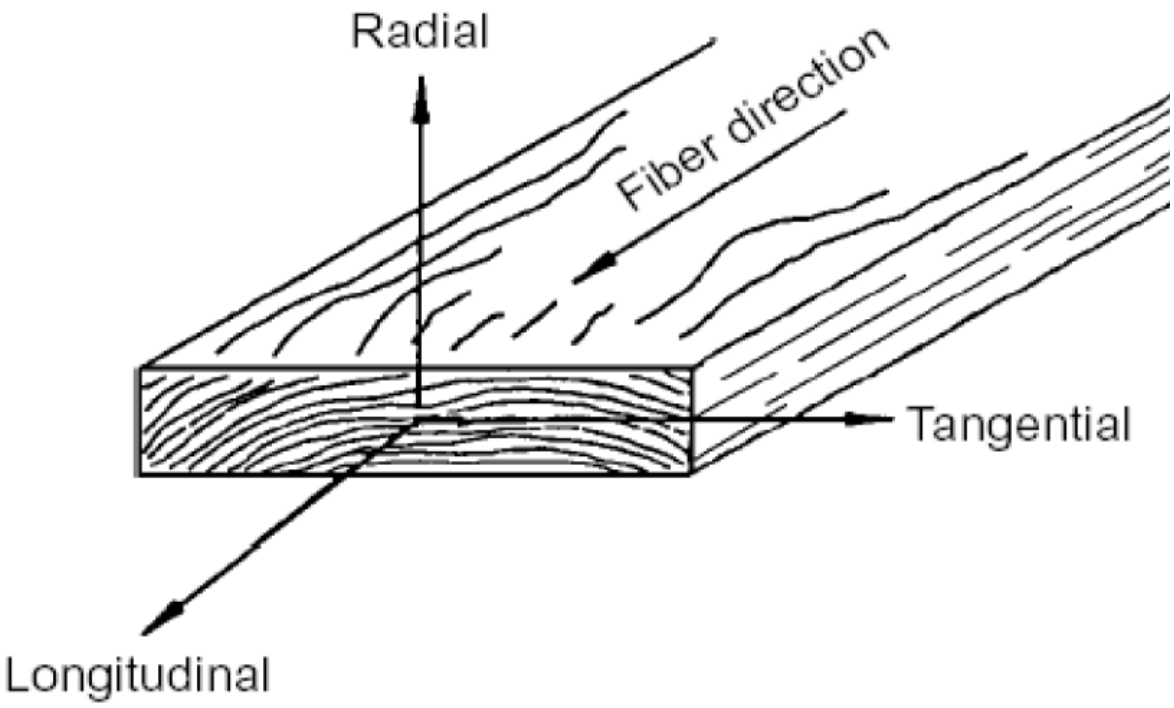

Figure 2.2. Wood plane of symmetry [Adopted from 13]

The Canadian Wood Council [15] provides a summary of wood properties as shown in Table 2.1.

Table 2.1. Material properties of wood [Adopted from 15]

Material properties	**Approximate values**
Density (kg/m^3)	400-600
Modulus of Elasticity (MPa)	8000-11000
Compressive strength (MPa) Parallel	30
Compressive strength (MPa) Perpendicular	8
Tensile Strength (MPa) Parallel	6
Tensile Strength (MPa) Perpendicular	1

Figure 2.3 shows the stress-strain relationship of wood and the two failure modes that occur in wood connections, brittle (splitting) failure and ductile failure. The former involves fracture of the wood around the connection while the latter occurs when the wood is crushed under the bolt shank as stress reaches the plastic state. Most beam to column connections where the loads are applied perpendicular to grain fail by splitting due to the use of bolts [16 - 18]. Habkirk and Quenneville [19] found out that pure brittle and ductile behavior are rare, in their experiments, ductile behavior occurred first, and then, with increasing load, the wood member failed due to brittle fracture.

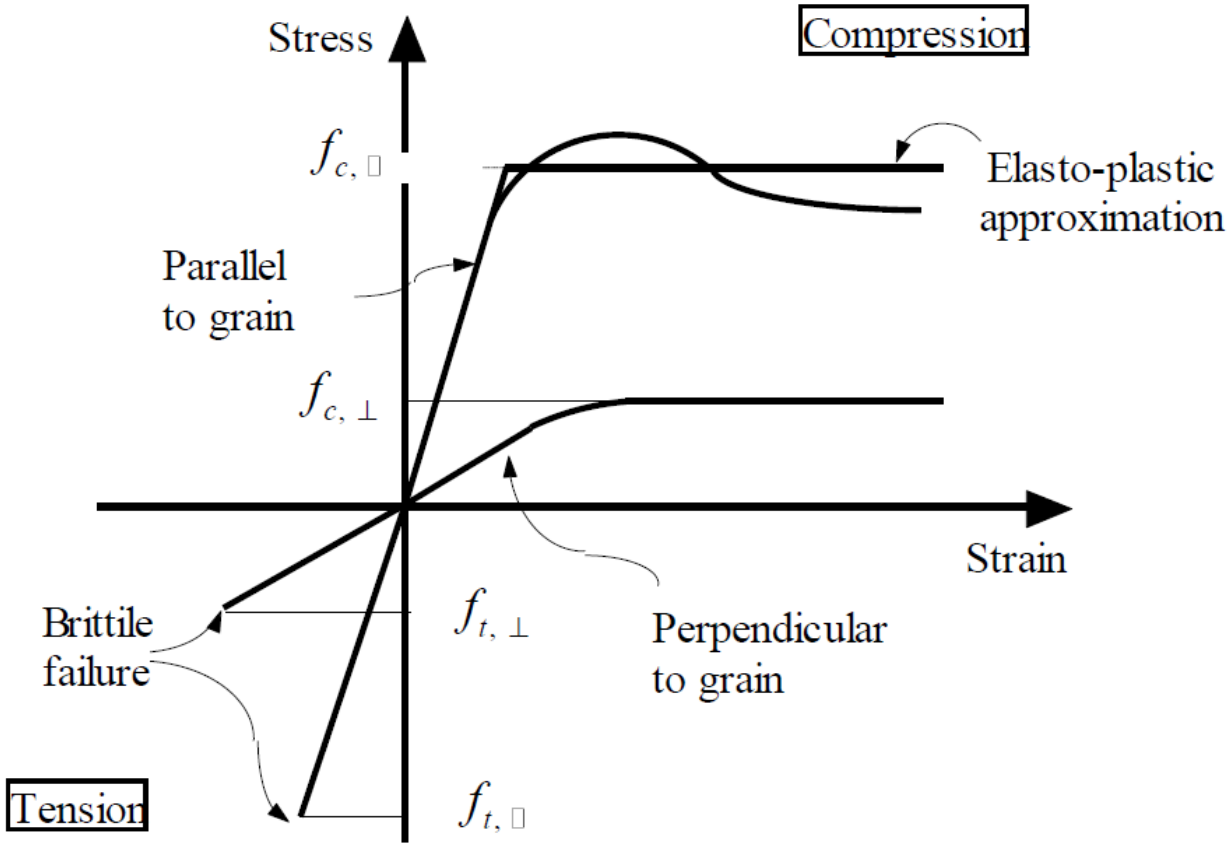

Figure 2.3. Stress-strain relationship for wood [Adopted from 1]

2.2.2 Steel at ambient temperature

Steel is an isotropic man-made material obtained from iron. Unlike wood, steel has the same properties in all directions. Steel can be designed for long spans and can take higher loads than timber.

Table 2.2 shows a summary of the material properties of steel provided by the Canadian Wood Council [15].

Table 2.2. Material Properties of steel [Adopted from 15]

Material properties	**Approximate values**
Density (kg/m^3)	7800
Modulus of Elasticity (MPa)	200000
Poisson ratio	0.3-0.31
Compressive strength (MPa)	400-1000
Tensile Strength (MPa)	400-1000
Yield (MPa)	350

2.2.3 Properties of wood at elevated temperatures

When wood is exposed to elevated temperatures; factors like charring rate, thermal properties (thermal conductivity, specific heat, density) and mechanical properties (modulus of elasticity, tensile strength, compressive strength) must be considered.

2.2.3.1 Charring rate of wood

Wood undergoes thermal degradation when exposed to fire. Thermal degradation or pyrolysis reduces the wood density by converting the wood to char and vapour. Thermal degradation, charring, and combustion of wood have been studied by many researchers [20 - 24].

When as wood is exposed to fire, charring reduces the cross section of the member and the residual structural capacity is affected by the elevated temperature gradient within the uncharred wood [1].

Figure 2.4

Wood starts charring at a temperature between 280℃ to 300℃ degrees, specifically 288℃ [25, 26 and 27], however the charring rate depends on the wood species, density, section size and moisture content [22]. Charring rate plus an assumed zero-strength layer reduces the wood section

because char does not contribute to the strength. The charred layer serves as an insulation that reduces heat transfer to the wood core hence reducing the charring rate [1 and 28].

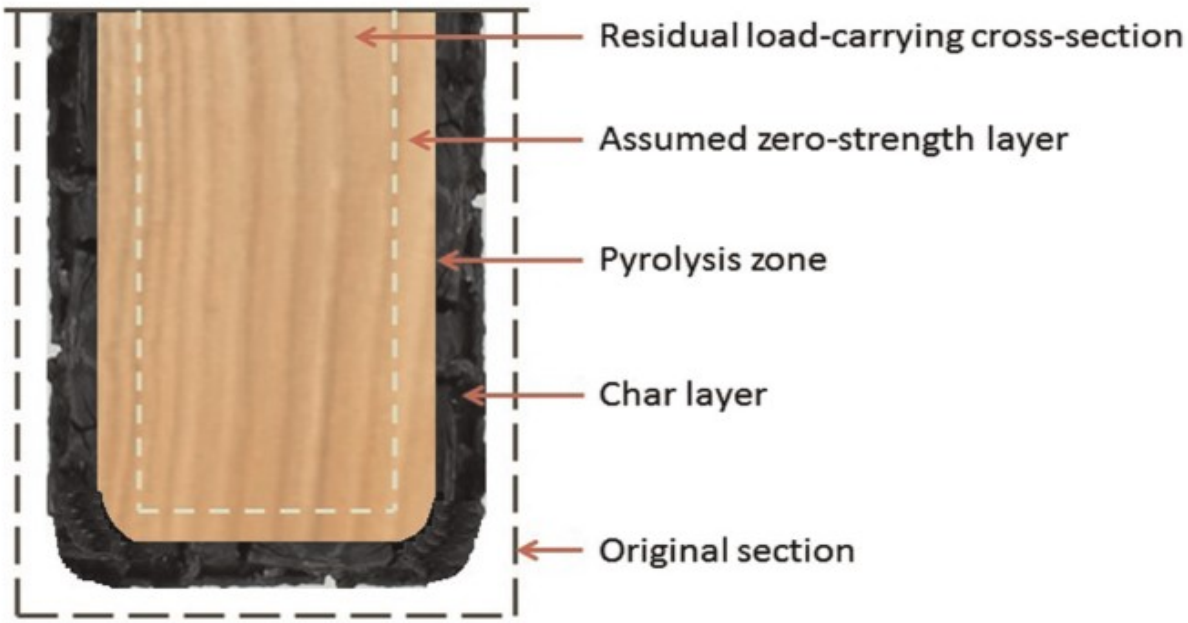

Figure 2.4. Illustration of char layer and zero-strength layer model of fire-damaged wood beam. [Adopted from 29]

König [30] investigated the relationship between the charring depth at 300-degree isotherm and ISO 834 fire exposure time for heavy timber members, Figure 2.5. A1, A2, A3 and A4 represent four similar tests, and the curves are almost linear for all tests.

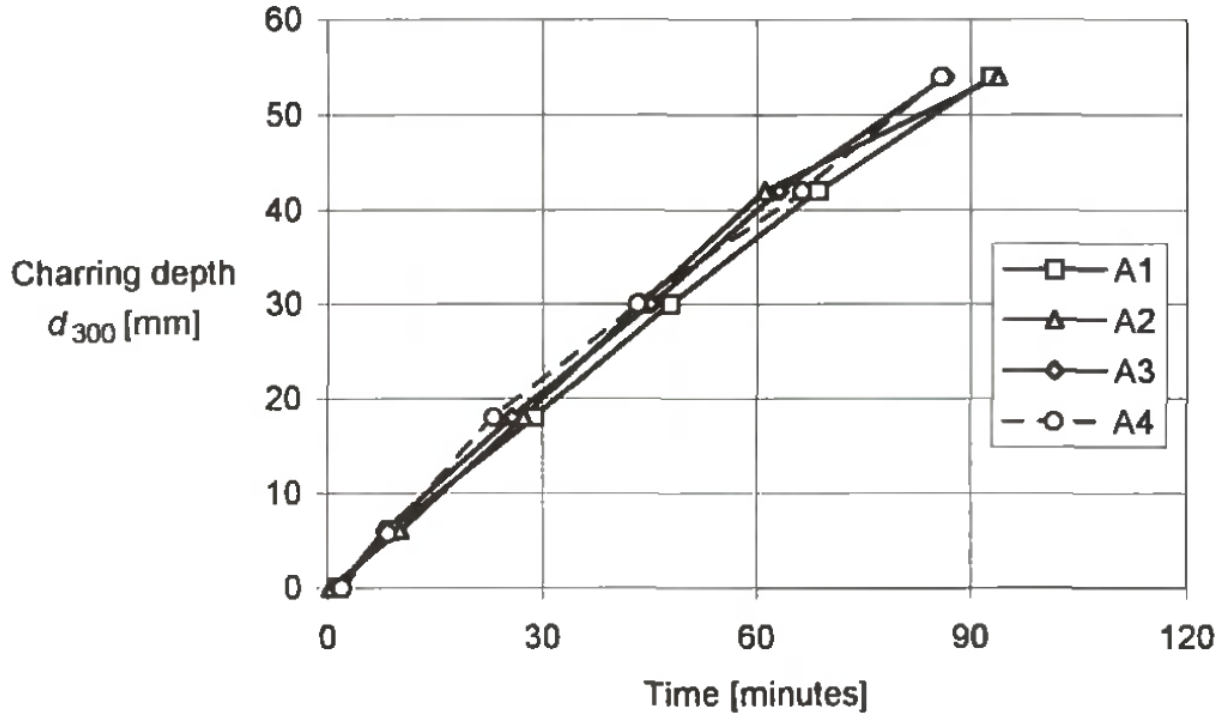

Figure 2.5. Charring depth versus time [Adopted from 30]

Most building codes specify a constant charring rate during standard fire exposures. The acceptable charring rate varies between the different national codes; in the United States, a charring rate of 0.635 mm/min is used for solid wood and glulam [31]. The NBCC [2] uses 0.60 mm/min based on Lie [32] who developed calculation methods for columns and beams. Eurocode 5 [33] uses a charring rate of 0.65 mm/min and 0.5 mm/min for softwood and hardwood respectively. Eurocode 5 [33] also considers the effect of corner rounding. White [17] developed an accepted empirical model (Equation 1) for calculating the charring rate in the ASTM E119 fire tests. The charring rate can be calculated using White's empirical model:

$$t = m\, x_c^{1.23} \qquad \textbf{Equation 2.1}$$

where:

t is the time of exposure (min),

x_c is the char depth (mm)

m is the char rate coefficient (min/mm $^{1.23}$)

m is expressed as a function of density, moisture content, and a char contraction factor. The char contraction factor is the ratio of the thickness of the char layer at the end of the fire exposure divided by the original thickness of the wood layer that charred.

2.2.3.2 Thermal conductivity

Knudson [34], Fredlund [35], Mehaffey [36], Janssens [37] and Konig [38] investigated the thermal conductivity of wood and obtained values shown in Figure 2.6. Knudson [34] used a linear relationship to represent the thermal conductivity of wood from 20℃ to 200℃, a linear curve between 200℃ to 350℃ and a linear relationship for char beyond 350℃. Fredlund [35] assumed the transformation from wood to char occurred at 300℃. Mehafffey [36] derived his values from Lie [39]. Janssens used expressions to derive his values based on wood oven-dry density and moisture content. Konig's [38] research dealt with charring of timber members of spruce exposed to fire with thermal conditions of one-dimensional heat transfer as in semi-infinite slabs. From his values, the thermal conductivity increases at temperatures over 500℃. He explained that he considered the influence of cracks and shrinkage of the charred layer. The difference in values from the researchers may be due to the variation in their wood species, moisture content and densities.

In general, most researchers agree that the thermal conductivity increases linearly up to 200℃ then decreases linearly to 350℃ and increases after 350℃.

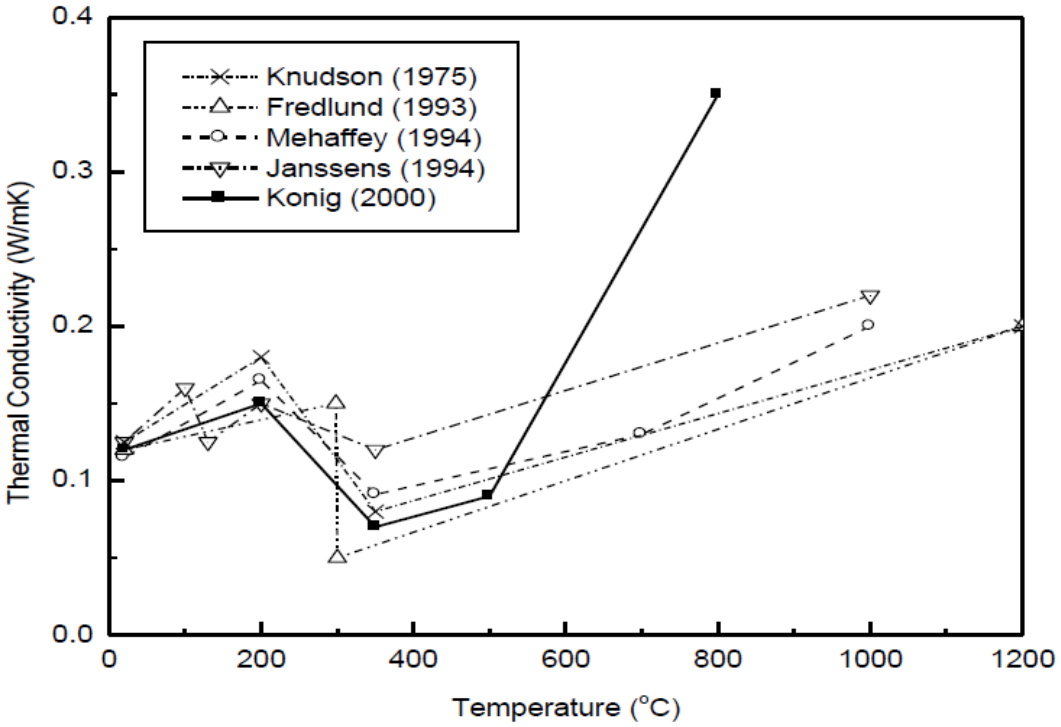

Figure 2.6. Thermal conductivity of wood at elevated temperatures [Adopted from 6]

2.2.3.3 Specific heat

The specific heat of wood at elevated temperatures was studied by various researchers, Mehaffey [36] and Konig [38] examined a specific heat have a peak between 100℃ and 120℃ because of the extra energy required to evaporate moisture, as show in Figure 2.7. The specific heat can be calculated using Gammon's equation [40] as shown in Equation 2.2.

$$C_p = (\alpha+bT+ 4.187u)/ (1+u) +\Delta c \qquad \textbf{Equation 2.2}$$

Where;

C_p (kJ/kgK): is the specific heat,

T (°C): is the temperature

u (kg/kg): is the moisture content.

a and b: are the coefficients that depend on wood species.

Δc: is the moisture correction used only by Janssens [37].

$$\Delta c = (23.55T - 1326u + 2417)\, u \qquad \textbf{Equation 2.3}$$

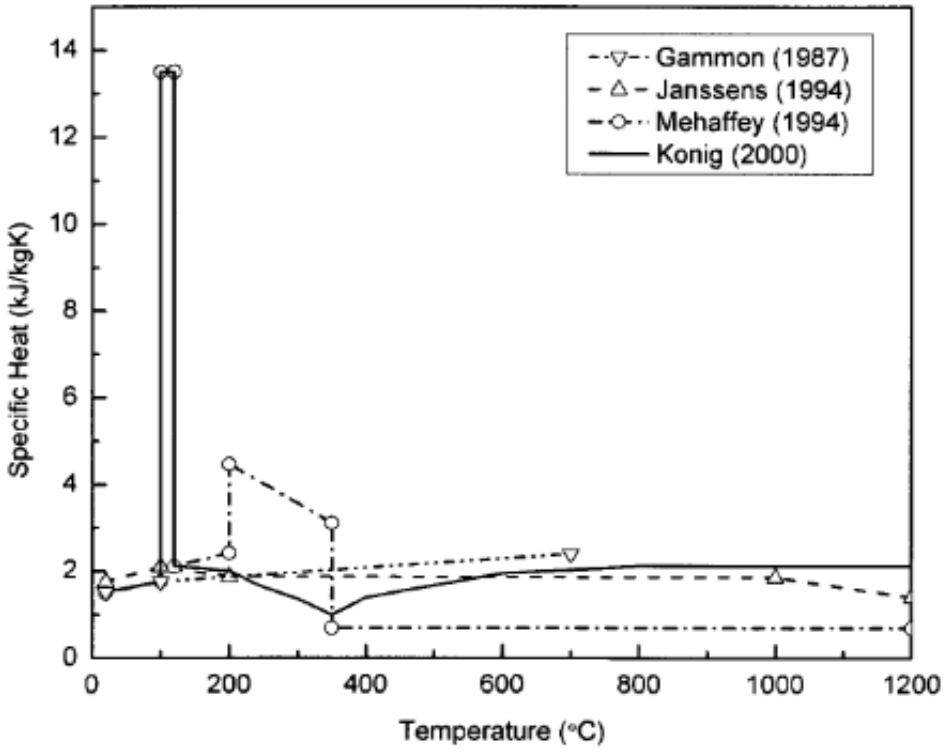

Figure 2.7. Specific heat of wood at elevated temperature [Adopted from 6]

2.2.3.4 Density

Lie [39], Takeda and Mehaffey [41] and Janssens [37] represent the density ratio as a function of temperature as shown in Figure 2.8. From their results the density of wood changes at elevated temperatures and this is due to moisture evaporation and thermal degradation of the wood fibers. It can be observed that at 200°C the density ratio reduces to a value between 0.9 and 0.95 and there

is a significant drop from 0.9 or 0.95 to 0.3 or 0.2 between temperatures 200℃ and 350℃ due to thermal decomposition. From this point the char density decreases slowly.

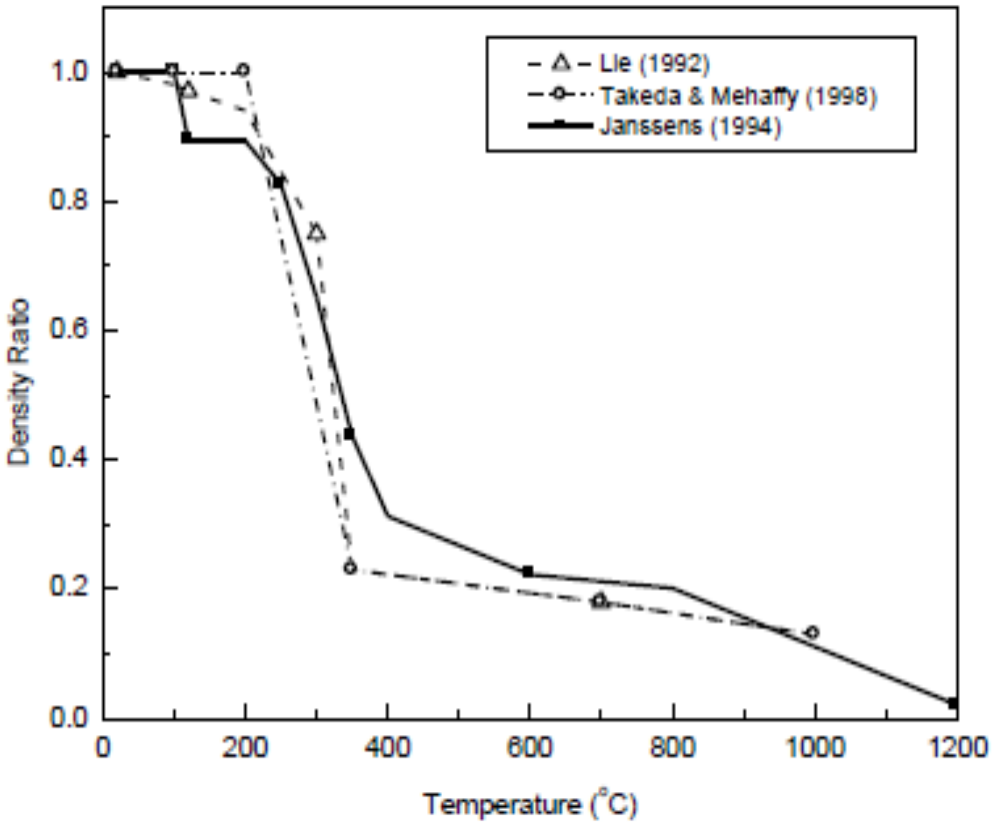

Figure 2.8. Density of wood at elevated temperature [Adopted from 6]

2.2.3.5 Modulus of elasticity

Similarly, to density, the modulus of elasticity reduces to 0.9 at a temperature of 200℃. The value reduces drastically after about 200℃ [39 - 45] as shown in Figure 2.9.

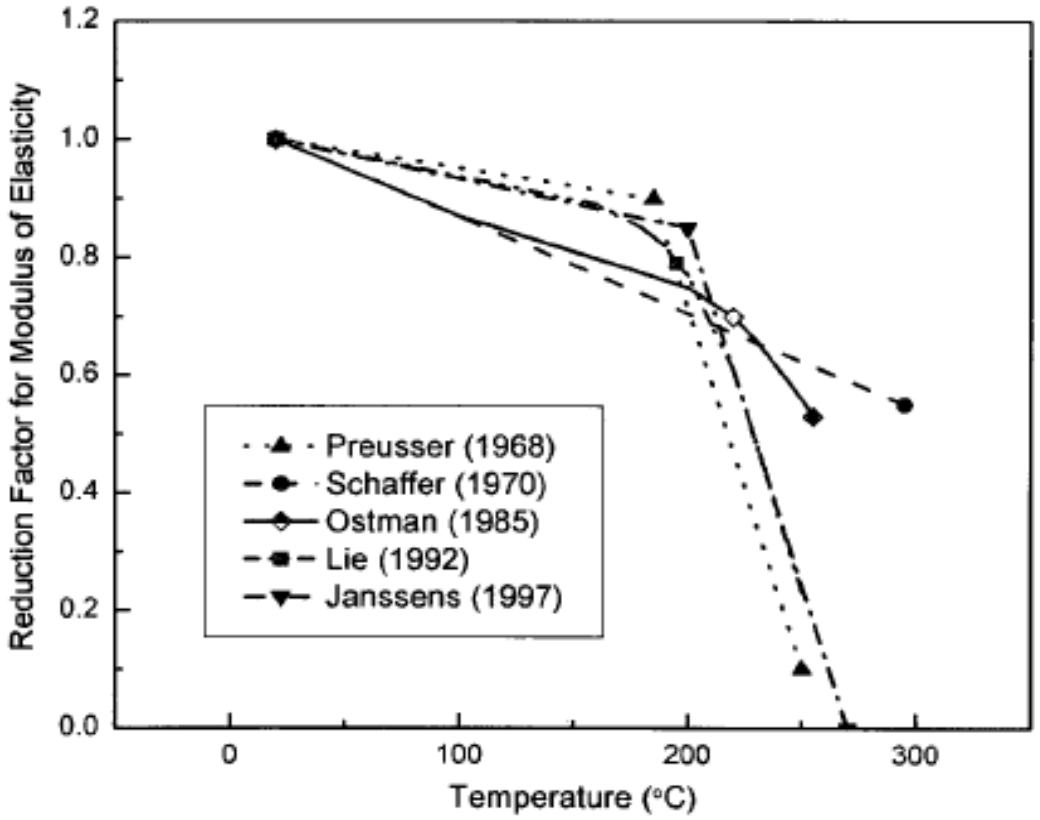

Figure 2.9. Elastic modulus of wood at elevated temperature (1) [Adopted from 6]

Konig [38] and Thomas [46] also investigated the reduction factor for modulus of elasticity at elevated temperatures. They noticed that the behavior varies for tension and compression as shown in Figure 2.10.

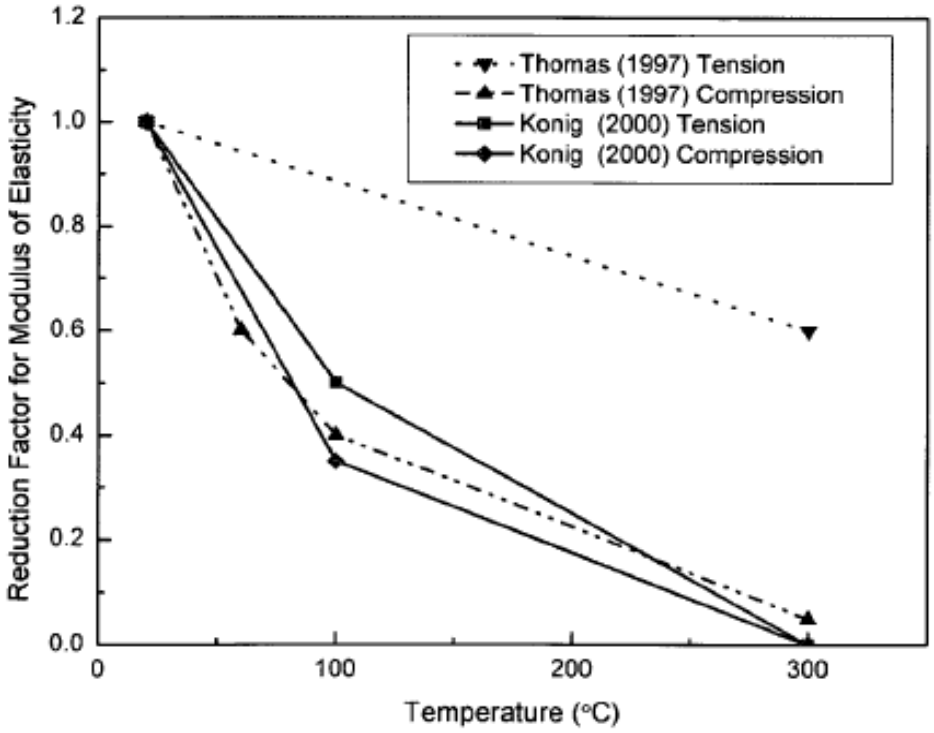

Figure 2.10. Elastic modulus of wood at elevated temperature (2) [Adopted from 6]

2.2.3.6 Tensile strength

As expected, the tensile strength of wood decreases with the increase in temperature until it becomes negligible when wood becomes char. Figure 2.11 shows the reduction factor for tensile strength with temperature. Konig [38] found out that when assuming a bilinear relationship, the reduction in tensile strength is similar to the reduction in density and modulus of elasticity. Lie [39] and Thomas [46] also used a decreasing linear relationship from 20℃ to 300℃. Schaffer [43] assumed a gradual decrease until 200℃, after which there was a rapid decline in tensile strength. According to Thomas [46] the tensile strength of wood dropped linearly between 80℃ and 295℃ and it loses its strength at 310℃. Similar to the modulus of elasticity, the reduction in tensile

strength is assumed to be the same in both directions parallel and perpendicular to grain [47 and 48].

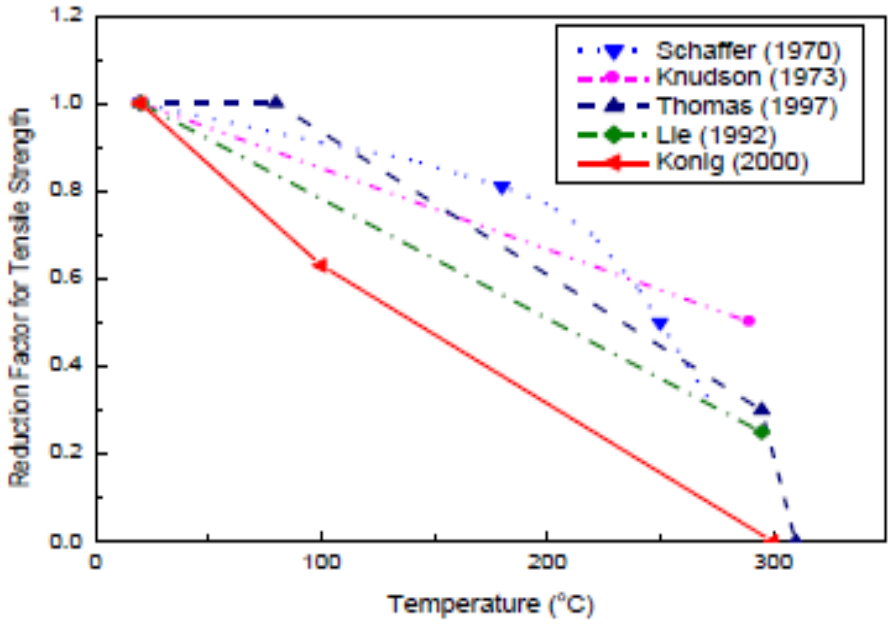

Figure 2.11. Tensile strength of wood at elevated temperature. [Adopted from 6]

2.2.3.7 Compressive strength

Results from Schaffer [43] and Lie [39] shown in Figure 2.12 revealed that compressive strength acts similarly to the tensile strength at elevated temperatures. Others also found out that the reduction in the compressive strength in both directions, perpendicular and parallel to grain, is like reduction of the tensile strength. Konig [38] and Thomas [46] assumed a bilinear relationship similar to the tensile strength.

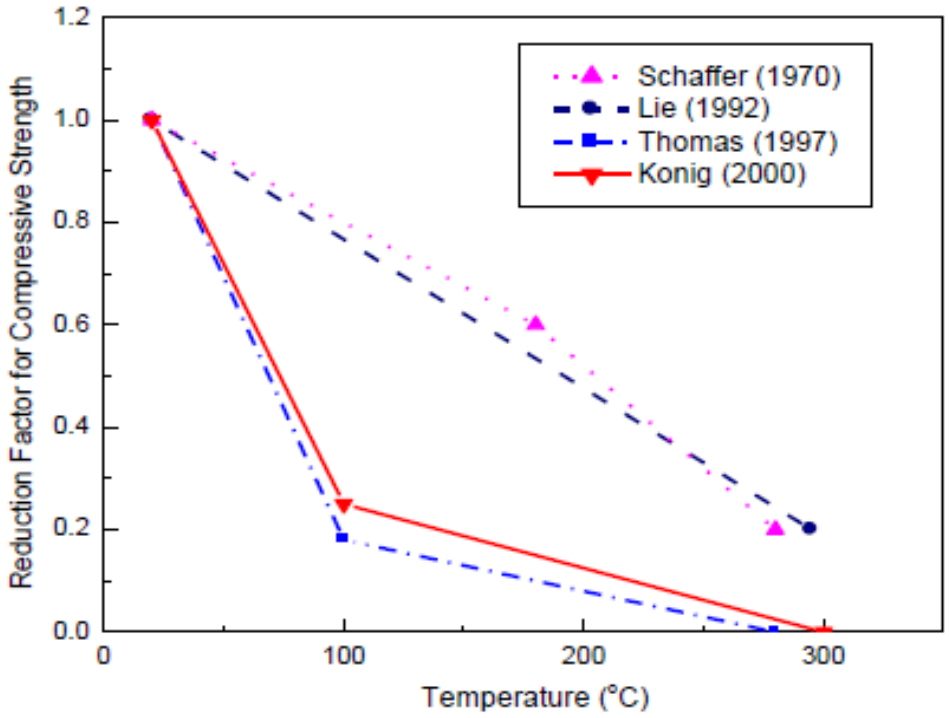

Figure 2.12. Compressive strength of wood at elevated temperature [Adopted from 6]

2.2.4 Properties of steel at elevated temperatures

This session discusses how increase in temperature can affect the yield strength, thermal conductivity, specific heat and density of steel. These properties are essential in determining the residual capacity and heat transfer in steel.

2.2.4.1 Yield strength

Unlike wood, steel is an isotropic material that does not undergo thermal decomposition. However, steel maintains its yield strength up to temperatures of about 400°C as shown in Figure 2.13. Steel's ultimate strength increases slightly at medium temperatures but significantly decreases at elevated temperatures [1]. The cross-sectional area and exposed area of steel to heat plays an important role in heat transfer through the steel core and hence to the reduction in strength.

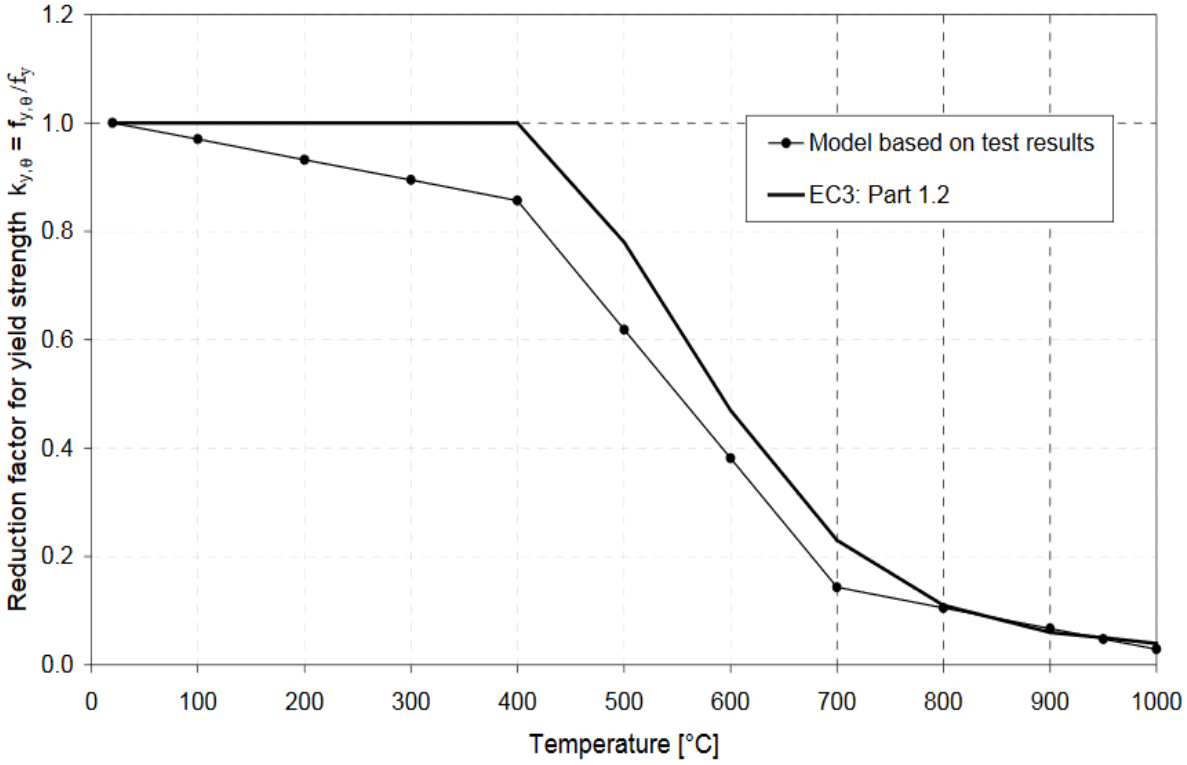

Figure 2.13. Steel yield strength with temperature [Adopted from 48]

2.2.4.2 Thermal conductivity of steel

Steel is a very good conductor of heat; therefore, it heats up very quickly if exposed directly to fire. The rate of heating depends on its thermal conductivity, specific heat and density. Figure 2.14 shows the thermal conductivity of steel at elevated temperatures. From the graph, steel's thermal conductivity reduces linearly from about 55 W/mK at 0°C to 27 W/mK at 800°C and remains constant with further increase in temperature [49].

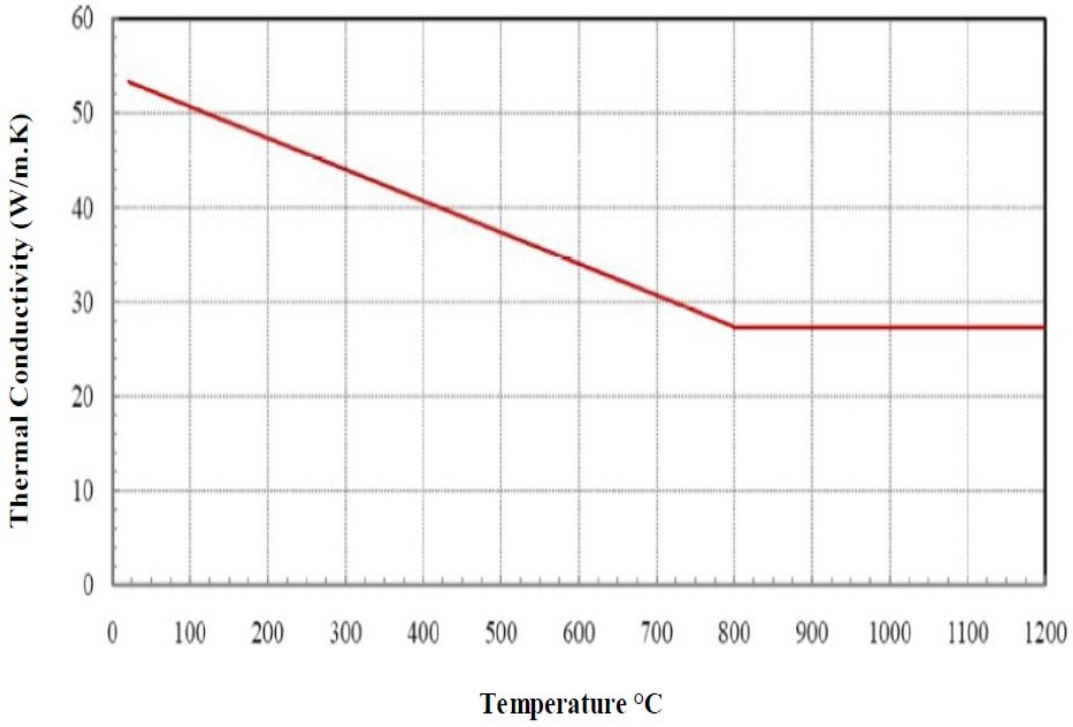

Figure 2.14. Thermal conductivity of steel with variation in temperature [Adopted from 48]

2.2.4.3 Specific heat of steel

As shown in Figure 2.15 the specific heat of steel increases gradually from 400 J/kg.K to 700 J/kg.K from 0°C to 700°C, respectively. However, there is a sudden rise and fall in specific heat, between 700°C and 850°C; after which a constant specific heat of 650 K/kg.K is obtained [43]. This peak is due to changes in the microstructure of steel.

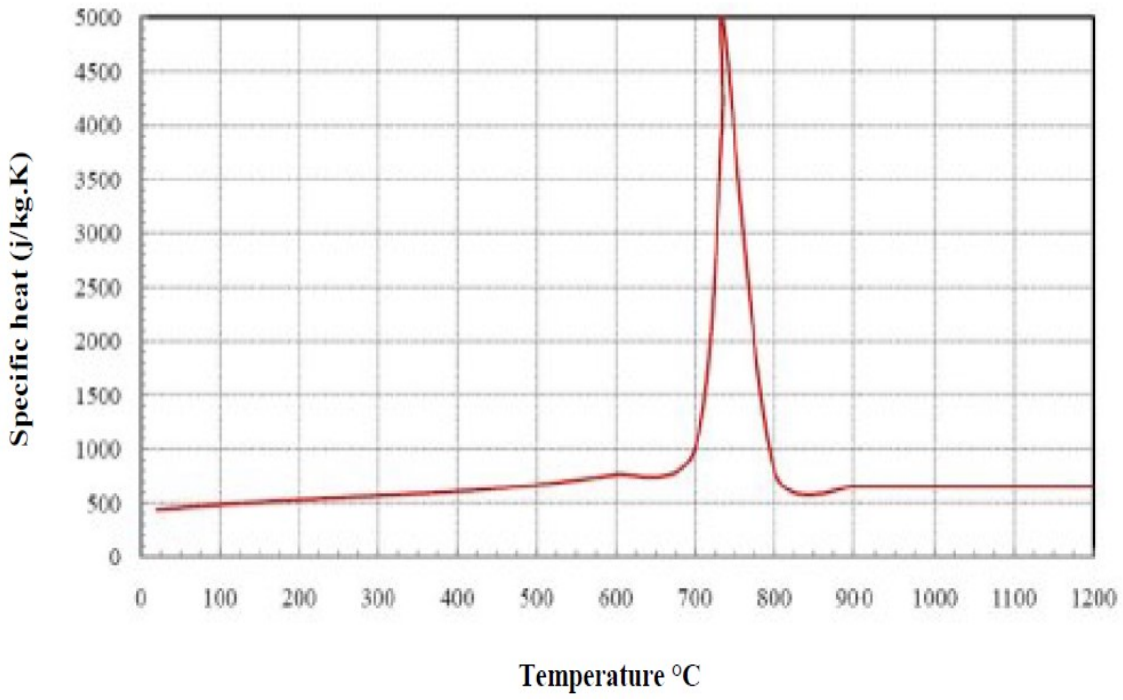

Figure 2.15. Specific heat of steel with variation in temperatures [Adopted from 48]

Contrary to wood, steel does not char and therefore maintains its density similar to the density at ambient temperature, that is 7850 kg/m^2. [43]

2.3 Wood and Steel Hybrid Connections

Hybrid connections combine the properties of the individual materials to achieve high structural capacities. There are different types of wood and steel hybrid connections depending on the steel shear taps. Figure 2.16 shows some common types of steel shear taps, that is concealed, exposed and seated. This section discusses the performance of wood-steel hybrid connections at both ambient and elevated temperatures, as well as the possible failure modes.

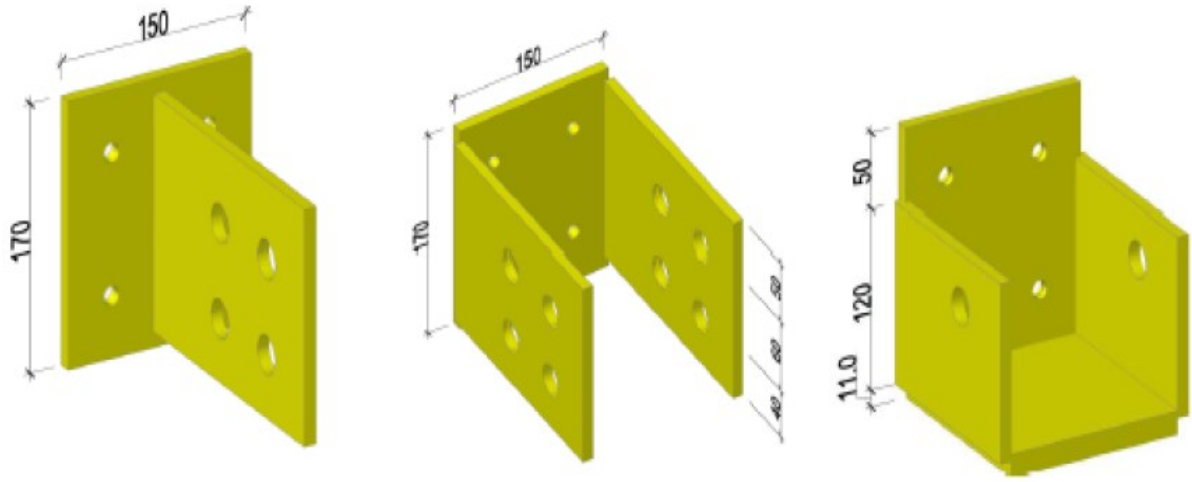

(a) Concealed (b) Exposed (c) seated

Figure 2.16. Steel plate connection types [Adopted from 3]

2.3.1 Connection behavior at ambient temperature

Connections are a critical aspect of wood structures as they transfer the loads from one member to another. Mostly, steel fasteners such as nails are used to connect light framing members, while bolts with steel plates are used for heavy member connections. Design codes provide guidance on fastener spacing and how to design for the different failure modes. Figure 2.17 shows the various possible failure modes depending on the direction of the applied load. In general, the main failure modes are yielding and splitting.

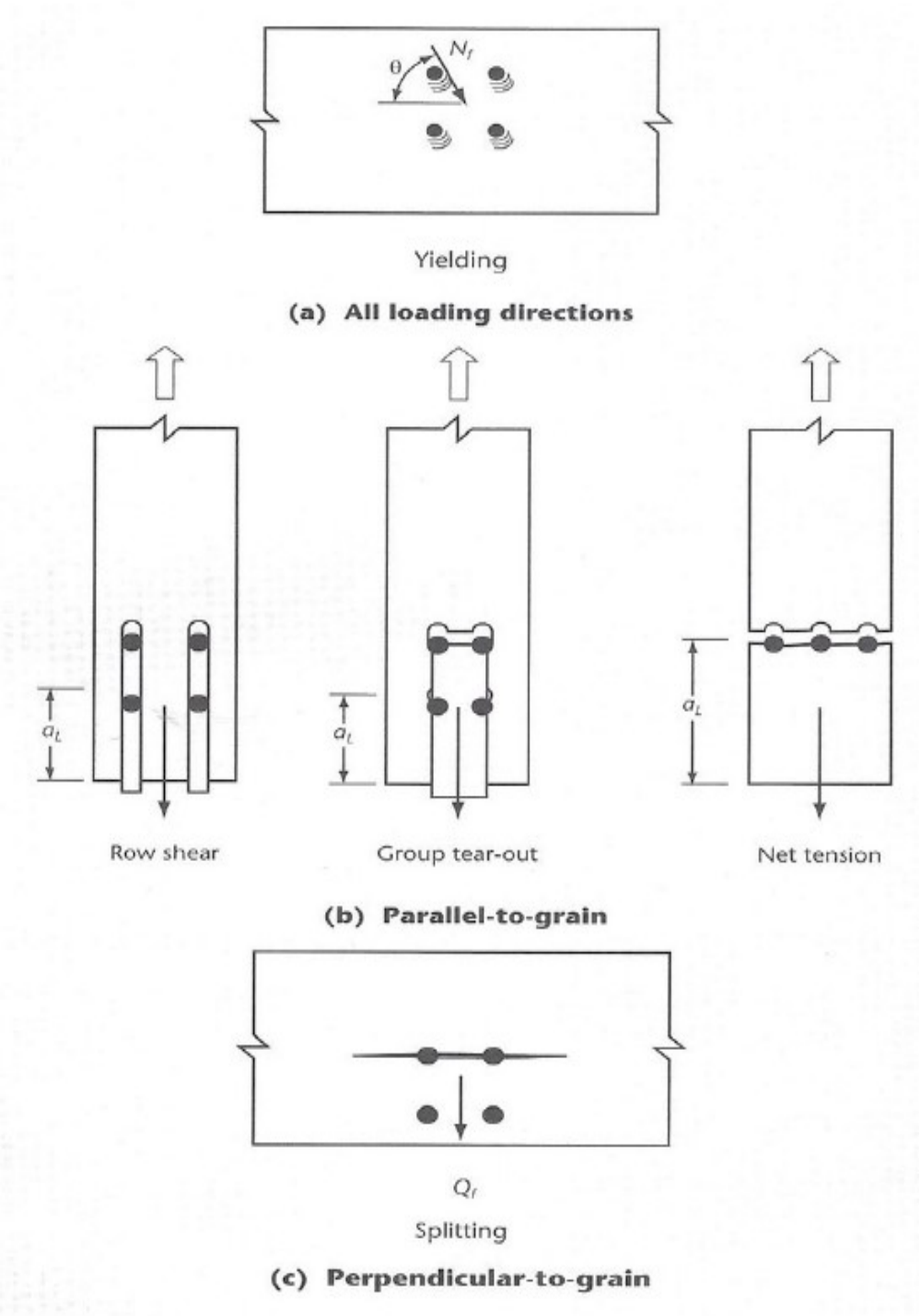

Figure 2.17. Failure modes of wood connections [Adopted from 4]

2.3.1.1 Splitting

The ductile and brittle failure modes are explored in the Canadian design standard (CAN/CSA O86-14) [13] for bolted timber connections. It establishes the requirements for splitting as shown in Equation 2.4 which occurs at joints loaded perpendicular to the grain,

$$Qf \leq Qr \qquad \textbf{Equation 2.4}$$

where:

Qf: is the factored load perpendicular to the grain

Qr: is the factored splitting resistance

The factored splitting resistance is calculated as follows (clause 12.4.4.7):

$$\boldsymbol{Qr}=\boldsymbol{QSr}\mathrm{T} \qquad \textbf{Equation 2.5}$$

The total factored splitting resistance of a connection shall be calculated as the sum of the splitting resistance of the wood member resisting the load and shall be the following:

$$QSr\mathrm{T}=\Sigma QSr\mathrm{i} \qquad \textbf{Equation 2.6}$$

The factored perpendicular-to grain splitting resistance of wood member *i, N*, shall be calculated as follows:

$$QSr\mathrm{i}=\emptyset w\ QSi\ (K_{\mathrm{D}}\ K_{\mathrm{SF}}\ K_{\mathrm{T}}) \qquad \textbf{Equation 2.7}$$

$$QSi=14\ t\ \sqrt{\frac{de}{1-\frac{de}{d}}} \qquad \textbf{Equation 2.8}$$

t = the thickness of the side member, mm

d_{e}= the effective depth of the member, mm

$$d_{\mathrm{e}}=\mathrm{d}\text{-}\mathrm{e_p} \qquad \textbf{Equation 2.9}$$

Where;

d = the total depth of the wood member, mm

e_p = unloaded edge distance, mm

$\emptyset_w$ = 0.7 is the resistance factor for brittle failures

K_D = the duration of the load factor (values can be found at Clause 5.3.2.2)

K_s = the service condition factor (values can be found at Table 6.4.2)

K_T = the fire-retardant treatment factor (values can be found at Table 6.4.3)

2.3.1.2 Yielding

CAN/CSA O86-14 establishes the requirement for yielding as shown in Equation 2.10 which occurs at joints loaded in all directions.

$$Nf \leq Nr \qquad \textbf{Equation 2.10}$$

Where;

N_f: is the factored load on the joint

N_r: is the factored lateral yielding resistance

The factored lateral yielding resistance is:

$Nr = \emptyset_y \, n_u \, n_s \, n_f$

$\emptyset_y$: = 0.8 is the resistance factor for yielding failures

n_u = unit lateral yielding resistance, N (Clause 12.4.4.3.2)

n_s = number of shear planes in the joint

n_f = number of fasteners in the joint

The unit lateral yielding resistance nu shall be taken as the smallest value from the following expressions

(for two shear plane):

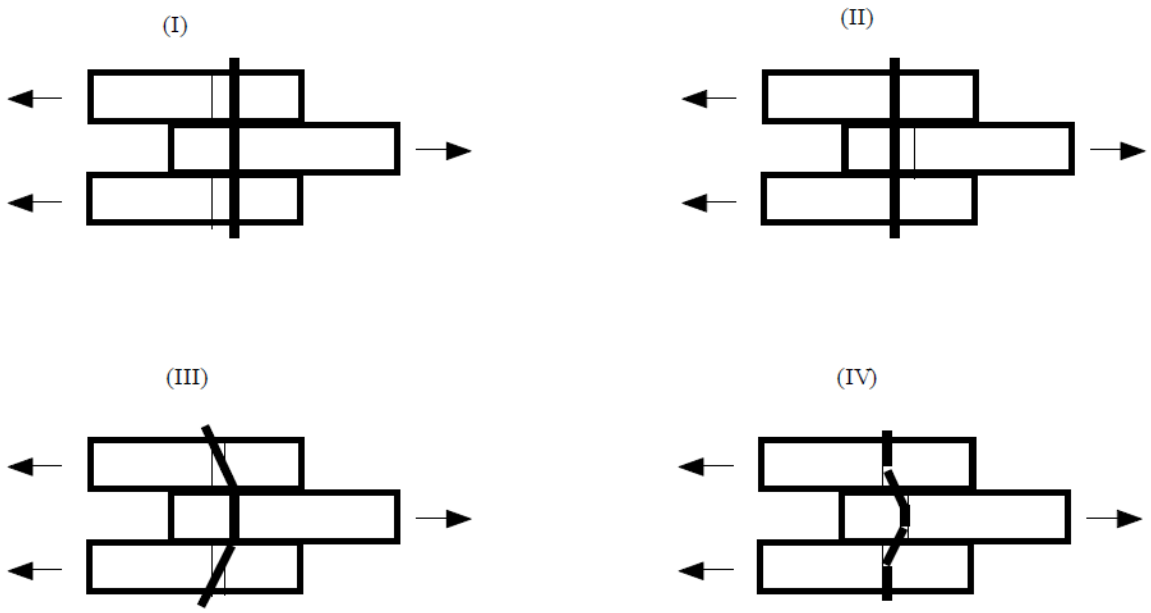

Figure 2.18. Ductile failure modes for double shear timber connections [Adopted from 4]

- For I: $n_u = f_1\, d_f\, t_1$ **Equation 2.11**

- For II: $n_u = \frac{1}{2} f_2\, d_f\, t_2$ **Equation 2.12**

- For III: $n_u = f_1\, d_f^2 \left[\sqrt{\frac{1}{6}\frac{f_2}{(f_1+f_2)}\frac{f_y}{f_1}} + \frac{1}{5}\frac{t_1}{d_f}\right]$ **Equation 2.13**

- For IV: $n_u = f_1\, d_f^2 \left[\sqrt{\frac{2}{3}\frac{f_2}{(f_1+f_2)}\frac{f_y}{f_1}}\right]$ **Equation 2.14**

where;

f_1: is the embedment strength of side member, Mpa

f_2: is the embedment strength of main plate, Mpa

f_y: is the bolt's yield strength, MPa

t_1: is the side member's thickness, mm

t_2: is the main member's thickness, mm

d_f: is the fastener's diameter, mm

For wood member embedment strength:

f_1=22 $G(1-0.1df)$ (for fastener bearing perpendicular to grain) **Equation 2.15**

For steel member embedment strength:

f_2=3f_u ($\emptyset_{steel}$ $\emptyset_y$) **Equation 2.16**

where;

G: is mean relative density

f_u: is the ultimate strength of steel grade, MPa

$\emptyset_{steel}$: = 0.67, is the resistance factor for metal member

$\emptyset_y$ = 0.8, is the resistance factor for yielding failures

Mail Geyloff, Maximilian Closen and Frank Lam [49] investigated the ambient behavior of reduced edge distance in bolt timber moment connections with perpendicular to grain reinforcement**.** The experiments were conducted to study the influence of reduced edge distances of bolts and self-tapping screws (STS) as reinforcement perpendicular to grain on the performance and ductility of a moment resisting timber connection. They used glulam 24- E Douglas Fir 130 x 304 for beams and columns. Column and beam length were 1000 mm and 830 mm respectively. The beam was sandwiched between two columns and connected to the column with a concealed 9.5 mm steel plate and 25.4 mm carbon steel bolts. All test samples were reinforced perpendicular to grain and the tests were repeated five times using a displacement controlled reverse cyclic loading as shown in Figure 2.19.

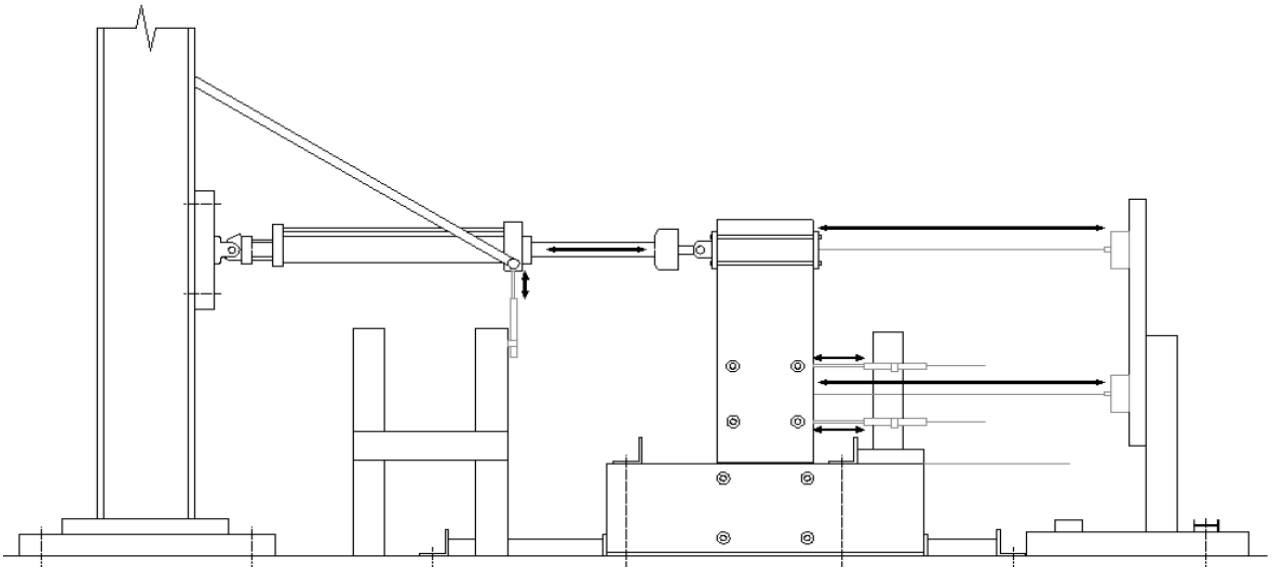

Figure 2.19. General Setup (Geyloff) [Adopted from 49]

Three (3) series of tests were conducted, that is, A-CR, B-CR, and C-CR, with varying end distance as shown in Figure 2.20. A-CR had an edge distance of 94.5 mm which was reduced to 49.5 mm for the B-CR series and C- CR series. However, the layout of the self tapping screws varied.

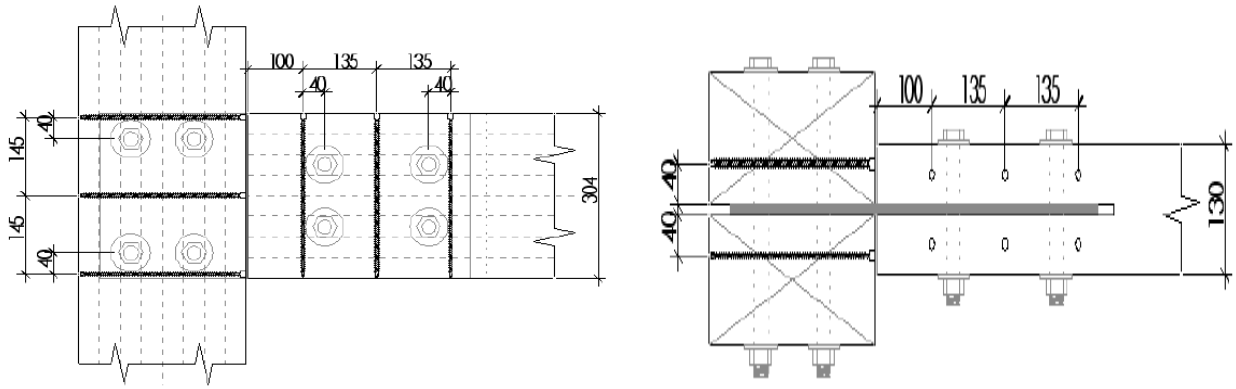

a) *(b)*

A-CR STS Layout

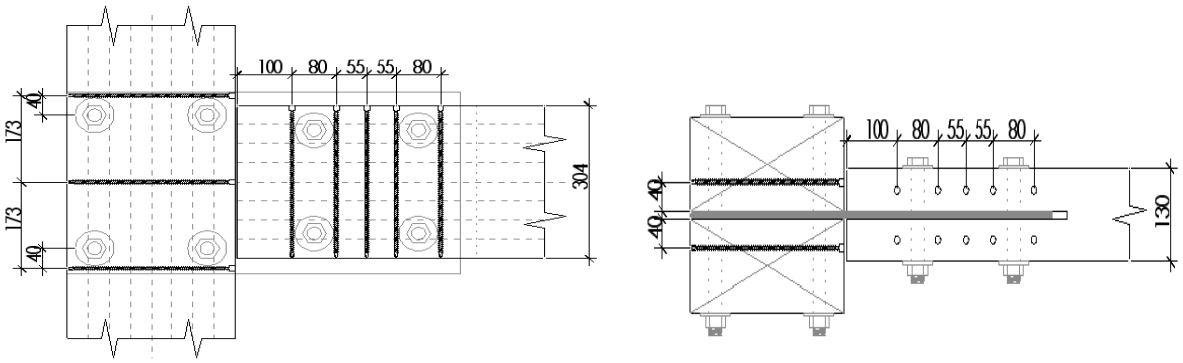

(a) *(b)*

B-CR STS layout

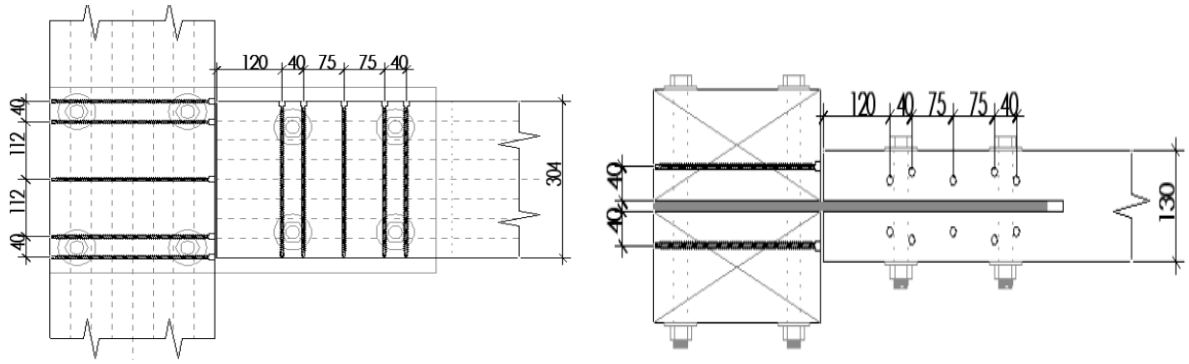

(a) *(b)*

C-CR STS layout

Figure 2.20. Steel-Tapping Screw layout [Adopted from 49]

At the end of the test the A-CR had an ultimate moment capacity of 76.64 kNm while B-CR achieved a higher capacity of 103.83 kNm due to the reduced edge distance. C-CR had the self-tapping screw placed closer to the bolt, allowing an additional increase of ultimate capacity to 105.9 kNm. Figure 2.21 shows the typical moment rotation plot for the three series of tests.

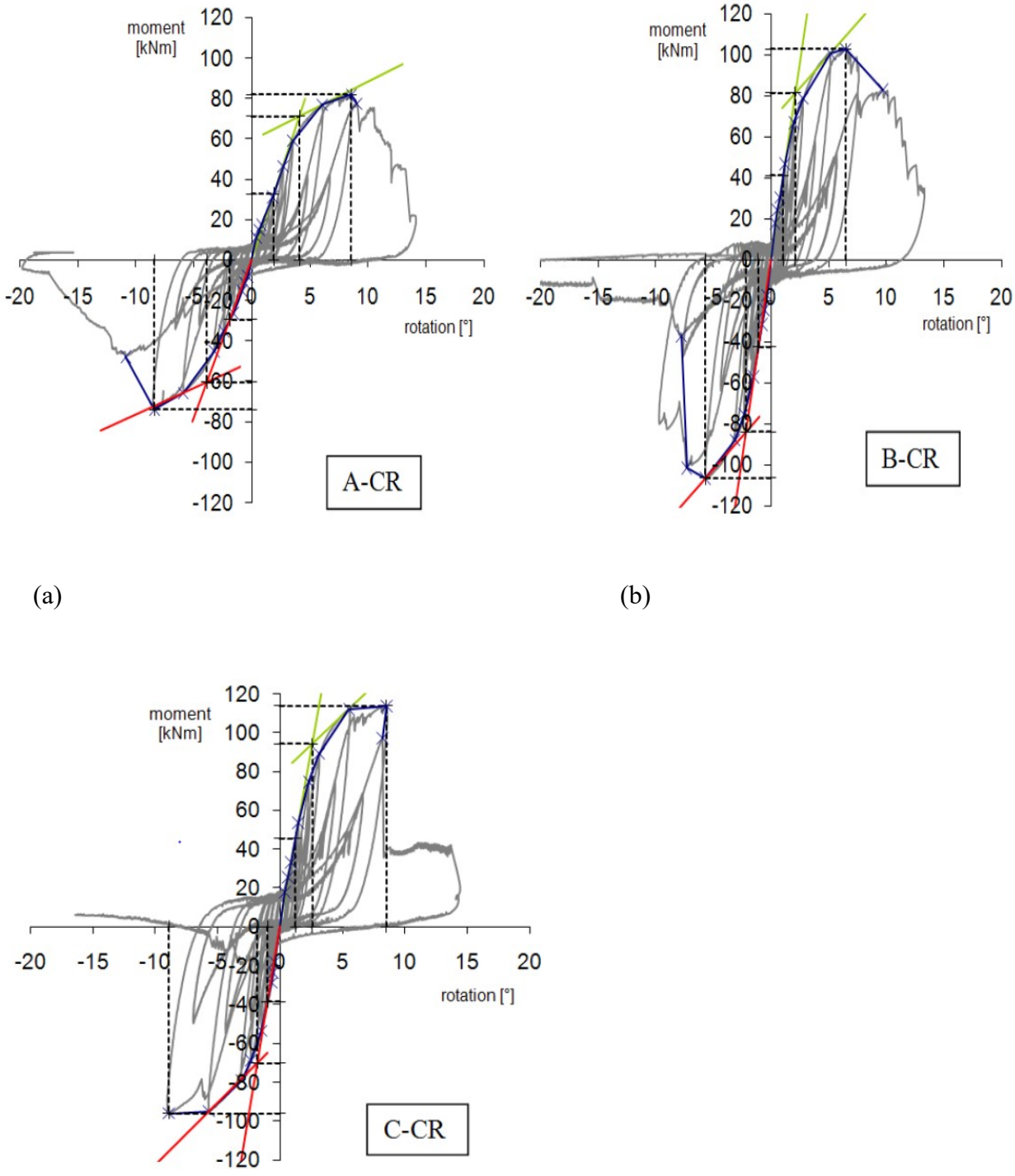

(a)

(b)

(c)

Figure 2.21. Moment-rotation relationships of test species [Adopted from 49]

At the end of the research, it was concluded that the combined use of large diameter bolts and significantly reduced edge distances increased the tendency of splitting but improved the effectiveness of the reinforcing self-tapping screws. Moreover, there was an increase in the yield moment of 31.1 % and 25.2 % in series C-CR and A-CR, respectively as compared to the A-CR. Finally, the reduced bolt edge distance for the B-CR and C-CR series shows that when the spacing of the bolts increased by a factor of 1.9, the elastic stiffness increased by a factor of 2.04 when compared with the A-CR series.

2.3.2 Connection behavior at elevated temperatures

Predicting the behavior of hybrid connections between steel and wood when exposed to high temperatures is complex, because of the difference in the thermal properties of wood and steel, and wood charring.

Ali and Hadjisophocleous [3] investigated the fire performance of hybrid connections between steel columns and a glulam beam. He considered concealed shear tap, exposed shear tap, and seated beam connections. The tests were done using two pin-pin steel columns (W150 X 37), 3200 mm long glulam beam (Nordic Lam 24F/ES12) 140 X 191 X 1900 loaded using two-point loads at one third mid-section. He used a shear plate with a thickness of 9.5 mm and bolts with diameter of 12.7 mm and 19.1 mm to connect the steel column to the beam. The number of bolts was also varied from 2 to 4. All specimens were exposed to the standard time temperature curve defined by CAN/ULC-S101 and subjected to load ratios of 30%, 60% and 100%. The steel columns were protected fully however the beam was only protected at the top surface.

During the tests, he observed elongation and charring around the bolts as a result of heat transfer from the bolts to the interior of the wood section, Figure 2.22. Figure 2.23 shows the failure times for the different specimens with different load ratios.

Figure 2.22. Elongation of holes and charring around the holes [Adopted from 3]

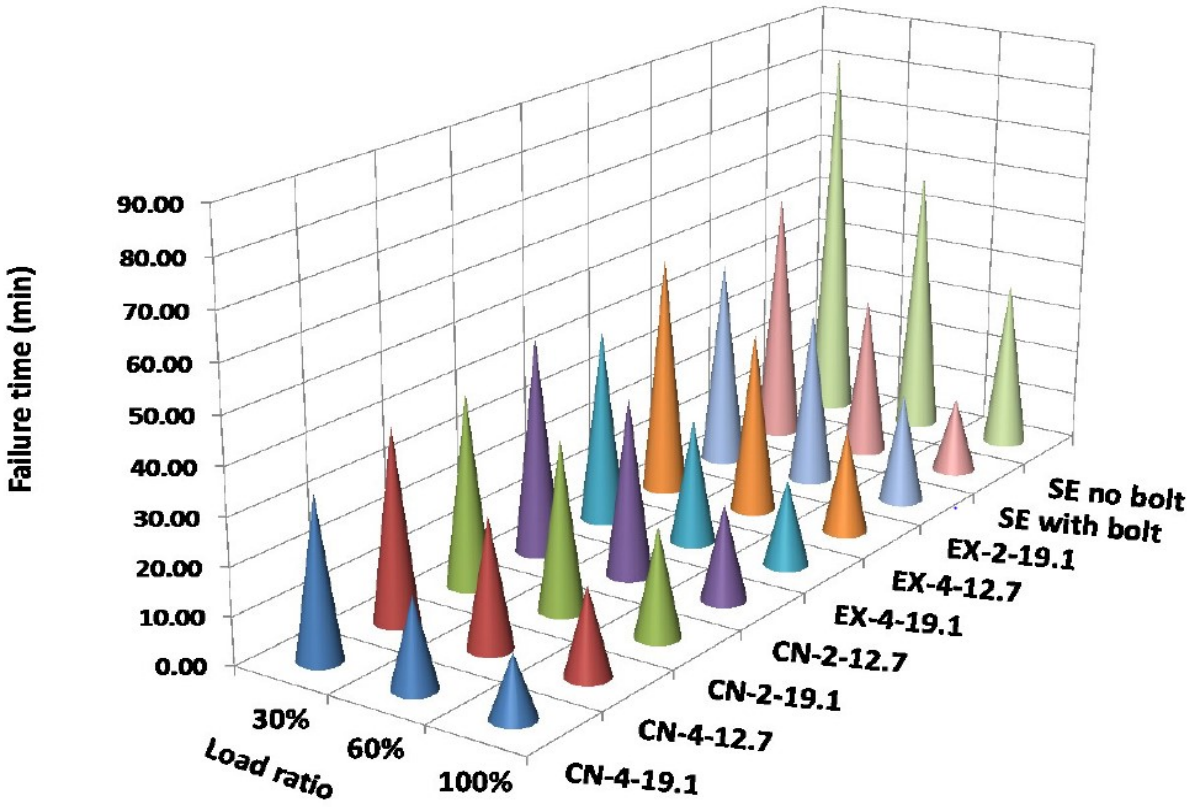

Figure 2.23. Failure time for different types of connections [Adopted from 3]

After the full-scale tests, the results were analysed, and the following conclusions were made

- The type of connection has a major role to play on failure time. For concealed connections, the steel plate notch reduces the member section and the steel plate transmit more heat to the core of the wood. However, in the case of the exposed connection, the steel plate provides initial protection to the wood thereby increasing the failure time.
- The seated connection without the bolt had a higher failure time than the other connection types.
- Partial deflection recovery was observed on both sides of the beam during the first 2-5 minutes of fire exposure and beam deflection increased with time.

- The charring rate of the wood species observed was in the range of 0.63 and 0.76 mm/min.
- Most of the test specimens failed by splitting of the wood, starting from the bolt hole and propagating towards the mid-span.
- The results showed that the failure time was reduced by a range of 12% - 45% and 43% 69% when the load ratio increased from 30% - 60% and 30% - 100% respectively.

He finally recommended that further research can be done on different material protection against fire, and the effect of varying bolt diameters.

Petrycki and Salem [4] also investigated the behavior of concealed steel-glulam bolted connections subjected to monotonic loading at both ambient and elevated temperatures. At ambient temperature, sixteen full-size test assemblies were examined, representing a total of thirty-two beam-to-column glulam bolted connections. Eight of the test assemblies were strengthened perpendicular to the wood grain with long self-tapping screws (STS) as shown in Figure 2.25. For all unstrengthen and strengthened connections, he increased the number of bolt rows, each row having two bolts. Figure 2.24 shows the test setup for both ambient and fire tests. From the ambient tests, it was observed that increasing the bolt rows from two to three had a higher increase in the connection's moment capacity than by increasing the bolt's end distance from four to five-times bolt diameters. The connections failed in a relatively ductile manner in contrast to the unstrengthen connections. After the tests, he observed that the increase in the number of bolts to six bolts in three rows in strengthened connections reduced the occurrence of brittle failure modes compared to the connections with four bolts in two rows. STS-strengthened connections experienced an increased moment-resisting capacity between 1.3 and 2.4 folds.

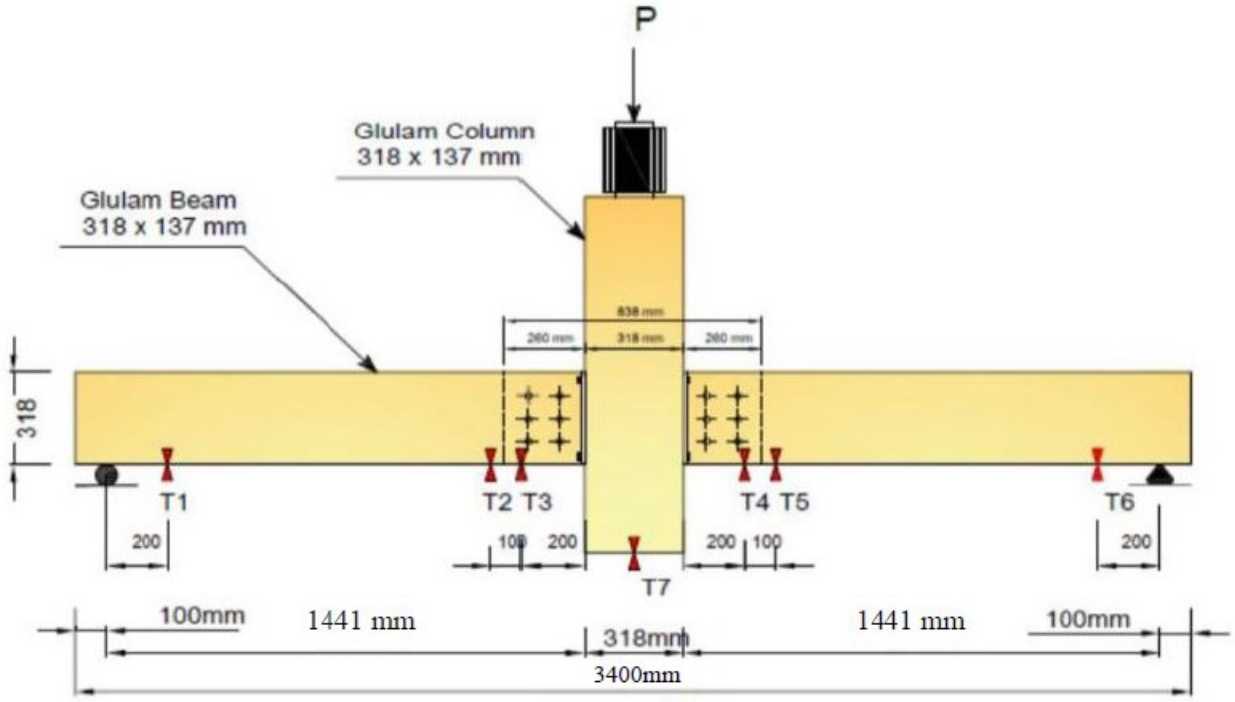

Figure 2.24. Experimental setup [Adopted from 4]

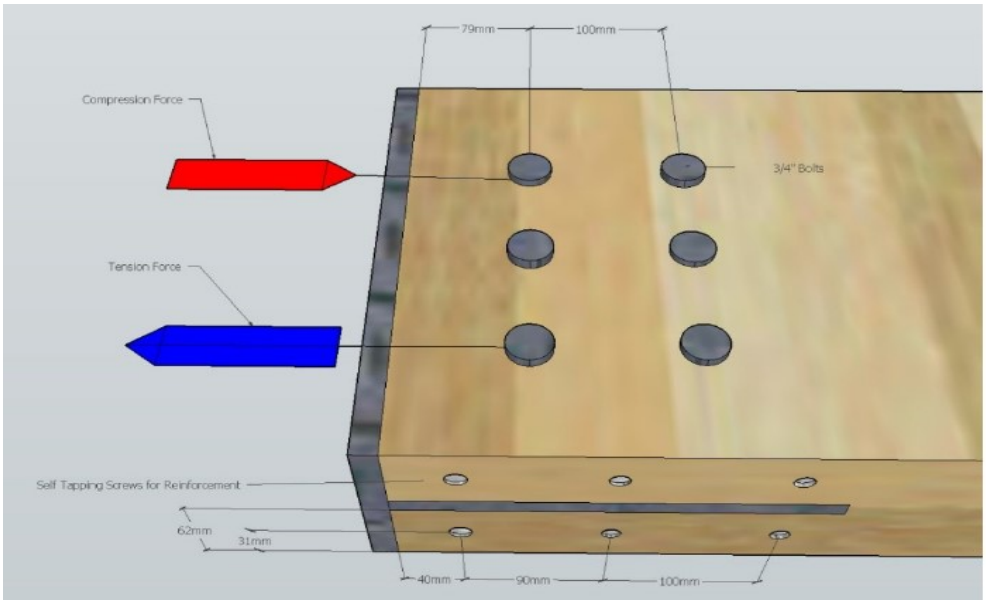

Figure 2.25. Steel connector with four-times bolt diameter end distance, six bolts and STS strengthening [Adopted from 4]

The results of the fire resistance tests showed that by increasing the number of bolt rows from two to three, (each two bolts), increased the glulam beam-to-column connection fire resistance time than increasing the bolt's end distance from four to five-times the bolt diameter. Moreover, the strengthened connections were found to have an increased fire resistance time compared to the unstrengthened connections. The STS increased the fire resistance time of the glulam connections. Table 2.3 shows the results of his fire tests.

Table 2.3. Summary of fire resistance experimental testing results [Adopted from 4]

Assembly No.	End Distance	No. of Bolts	STS	Fire Resistance Time	
				Seconds	Minutes
1F	4*d*	4	No	817.0	13.62
1FS	4*d*	4	Yes	1020.0	17.00
2F	4*d*	6	No	969.0	16.15
2FS	4*d*	6	Yes	1092.0	18.20
3F	5*d*	4	No	921.0	15.35
3FS	5*d*	4	Yes	1028.0	17.13
4F	5*d*	6	No	1050.0	17.50
4FS	5*d*	6	Yes	1140.0	19.00

Boadi and Hadjisophocleous [50] investigated the influence of parameters of load ratio (60% and 100%) of different shear tab connections on the behavior of unprotected hybrid timber-steel connection system in non-standard fires. He compared the performance of these hybrid timber-steel connection system when exposed to the standard CAN/ULC S101 and non-standard fire curves. He also confirmed the ability of the standard furnace to replicate real fires. In his research,

nine (9) unprotected hybrid connection assemblies involving glulam beams connected to insulated steel columns using 12.7 mm grade A325 bolts, were tested in a furnace under exposure to a modelled real fire curve. The glulam beams spanning 1.85 m were subjected to two-point constant transverse loads corresponding to load ratios of 60% and 100%. The columns were pinned at the top and bottom. Three main beam-to-column connections types were studied (seated, exposed and concealed). Figure 2.26 shows the summary of his test results

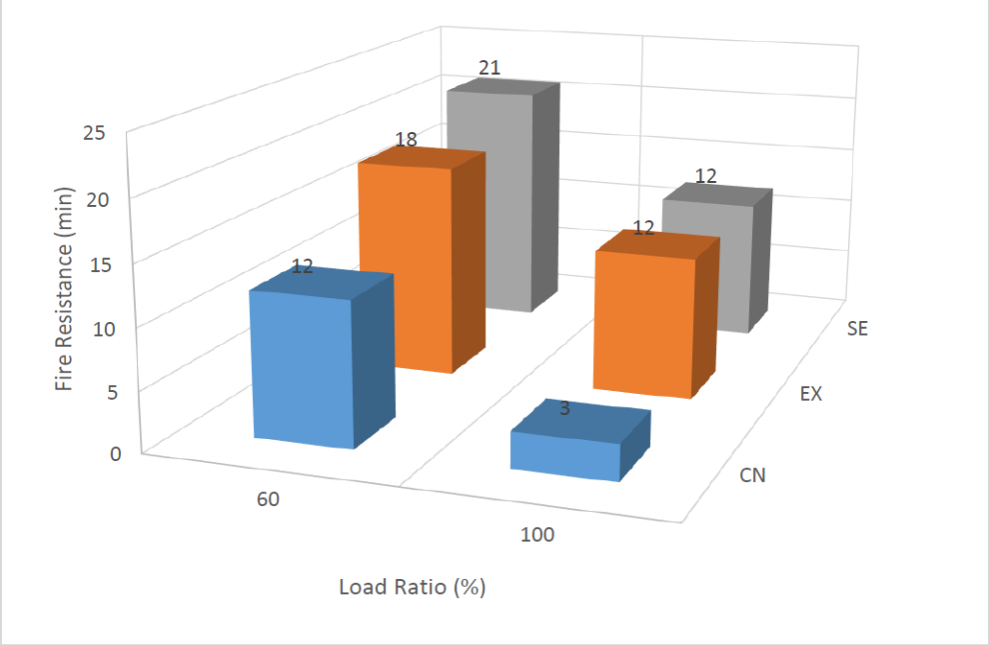

Figure 2.26. Relative fire resistance of the connections [Adopted from 50]

After analysing the test results, he drew the following conclusions;

- Charring rate of wood in natural fires exceed the suggested value of 0.65 mm/min usually employed in design of wood for fire safety. In his research, charring rate values exceeding 1.0 mm/min were recorded for the glulam beams.
- Though the assemblies were designed to fail in one dominant mode, it was observed that splitting of wood was the dominant failure mode for the exposed and concealed connection,

with an accompanying embedment of bolt holes, and fracture of glulam beam at mid-span in the tensile regions.

- There was significant effect of the ratio of applied load in fire to the capacity of a member in ambient conditions. Decrease in load ratio from 100% to 60% significantly increased the fire resistance of the tested connection assemblies. The seated connection had a 75% increase in fire resistance, and the exposed an increase of 50%.

  Based on the analysis of the results obtained, he concluded that the seated connection offers the best fire resistance rating. Which was 17% and 75% higher than the exposed and concealed connection respectively under load ratio of 60%.

Palma [51] also investigated the behaviour of timber beam-to-column shear connections. The objectives of the experimental research were to study the mechanical behavior of beam-to-column connections loaded in shear at normal temperature and elevated temperature. Beam-to-column connections comprised two parts: a column-side, and a beam-side connection. In his research, he focused on the beam side of the connections, which was assumed to be the most exposed to fire. He performed twenty-six full-scale tests at normal temperature, covering eleven different connection types, and twenty-one loaded fire resistance tests were conducted, involving thirteen connections types. He varied the beam section, dowel diameter, number of dowels, dowel spacing, unloaded end distance, loaded edge distance, unloaded edge distance, and the gap between beam and column, as shown in Table 2.4. Figure 2.27 shows his beam-to-column test setup at ambient temperature which was very similar to the set up elevated temperature. He summarised the results of his ambient test and compared it with the estimated values as shown in Table 2.5.

Table 2.4. Geometries of the beam side of the tested connections [Adopted from 51]

Connection typology	$b \times h$ [mm^2]	d [mm]	n_d [ ]	h_e/h [ ]	a_2 [mm]	a_3 [mm]	$a_{4,t}$ [mm]	$a_{4,c}$ [mm]	g [mm]
A.1, A.4	160 × 260	12	4	0.71	36	84	76	76	10
A.2	160 × 260	12	4	0.71	36	84	76	76	20
A.3	160 × 260	12	4	0.71	36	84	76	76	0
A.5	160 × 260	12	4	0.73	40	80	70	70	6
A.6	240 × 340	12	4	0.66	36	84	116	116	10
B.1	160 × 260	8	4	0.64	24	56	94	94	10
B.2	160 × 260	8	4	0.91	24	56	164	24	10
C.1	160 × 260	8	7	0.91	24	56	92	24	10
C.2	240 × 340	8	7	0.81	24	56	132	64	10
D.1	160 × 260	-	-	-	-	-	-	-	18

From Table 2.4, b and h are the width and the height of the beam; d is the dowel diameter and n_d is the number of dowels; h_e is the distance from the most distant fastener to the loaded edge; α_2, α_3, $\alpha_{4,t}$, and $\alpha_{4,c}$ are the dowel spacing, unloaded end distance, loaded edge distance, and unloaded edge distance, respectively; and g is the gap between the beam and the column.

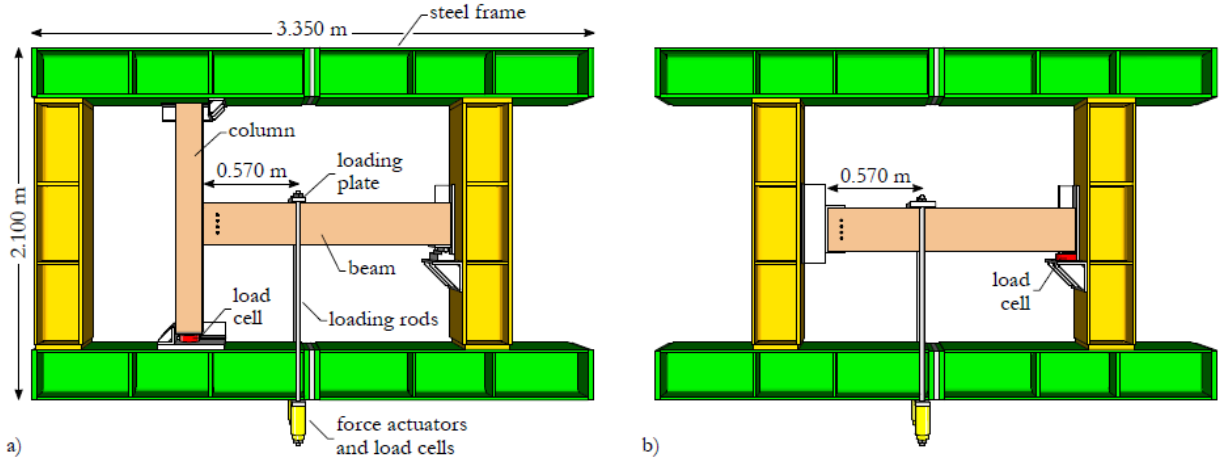

Figure 2.27. Test set-ups: a) beam-to-column connections (same as for fire resistance test); b) beam side connections [Adopted from 51]

Table 2.5. Estimated and experimental load-carrying capacities of the connections tested at normal temperature [Adopted from 51]

Connection typology	Experimental load-carrying capacity				Estimated load-carrying capacity [d]	
	Test values $R_{exp,i}$ [kN]	Mean value $R_{exp,mean}$ [kN]	Characteristic value [c] $R_{exp,k}$ [kN]	Failure mode	Characteristic value $R_{est,k}$ [kN]	Failure mode
A.1	51.5; 55.1; 48.0	52 (7%) [b]	44	Splitting	27	Splitting
A.1-X [a]	51.2	51 (n.a.)	n.a.	Splitting	27	Splitting
A.4	66.8; 62.4; 65.2	65 (3%)	55	Shear	n.a.	n.a.
A.5-X [a]	39.3	39 (n.a.)	n.a.	Splitting	29	Splitting
A.6	52.5; 57.5; 65.6	59 (11%)	50	Splitting	42	Splitting
B.1	31.5; 31.6; 34.1; 35.4; 36.9	34 (5%)	30	Splitting	23	Splitting
B.2	42.4; 45.8; 49.1; 46.0; 50.3	47 (7%)	41	Dowel (failure mode 2)	46	Dowel (failure mode 2)
C.1	62.4; 72.3; 71.1	69 (8%)	58	Shear/dowel (failure mode 2)	55	Splitting
C.2	88.3; 93.7; 86.0	89 (4%)	76	Dowel (failure mode 3)	63	Dowel (failure mode 3)
D.1	60.3	60 (n.a.)	n.a.	Screws (withdrawal)	n.a.	n.a.

[a] Entire beam-to-column connections (not only the beam side, as in the other tests); failed on the beam side.
[b] Coefficient of variation between parentheses.
[c] According to EN 14358:2006.
[d] According to EN 1995-1-1:2004.

After analysing his results, he drew the following conclusions,

- Timber members end loaded in the direction perpendicular to the grain by steel-to-timber connections with dowels in double shear can exhibit ductile and brittle failures.
- Connection' failures in the direction perpendicular to the grain limited the load-carrying and deformation capacities of the connections.
- The loaded edge distance of the most distant fastener (h_e) appeared to be the most relevant parameter.
- The reinforcement with self-tapping screws was effective at delaying the splitting failure, increasing the connections' load-carrying and deformation capacities.

All specimen tested at ambient temperature were examined at elevated temperature while loaded between 23% to 39% of the connections' tested ambient load capacities as shown in Table 2.6.

From the elevated temperature test, it was observed that as charring from the sides was mostly prevented in the column-members, the heat damage to the column side came mostly from top and bottom the header plate, directly affecting the outermost nails in withdrawal and the compression zone under the header plate, allowing it to rotate. Also, the charring of the end surface of the beam was much more substantial for a 20 mm gap than for a 10 mm gap, which is mostly comparable to that of a 0 mm gap. The connection reinforced with self-drilling screws (A.4) exhibited a fire resistance 5 minutes shorter than the corresponding unreinforced connection (A.1).

Table 2.6. Results of the fire resistance tests [Adopted from 51]

Connection		Tests at normal temperature	Fire resistance tests			
			Applied load	Displacement	Fire resistance	Failure mode
		$R_{20°C,mean}$ [a]	E_{fi}	$d_{t=tfi}$	t_{fi}	
Typology	Specimen	[kN]	[kN]	[mm]	[min]	
A.1	A.1.F-1	51.5	$15.3 = 0.30 \cdot R_{20C,mean}$	13.9	38.7	Column side
	A.1.F-2		$15.4 = 0.30 \cdot R_{20C,mean}$	12.5	44.1	Beam side
A.2	A.2.F-1		$15.4 = 0.30 \cdot R_{20C,mean}$	16.7	32.2	Column side
	A.2.F-1		$15.4 = 0.30 \cdot R_{20C,mean}$	15.7	34.0	Column side
A.3	A.3.F-1		$15.5 = 0.30 \cdot R_{20C,mean}$	9.0	48.0	Beam side
	A.3.F-1		$15.5 = 0.30 \cdot R_{20C,mean}$	11.0	46.8	Beam side
A.4	A.4.F-1	64.8	$19.4 = 0.30 \cdot R_{20C,mean}$	11.6	38.8	Beam side
A.5	A.5.F-1	39.3	$15.4 = 0.39 \cdot R_{20C,mean}$	18.3	37.8	Column side
A.6	A.6.F-1	58.5	$15.6 = 0.27 \cdot R_{20C,mean}$	10.4	76.6	Beam side
	A.6.F-2		$15.5 = 0.26 \cdot R_{20C,mean}$	18.4	82.8	Beam side
B.1	B.1.F-1	33.9	$9.4 = 0.28 \cdot R_{20C,mean}$	11.9	49.0	Beam side
	B.1.F-3		$9.5 = 0.28 \cdot R_{20C,mean}$	11.7	43.4	Beam side
B.2	B.2.F-1	46.7	$14.0 = 0.31 \cdot R_{20C,mean}$	14.1	43.3	Beam side
	B.2.F-2		$13.9 = 0.30 \cdot R_{20C,mean}$	13.5	44.5	Beam side
C.1	C.1.F-1	68.6	$20.5 = 0.30 \cdot R_{20C,mean}$	9.1	44.4	Beam side
	C.1.F-2		$20.6 = 0.30 \cdot R_{20C,mean}$	10.0	41.8	Beam side
C.2	C.2.F-1	89.3	$20.6 = 0.23 \cdot R_{20C,mean}$	14.1	77.6	Beam side
	C.2.F-2		$20.6 = 0.23 \cdot R_{20C,mean}$	13.1	72.8	Beam side
D.1	D.1.F-1	60.3	$18.1 = 0.30 \cdot R_{20C,mean}$	11.4	34.0	Connector

[a] Mean value of the experimental load-carrying capacity (beam side).

In conclusion Palma [51] stated that;

- The tested connection types of steel-to-timber dowelled connections reached more than 30 and even 60 minutes of fire resistance, for cross sections with 160 X 260 mm^2 and 240 X 340 mm^2, respectively, for degrees of utilisation E_{fi}=R20°C,$_{mean}$ between 0.23 and 0.39.
- Most connections failed after extensive embedment deformations in the beam side of the connection. He explained that aspects such as a wider gap between the beam and the

column and the presence of reinforcement with self-tapping screws showed a negative influence on the fire resistance and seemed to have induced premature embedment failures, after the wood between dowels was heated charred, especially in the case of the tested connections with 8 mm dowels. However, this spacing was dependent on the fastener diameter, which also affected the heat transfer into the cross section, and embedment failures were observed in connections with 8mm and 12 mm dowels. Therefore, it was unclear whether increasing the fastener spacing in the direction perpendicular to the grain would effectively increase the fire resistance.

- The failure mode at normal temperature and the dowel diameter did not seemed to have affected the fire resistance, indicating that the thickness of the side members and the degree of utilisation were more relevant. Moving the group of fasteners closer to the unloaded edge, therefore increasing the splitting resistance at normal temperature, exposed the lowermost fastener to higher temperatures earlier than if it was further away from the edge. This negative effect seemed to compensate the increased initial load-carrying capacity at normal temperature.

Based on the results of research performed by Ali and hadjisophocleous [3] and Boadi and Hadjisophocleous [50] on the different types of timber hybrid connection (concealed, exposed and seated), it can be said that even though concealed connections are aesthetically pleasing, they do not perform as good as the other types of connection in the case of fire as a result of reduced cross section due to the notch. The outcome of these research also shows that the seated connection performed better as compared to exposed and concealed connection, as a result of the absence of bolt. It happened that the bolt heats up very quickly and chars the surrounding wood leading to

earlier failure time in fire. The research reviewed in this report showed that the lesser the applied load ratio, the better the connections' failure time in fire. [3][50][51]. Palma varied different parameters to arrive at acceptable fire-resistant ratings for some of his beam-column shear tested connections [51]

Geyloff [49] investigated the ambient behavior of moment resisting hybrid connections and realised that the combined use of large diameter bolts and significantly reduced edge distances increased the tendency of splitting. Petrycki [4] made use of self tapping screws to help reduce the tendency of splitting occurring at a moment resisting connection. However, he recorded failure times below 20 minutes when his connections were tested in fire. He mentioned that the gap between the beam and column contributed to the earlier failure time which confirms Padro's discussion on his gap between beam and column. Petrycki also observed that increasing the bolt rows from two to three had an increase in the connection's moment capacity and failure time in fire [4]

Therefore, the research presented in this report focuses on investigating ways to improve the structural performance of moment- resisting concealed connection involving glulam beam and a supporting steel column. The effect of bolt pattern and bolt number were investigated to better understand how bolts affect the moment resistance and failure time in fire. Steel bolts and plates were fully protected with wood plugs, to reduce the transfer of heat from the steel components to the inner core of the wood section which affects the connections' failure time in fire. Also, a relatively larger section was used to account for the effect of reduced cross section. The beams were connected to the steel column such that there were zero gaps. Furthermore, all connections presented in this study were designed with adequate bolt spacing to avoid the earlier occurrence of splitting during the ambient and elevated temperature tests

3 EXPERIMENTAL PROGRAM

The experimental part of this study consisted of several full-scale ambient temperature and elevated temperature tests. The test assembly was composed of a 1600 mm long glulam wood beam connected to a supporting steel column (W shape).

3.1 Materials

3.1.1 Glulam beam

All glulam beams utilised in this study were manufactured from black spruce and had dimensions of 184 mm x 364 mm, with a stress grade of 24f-EX and architectural finish grade which is made up of 25 mm x 50 mm laminations. Table 3.1 shows the specific strengths of the glulam sections.

Table 3.1. Glulam section properties

Property	**Value**
Compression parallel to grain (MPa)	33.0
Compression perpendicular to grain (MPa)	7.5
Tension parallel to grain (MPa)	20.4
Longitudinal shear (MPa)	2.2
Flexural bending (MPa)	30.7
Modulus of elasticity (MPa)	2.2

3.1.2 Steel column and T-stub connectors

All glulam beam sections were connected to a 300W grade 200 mm x 200 mm steel column (Figure 3.1) with a flange and web thickness of 6 mm and 4 mm, respectively, using concealed steel T-

stubs fabricated from 300W grade steel using a 12.7-mm thick plate. The connections were secured to the column using four fully threaded 19.1-mm diameter rods. One end of the steel rods was welded to the face of the steel T-stub that flashes with the cross section of the beam to prevent creating notches at the cross section of the beam as a result of the presence of the bolt nuts. The other end of the steel rods was connected to the steel column using nuts. The concealed steel connector was inserted into the slotted cut of the glulam beam section (Figure 3.2). Depending on the test, four or six 19.1-mm diameter A325M high-strength steel bolts were used to secure the beam. A tolerance of 2 mm was used for both, the bolt holes and the slotted cuts.

Figure 3.1. Supporting steel column

Figure 3.2. Concealed steel plate inserted into glulam beam

3.2 Test Details

Fifteen assemblies were tested, five at ambient temperature and ten at elevated temperatures. The tests were conducted to investigate the effect of bolt number and bolt pattern on the load capacity for the ambient tests and the failure time for the fire tests. The connections were divided into two groups based on bolt number: four bolts and six bolts. For each group, two bolt patterns were considered. In one pattern, two rows of bolts, each with two bolts, were symmetrically positioned near the top and bottom sides of the beam cross section. While in the other bolt pattern, the bottom bolt row was shifted upwards to be located at the mid height of the beam section so it can contribute to the moment-resisting capacity of the connection. All test assemblies describe above were repeated with the same bolt arrangement however the bolts and steel plates were protected with glued-in wood plugs. The wood plugs used to cover the bolt heads and the top and bottom of the steel plate, and nuts had thicknesses of 30 mm and 20 mm, respectively (Figure 3.3). All beam to column connections required that a vertical slotted cut be made in each beam section using a portable bandsaw. A slotted cut of about 15-mm wide was prepared at the center of the beam cross section to accommodate the steel plate, allowing a clearance of 1 to 2 mm, as per CSA 086-14. Two test assemblies were prepared with the beam connected to the steel plate using four bolts in

two rows (Figure 3.4(a)). Another two tests assemblies were made with the beam connected with the same number of bolts but, with the bottom bolt row shifted upwards to be located at the mid-height of the beam section (Figure 3.4(b)). The expectation is that at this location the bolts will end up in the top tensile stress zone of the beam cross section and contribute to the moment-resisting capacity of the connection. Four beams were prepared using six bolts and following the same bolt configuration and bolt spacing as described above for four bolts. Table 3.2 below summarizes the test matrix for this research. Seven other beams were prepared for protected connection configuration. Three with four bolts arranged in pattern one (Figure 3.4(c)), two with six bolts in pattern one, and one each prepared for pattern two of four and six bolts.

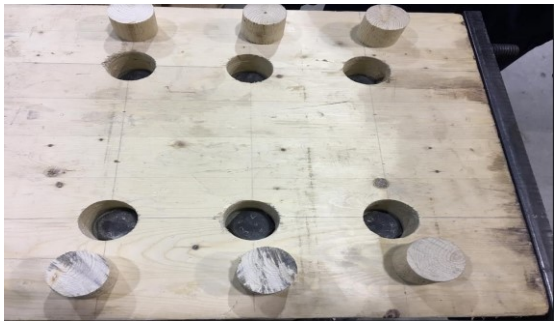

Figure 3.3. 30 mm thick wood plugs for the bolt heads

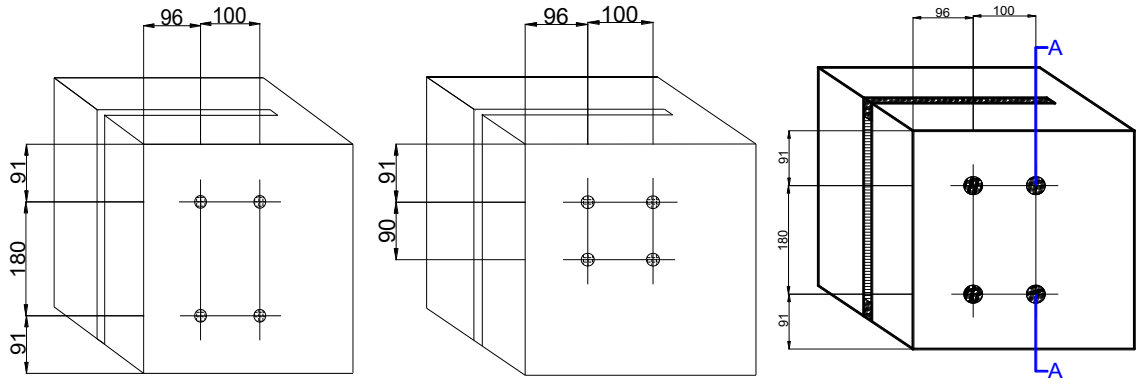

(a) Pattern one unprotected *(b) Pattern two unprotected* *(c) Pattern one protected*

Figure 3.4. Connection configurations with four bolts

Table 3.2. Test matrix

Test No.	Number of bolts	Bolt position	Protection	Test Type	Number of tests
$4BP1NA_1$	4	1	Not Protected	Ambient	1
$4BP2NA_1$	4	2	Not Protected	Ambient	1
$6BP1NA_1$	6	1	Not Protected	Ambient	1
$6BP2NA_1$	6	2	Not Protected	Ambient	1
$4BP1PA_1$	4	1	Protected	Ambient	1
$4BP1NF_1$	4	1	Not Protected	Fire	1
$4BP2NF_1$	4	2	Not Protected	Fire	1
$6BP1NF_1$	6	1	Not Protected	Fire	1
$6BP2NA_1$	6	2	Not Protected	Fire	1
$4BP1PF_1$	4	1	Protected	Fire	1
$4BP2PF_1$	4	2	Protected	Fire	1
$6BP1PF_1$	6	1	Protected	Fire	1
$6BP2PF_1$	6	2	Protected	Fire	1
$4BP1PF_2$	4	1	Protected	Fire	2
$6BP1PF_2$	6	1	Protected	Fire	2

3.3 Ambient Temperature Tests

The ambient experiments presented in this research were conducted at Lakehead University's Civil Engineering Structures Laboratory. Each glulam beam was fixed to a steel column at one end using a T-stub steel connector that was attached to the supporting steel column. A point load was applied

1400 mm away from the beam support using a Universal Testing Machine (UTM) as shown in Figure 3.5. During testing, the deflections of the beam in response to the gradually increased loading were measured using two Linear Variable Differential Transformers (LVDTs): one was located 200 mm from the support; and the other at the location where the load was applied, near the free end of the beam. All test specimens were loaded until the beam-to-column assembly failed.

Figure 3.5. Ambient test setup

All four connection types were designed for yielding, splitting and row shear out, according to CSA 086-14. All connection types were governed by splitting failure.

3.4 Elevated Temperatures Tests

3.4.1 Fire test furnace

The elevated temperature tests were conducted at Lakehead University's Fire Testing and Research Laboratory (LUFTRL) at Thunder Bay campus, Ontario. The laboratory shown in Figure 3.6, accommodates a large custom-designed furnace with two natural-gas fed burners that can raise the furnace' temperature up to 1300°C. The furnace compartment is housed within a large steel

loading frame (Figure 3.7). The furnace is made from strengthened heavy-steel plated walls that are lined with thick Fiberfrax blankets from inside. The furnace large door and the roof can be removed using the 1-ton jib crane installed in the facility. Additional vents on the furnace's floor and roof are present to facilitate the access of instrumentation and set up of experimental assemblies. These features of the furnace allowed for tests conducted at elevated temperatures to follow a similar experimental setup and methodology as that used during ambient temperature testing.

Figure 3.6. Lakehead University Fire Testing and Research Laboratory (LUFTRL).

Figure 3.7. Large fire testing furnace accommodated at LUFTRL.

Thermal measurements were required to be captured during the fire resistance test. Temperature data of the furnace compartment was used to control the furnace temperature to follow the standard time-temperature curve, or any other desired curve, using a computer system built into the furnace control panel. (Figure 3.8).

Figure 3.8. Human-Machine Interface (HMI) touch screen of the furnace's control panel

3.4.2 The thermocouples

For fire resistance tests, the connection configuration with no fire protection, labelled (N), had twelve metal-shielded K-type thermocouples (TC) installed at different locations: four TC from the beam front face (TC1 through TC4), six from the beam back face, one from the beam top side (TC11) and one from the beam bottom side (TC12), as shown in Figure 3.9. The figure also indicates the depth (mm) at which each TC was embedded inside the wood section. For instance, TC1 and TC2 were installed at a depth of 60 mm from the beam front face; TC3 and TC4 were at 20 mm depth from the beam front face; TC7 and TC8 at 40 mm depth; and TC9 and TC10 10 mm depth. TC5 and TC6 were employed to measure the steel plate temperatures, whereas, TC11 and TC12 measured the temperature of one of the top bolts and one of the bottom bolts, respectively. For the connection configuration with fire protection, labelled (P), fourteen metal-shielded K-type thermocouples (TC) were used: six were installed from the beam front face and eight from the beam back face, TC5 and TC6 measured the steel plate temperatures. TC11 and TC12 measured the temperatures of the bolt nuts underneath the 20 mm thick wood plug; whereas TC13 and TC14 measured the temperatures of the bolt heads underneath the 30 mm thick wood plug (Figure 3.10).

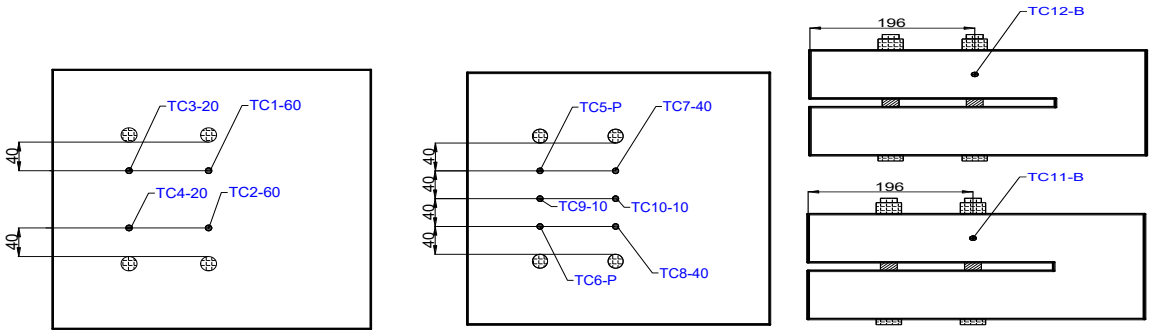

(a) Pattern one

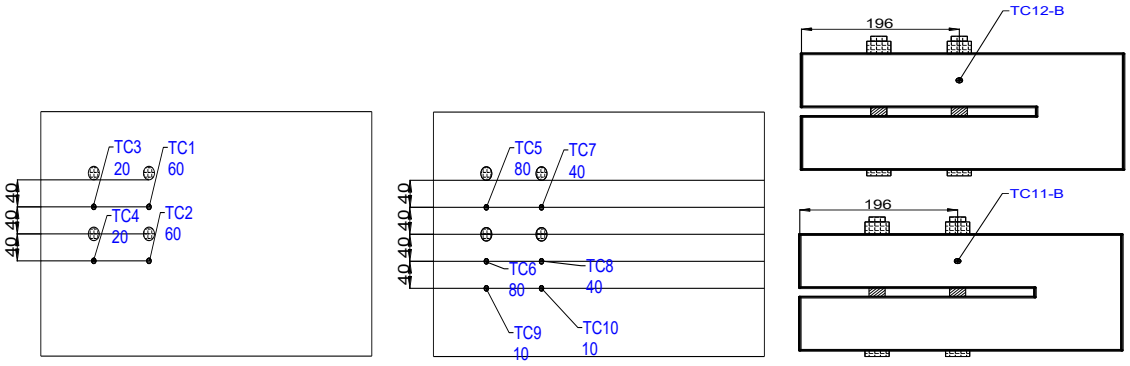

(b) Pattern two

Figure 3.3.9. Typical thermocouple layout for unprotected connection of 4 bolts

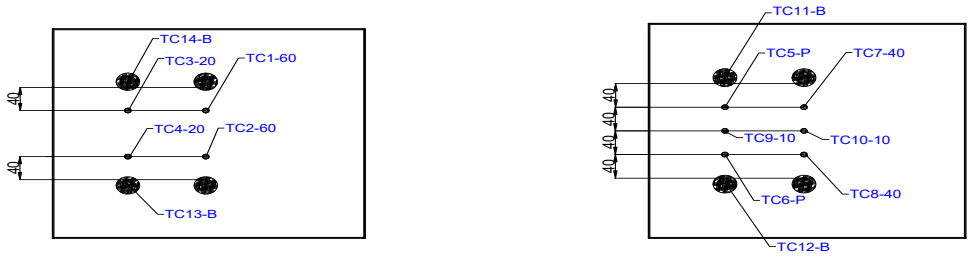

Figure 3.10. Typical thermocouple layout for protected connection of 4 bolts

3.4.3 Fire tests setup and procedure

The supporting steel column and the top side of the glulam beams were protected using a 25 mm thick ceramic-fibre blanket. Figure 3.11 shows a specimen inside the test furnace. The failure criterion used for the fire tests was based on the beam deflection. Failure was assumed to occur when the beam deflection at 1400 mm from the support reached a magnitude corresponding to a beam rotation of 0.1 radians. The fire test continued beyond this point until the beam could not sustain any load increase. One low-thermal elongation ceramic rod was placed vertically through a small hole in the roof of the furnace and was attached to a displacement transducer that was installed outside the furnace to allow the measurement of the beams vertical displacement 200 mm from the beam supporting column, as shown in Figure 3.11.

As discussed earlier, twelve metal-shielded K-type thermocouples (TC) were connected to each test specimen at several locations of the beam connection. Thermocouples were inserted at different depths of the beam section to determine the temperature variations due to heat transfer with time. The measured temperatures were used to determine the average charring rate of the beam. The charring rate could not be determined using the residual wood, because by the time that the furnace could safely open there was total burnout of the beam. The temperatures measured at the top and bottom steel bolts were used to determine how the bolts contributed to the heat transfer within the wood section.

Figure 3.11. Fire resistance test setup inside LUFTRL's furnace

3.4.4 Applied loads

For the fire tests, the test assemblies were subjected to CAN/ULC-S101 standard fire and loaded to 100% of the ultimate design load capacity of the weakest connection configuration. For the purpose of this study, all connection configurations were loaded with 100% splitting failure load (Ultimate capacity) of the weakest connection determined by Cl. 12.4.4.7 from the Canadian Wood Design Handbook (2015)-CSA 086-14 (Equations 2.6 to 2.8). This load is higher than the actual loading in fire as suggested by the Eurocode.

This load was maintained on the test assembly over the course of the fire exposure period until the assembly met the required failure criterion. Based on Equation 3.1 to 3.3, the following design calculation for the connection configuration of four bolt position one was used to determine appropriate loading for the specimens.

$$QS_{i=}14t\sqrt{\frac{de}{1-\frac{de}{d}}} = 14 \times 85\sqrt{\frac{271}{1-\frac{271}{362}}} = 39.07kN \qquad \textbf{Equation 3.1}$$

t = 85mm (thickness of member)

de=d-ep (effective depth)

where;

d = 362 (depth of member)

ep =91 (unloaded edge distance)

$$QSri = 0.7 \times 39.07 = 27.35\ kN \qquad \textbf{Equation 3.2}$$

$$QSrT = \Sigma(QSri) = 2 \times 27.35 = 54.7kN \qquad \textbf{Equation 3.3}$$

Once the splitting resistance was determined, the load required to generate a moment equivalent to the tensile force causing splitting failure was determined as follows;

The couple moment between the compression and tension zone is equal to the force acting along one axial direction times the moment arm which was 271 mm for all connections.

$$Mi = QSrT * L = 54.7 * 271 * 10^{-6} = 14.8\ kNm \qquad \textbf{Equation 3.4}$$

4 RESULTS AND DISCUSSION

For each test assembly, the vertical displacements measured using the installed LVDTs were used to calculate the gradual change in the angle of rotation of the beam-to-column connections. The data collected from the ambient and elevated temperatures tests were analysed in terms of failure loads, failure modes and connection rotations. In addition, for the fire resistance tests, the average charring rates and temperatures with respect to time were analysed.

4.1 Ambient Temperatures Tests

Table 4.1 lists the failure load and the corresponding maximum moment-resisting capacity of each of the two test assemblies.

The maximum moment capacity of each connection configuration was pre-determined by adapting the clauses and equations in CSA 086-14 in conjunction with principle mechanics equations using a moment arm of 1400 mm, which is the distance from the beam end at the interface of the beam-to-column connection to the point where the transverse load was applied.

Table 4.1. Summary of ambient tests results

Connection Bolt Pattern	**Failure Load (kN)**	**Max Moment (kN.m)**	**Maximum Rotation (Rad)**	**Mode of Failure (Analytical)**	**Mode of Failure (Experimental)**
4BP1NA$_1$	18.9	26.5	0.013	Splitting	Splitting
4BP2NA$_1$	36.3	50.9	0.047	Splitting	Splitting/eventual row shear out
4BP1PA$_1$	17.7	24.8	0.017	Splitting	Splitting
6BP1NA$_1$	31.4	44	0.015	Splitting	Splitting
6BP2NA$_1$*	38.2	53.5	0.023	Splitting	-

* the 6BP2 was not loaded to failure due to the failure of the steel column during the ambient test.

4.1.1 Effect of bolt pattern on the connection's rotational behavior

It was noticed that the beam connection configuration with the four bolts arranged in pattern two (4BP2NA$_1$), where the bottom row of bolts was raised to the mid-height of the beam section, supported a maximum moment of about 92% greater than that of the connection configuration with the four bolts arranged in pattern one (4BP1NA$_1$), where each of the two rows of bolts were symmetrically placed along the depth of the beam section, each 91 mm from the corresponding beam top and bottom side. Figure 4.1 shows the moment-rotation relationship developed in the two beam (4BP1NA$_1$ and 4BP2NA$_1$) end connections during the experiments at ambient temperature. The beam connection of bolt pattern one (4BP1NA$_1$) failed by splitting occurring at the top row of the bolts with a maximum rotation recorded at 0.013 rad, hence a sudden drop in the connection moment-resisting capacity occurred, as shown in Figure 4.1. However, the beam

connection was still able to sustain the load that was gradually increased after the sudden drop until another wood split developed in the bottom row of the bolts, Figure 4.2(a). For the other beam connection with the four bolts arranged in pattern two ($4BP2NA_1$), the connection's rotations increased with increased loading until the top row of bolts experienced a noticeable split, Figure 4.2(b). With increased loading, the bolts in the bottom row started to yield, and eventually this caused row shear out in the wood, Figure 4.2(c). It is worth mentioning that the yielding of the bolts in the bottom row of $4BP2NA_1$ contributed to the considerable increase in the connection's maximum moment that was about 92% greater than that of the other connection configuration with bolt pattern one ($4BP1NA_1$), Figure 4.2. It is also worth mentioning that all connection failure modes, represented in Figures 4.2(a), (b) and (c), have been predicted analytically.

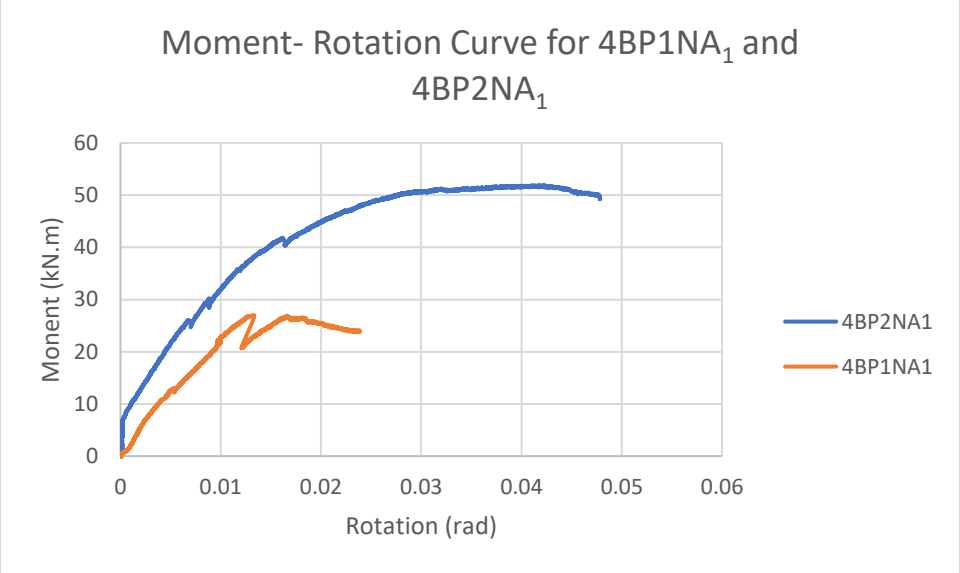

Figure 4.1. Moment-rotation relationships of the beam connections $4BP1NA_1$ and $4BP2NA_1$ tested at ambient temperature

(a) 4BP1NA$_1$ connection

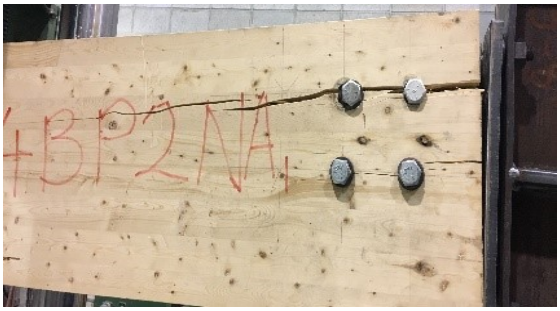

(b) 4BP2NA$_1$ connection

(c) bolt yielding in connection 4BP2NA$_1$

Figure 4.2. Failure modes of the four-bolt connections tested at ambient temperature

4.1.2 Effect of bolt number on the connection's rotational behavior

Figure 4.3 shows the moment-rotation relationships developed in the two beam end connections during the ambient temperature tests. The beam connection of bolt pattern one (4BP1NA$_1$) failed by splitting occurring at the top row of the bolts with a maximum rotation recorded at 0.013 rad, hence a sudden drop in the connection moment-resisting capacity occurred, as shown in Figure 4.1. For the other beam connection with six bolts arranged in pattern one (6BP1NA$_1$), the connection's rotations experienced a relatively higher moment rotation recorded at 0.015 before a noticeable split occurred at the top bolt row as shown in Figure 4.4. It was observed that the beam connection configuration with the six bolts arranged in pattern one (6BP1NA$_1$), where the bolts were arranged symmetrically along the beam section, sustained a maximum moment of about 66% greater than that of the connection configuration with the four bolts arranged in the same pattern

(4BP1NA$_1$). It is worth mentioning that the addition of a bolt column to the connection configuration with four bolts, increased the capacity by 66% in ambient temperature.

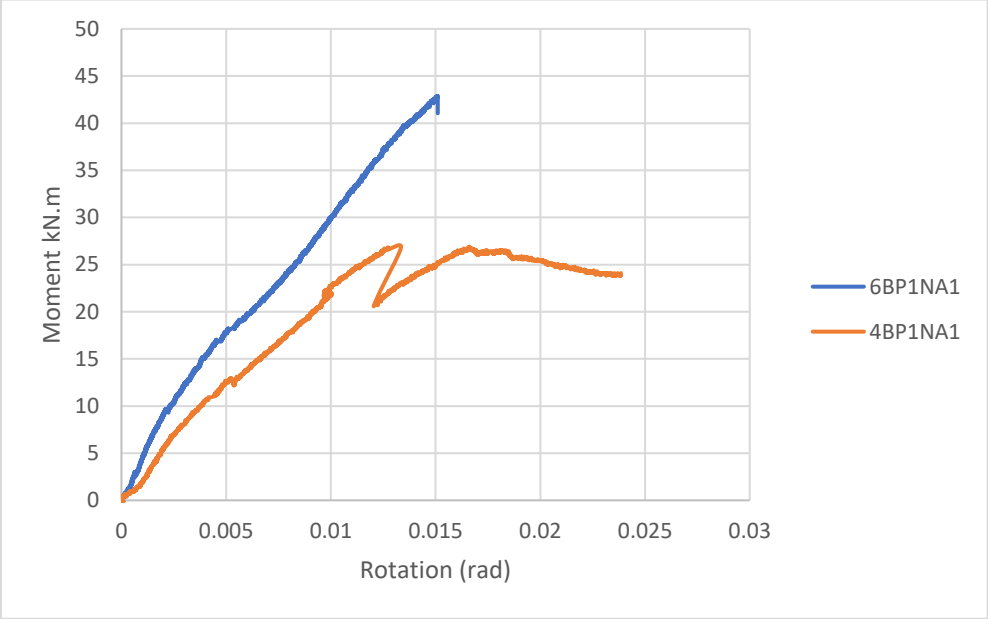

Figure 4.3. Moment-rotation relationships of the beam connections 4BP1NA$_1$ and 6BP1NA$_1$ tested at ambient temperature.

Figure 4.4. Failure mode of connection with six bolts tested at ambient temperature

4.1.3 Effect of protection on the connection's rotational behavior

Table 4.1. lists the connections' failure loads and their maximum moment-resisting capacities. It was noticed that the beam connection configuration with no protection ($4BP1NA_1$), where the steel plate and bolts were exposed, exerted a maximum moment that was 7% greater than that of the connection configuration where the steel plate and bolts were protected. This is due to the wood section reduction caused by embedding the bolts' heads and nuts into the glulam beam cross section in the protected connection configuration ($4BP1PA_1$).

Figure 4.5 shows the moment-rotation relationship obtained for the two connection configurations ($4BP1NA_1$ and $4BP1PA_1$) tested at ambient temperature. The beam connection without protection failed mainly by wood splitting which occurred at the top row of the bolts with a rotation recorded at 0.012 rad. Hence, a sudden drop in the connection moment-resisting capacity happened, as shown in Figure 4.5. However, the beam connection was still able to sustain the applied load, that was gradually increased at a rate of 2.0 kN per minute, after the sudden drop until another wood split developed at the bottom row of the bolts, as shown in Figure 4.6(a). For the other beam connection configuration with protection ($4BP1PA_1$), the rotation increased linearly with the gradually increased load until the connection experienced a sudden drop due to splitting of the top row of bolts under tensile stresses, Figure 4.6(b). With increased loading, the top row of bolts started to exhibit row shear out. It is worth mentioning that the reduction in the beam section effective width due to the circular notches created to accommodate the bolt heads and nuts in connection configuration ($4BP1PA_1$) contributed to the reduction in the moment-resisting capacity of this connection configuration compared to the connection configuration ($4BP1NA_1$), with no fire protection, which had moment-resisting capacity that was about 7% greater than that of

configuration (4BP1PA$_1$). It can also be said that both connection configurations exhibited brittle failure modes, such as splitting and row shear out, as shown in Figure 4.6.

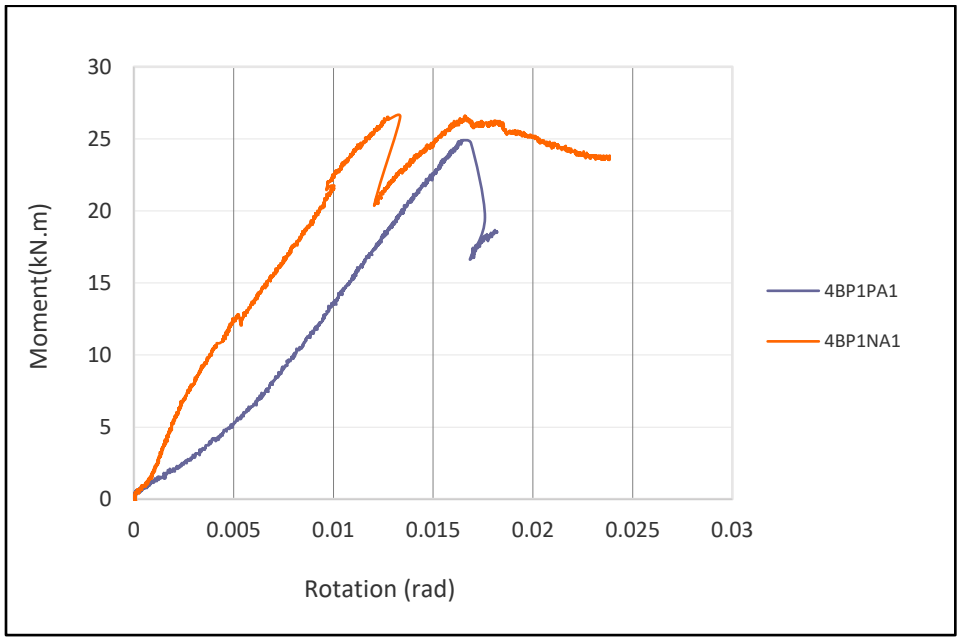

Figure 4.5. Moment-rotation relationships of the beam connection configurations with protection (4BP1PA$_1$) and without protection (4BP1NA$_1$)

(a) 4BP1NA$_1$ *(b) 4BP1PA$_1$*

Figure 4.6. Failure modes of the beam connection configurations in ambient temperature tests

4.2 Elevated Temperatures Tests

A total of 10 beam to column connections involving eight different configurations were tested for fire, test for connection configuration of four bolts and for six bolts. To confirm the results, two tests were repeated for the connection configurations with the best failure time for both connections of four (4) and six (6). The failure time, failure mode, charring rate, rotation behavior and time-temperature behavior are discussed in this section. Table 4.2 shows a summary of the results.

4.2.1 Failure time and mode

- Unprotected Connections

Table 4.2 summarizes the results of the ten fire tests. The table shows that the failure time of the unprotected connection configuration with bolt pattern one ($4BP1NF_1$) was 33.0 minutes, which is one minute more than that of the connection configuration of bolt pattern two ($4BP2NF_1$). However, the failure times of the connections with 6 bolts show that pattern two ($6BP2NF_1$) experienced a time to failure that is 5 minutes more than that of position one ($6BP1NF_1$). When considering the effect of bolt number on the same pattern, it can be seen from Table 4.2 that the connection configuration of four bolts performed better than that of six bolts with a difference of 11 and 5 minutes for position one and two respectively. It was also observed during the fire tests that both beam connections of four bolts began to experience slight wood splitting and row shear at the top bolt row which lead to the failure of the connections, Figure 4.7(a). However, the connection configuration with six bolts experienced a sudden split thereby increasing the rate of rotation which lead to a failure time that is less than that of the connection configuration with four bolts, Figure 4.7(b). It was noticed that splitting increased heat transfer into the wood core and hence reduced the overall fire resistance time of the connections with six bolts ($6BP1NA_1$ and

6BP2NA$_1$). As shown in Figure 4.7(b), splitting occurred along the glued line plane of the glulam beam.

(a) Connection of four bolts; 4BP1NA$_1$ (left) and 4BP2NA$_1$ (right)

(b) Connection of six bolts; 6BP1NA$_1$ (left) and 6BP2NA$_1$ (right)

Figure 4.7. Unprotected Connection's failure modes in fire test

- Protected Connections

From Table 4.2 connection configuration with protected bolts and steel plate arranged in pattern one, experienced the best failure time. therefore, the experiment was repeated for 4BP1PF$_1$ and 6BP1PF$_1$ for connection configuration of four (4) bolts and six (6) bolts respectively.

The table shows that the average failure time of the connection configuration with bolt pattern one (4BP1PF$_1$ and 4BP1PF$_2$) was 49.0 minutes, which is one minute more than that of connection

configuration of bolt pattern two ($4BP2PF_1$). The failure times of the connections with 6 bolts show that pattern one ($6BP1PF_1$) experienced an average time to failure that is 14 minutes more than that of position one ($6BP2PF_1$). When considering the effect of bolt number with the same pattern, it can be seen from Table 4.2 that the connection configuration of four bolts performed better than that of six bolts with a difference of 7 minutes and 8 minutes for pattern two ($4BP2PF_1$ and $6BP2PF_1$) and first test of pattern one ($4BP1PF_1$ and $6BP1PF_1$) respectively. However, the opposite happened when the pattern one tests were repeated, with the $6BP1PF_2$ exhibiting a failure time that is 20 minutes more than that of $4BP1PF_2$. When considering the failure mode, Figure 4.8 shows that all splitting occurred at the glue line plane that is aligned with the bolt rows. It was observed during the fire tests that both beam connections of four bolts ($4BP1PF_1$ and $4BP2PF_1$) began to experience wood split at the top bolt row which lead to the failure of the connections, Figure 4.8(a). However, the connection configuration with six bolt ($6BP1PF_1$) experienced a sudden split at the top and bottom row bolt (Figure 4.8(b)), thereby increasing the rate of rotation which lead to a failure time that is less than that of the connection configuration with four bolts, Figure 4.8(a). The connection configuration $6BP2PF_1$ experienced a complete split at the second row of bolts, which was along the glued plane, about 40 minutes into the test which lead to an unexpected failure. It was noticed that splitting increased heat transfer into the wood core and hence reduced the overall fire resistance time of the connections with six bolts ($6BP1PA_1$ and $6BP2PA_1$). It can be mentioned that the alignment of bolts with the glued line plane, also plays a role in the connection's failure time. This is because the repeated test for 4 bolts arranged in pattern one failed earlier due to an unexpected split at the glue line plane, whereas the repeated test for six bolts arranged in pattern one lasted longer in fire as a result of its gradual rotation with time.

(a) Connection of four bolts; 4BP1PF$_1$ (left) and 4BP2PF$_1$ (right)

(b) Connection of six bolts; 6BP1PF$_1$ (left) and 6BP1PF$_2$ (right)

Figure 4.8. Protected Connection's failure modes in fire test

4.2.2 Charring rate

The ten beam connections tested were completely burnout by the time the furnace was cooled down and opened. Therefore, there was no residual glulam sections to be used to determine the average charring rate. However, using Equation 4.1 along with the thermal measurements captured using the thermocouples installed at depths of 10 mm and 20 mm into the glulam section, the average charring rate was determined.

$$C = \beta t \qquad \text{Equation 4.1}$$

Where;

C is 10mm

t is the difference between the times the thermocouples at 10 mm and 20 mm depth reached 300 °C.

From Table 4.2 all connections experienced a notional charring rate that exceed the purported value of 0.7 mm/min employed by the Wood Design Manual 2015 (CSA-086-14, Table B.42). This is because the 0.7 mm/min used by CSA-086-14 is based on having a minimum residual section of 70 mm. When the residual minimum dimension is reduced to less than 70 mm, the charring rate increase as the temperature rise beyond the char front meets in the middle of the member. It is worth mentioning that for this study, the residual section of each wood side member was less than 70 mm hence contributing to the higher charring rates. A possible source of error that contributes to the variation of the charring rates is the location of the tip of the thermocouple. Although the hole was drilled to match the required depth, the thermocouple tip may have not reached the bottom of the hole due to the very low clearance between the hole and thermocouple diameter.

Table 4.2. Summary of fire resistance tests results.

Connection Bolt Pattern	**Applied Moment (kN.m)**	**Time to Failure (min)**	**Charring Rate (mm/min)**	**Failure Mode**
$4BP1NF_1$	14.8	33.0	0.73	Splitting/row shear
$4BP2NF_1$	14.8	32.0	0.82	Splitting/row shear
$4BP1PF_1$	14.8	56.0	0.9	Splitting
$4BP1PF_2$	14.8	42.0	0.96	Splitting
$4BP2PF_1$	14.8	48.0	1.0	Splitting
$6BP1NF_1$	14.8	22.0	0.81	Splitting
$6BP2NF_1$	14.8	27.0	0.8	Splitting
$6BP1PF_1$	14.8	48.0	1.03	Splitting
$6BP1PF_2$	14.8	62.0	0.85	Splitting/row shear
$6BP2PF_1$	14.8	41.0	0.77	Complete splitting

4.2.3 Connection rotations

It was observed during the fire tests that the 10 beam-to-column connection configurations underwent similar trends of increased rotations with time. All ten connection configurations experienced very slight linear increase in rotation values early in the fire tests; however, the rotation values increased exponentially after about 20 minutes and 40 minutes into the fire test, for the unprotected and protected connections respectively.

- Unprotected Connections

(a) Effect of bolt pattern on the connection's rotational behavior

(i) Four bolts

It was observed that although the connection's moment-resisting capacity and rotations were significantly affected by the bolt pattern in ambient temperature tests, there was almost no effect on the connection's rotation values for the connection configurations of the two bolt patterns ($4BP1NF_1$) and ($4BP2NF_1$) in the fire resistance tests as shown in Figure 4.9.

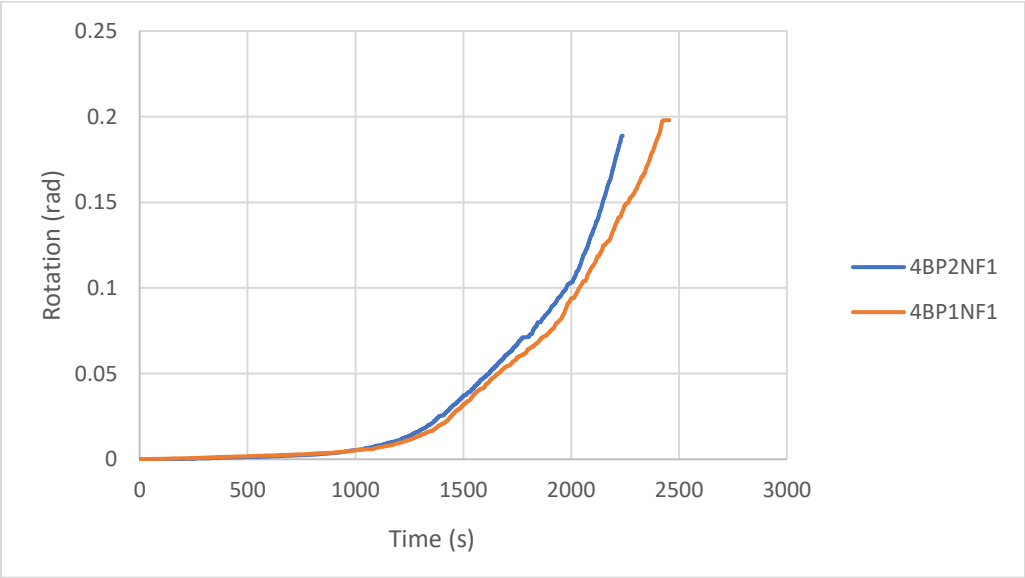

Figure 4.9. Time-rotation relationships of the beam connections 4BP1NF$_1$ and 4BP2NF$_1$ tested at elevated temperatures

(ii) Six bolts

When considering the six bolt connections, it was noticed that both connections exhibited the same time rotation trend for about nineteen (19) minutes, after which the configuration with the bolts arranged symmetrically along the beam (6BP1NF$_1$) experienced a steeper exponential increase as compared to that of the connection configuration with the bottom row bolt arranged at the mid height (6BP2NF$_1$), Figure 4.10. It was also observed that the connection 6BP1NF$_1$ underwent a sudden split about nineteen (19) minutes into the test thereby increasing the rotation and reducing the failure time.

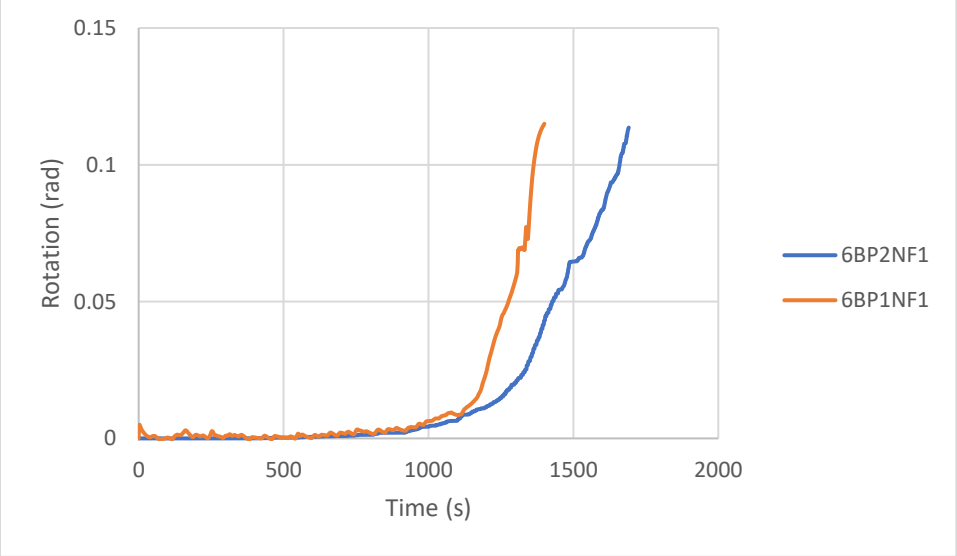

Figure 4.10. Time-rotation relationships of the beam connections 6BP1NF$_1$ and 6BP2NF$_1$ tested at elevated temperatures

(b) Effect of bolt number on the connection's rotational behavior

The connection configuration with four bolts behaved better than that with six bolts which was the case for both bolt patterns one and two. This is likely due to the increase in heat transfer through

the bolts, which increases the rate of rotation and chances of splitting, and hence reducing the time to failure of the connections with six bolts.

(i) Pattern one

It was observed that although the moment-resisting capacity of connection $6BP1NF_1$ was 66% greater than that of $4BP1NF_1$ in ambient temperature the opposite occurred when the two connection types were exposed to the standard fire. Both connections, $6BP1NF_1$ and $4BP1NF_1$ experienced similar time -rotation trend for about 20 minutes after which the former rotated rapidly leading to a failure time that is 11 minutes less than latter, Figure 4.11.

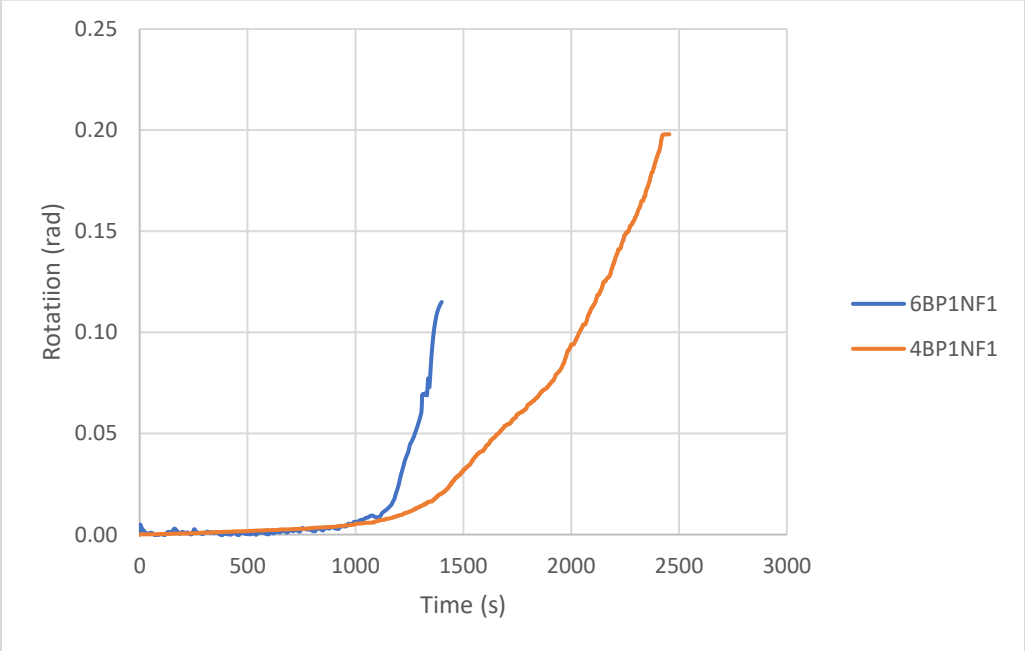

Figure 4.11. Time-rotation relationships of the beam connections $4BP1NF_1$ and $6BP1NF_1$ tested at elevated temperatures

(ii) Pattern two

Similarly, the rotation of connection configuration of bolt pattern two, both six and four bolts configurations exhibited similar trends for about twenty minutes into the test. However, after 20 minutes the rotation of connection configuration with six bolts ($6BP2NF_1$) increased faster than the rotation with four bolts ($4BP2NF_1$), as shown in Figure 4.12. Therefore, the connection $4BP2NF_1$ exhibited a failure time which is ten (10) minutes more than that of connection $6BP2NF_1$.

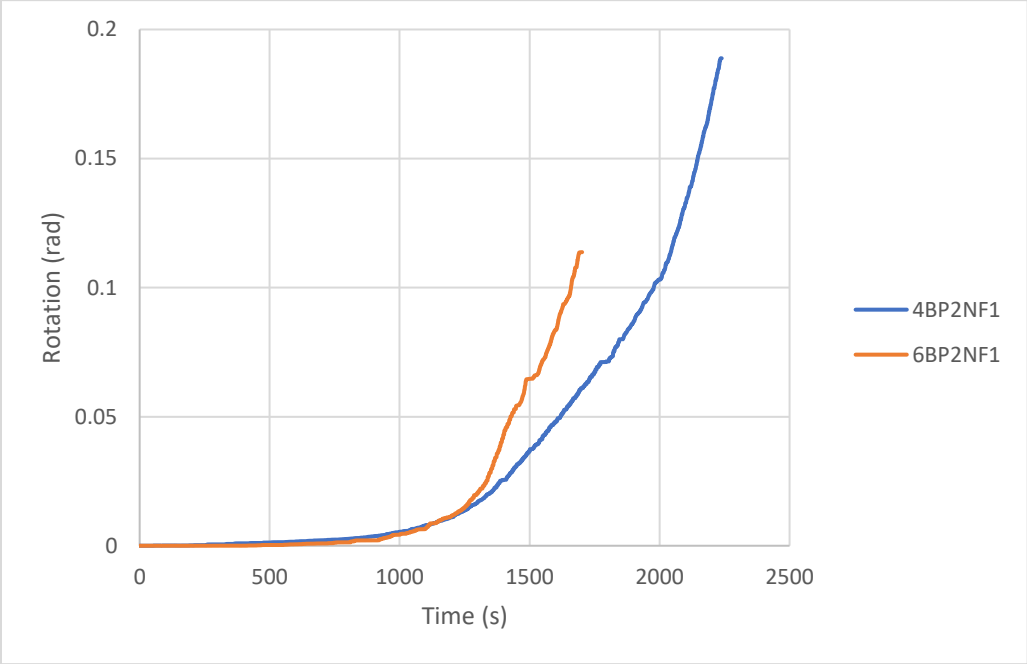

Figure 4.12. Time-rotation relationships of the beam connections $4BP2NF_1$ and $6BP2NF_1$ tested at elevated temperatures

- Protected Connections

(a) Effect of bolt pattern on the connection's rotational behavior

(i) Four bolts

From Figure 4.13, beam configurations $4BP1PF_1$ and $4BP2PF_1$ experienced a linear increase in rotation for about 40 minutes however the former had a higher slope than the latter. After 40 minutes the connection configuration with pattern two experienced a rapid exponential increase that led to a failure time that is 8 minutes less than that of $4BP1PF_1$. It can be mentioned that the $4BP2PF_1$ underwent a significant splitting failure along the glue line plane as shown in Figure 4.8(a) while the connection configuration with $4BP1PF_1$ experienced a gradual failure.

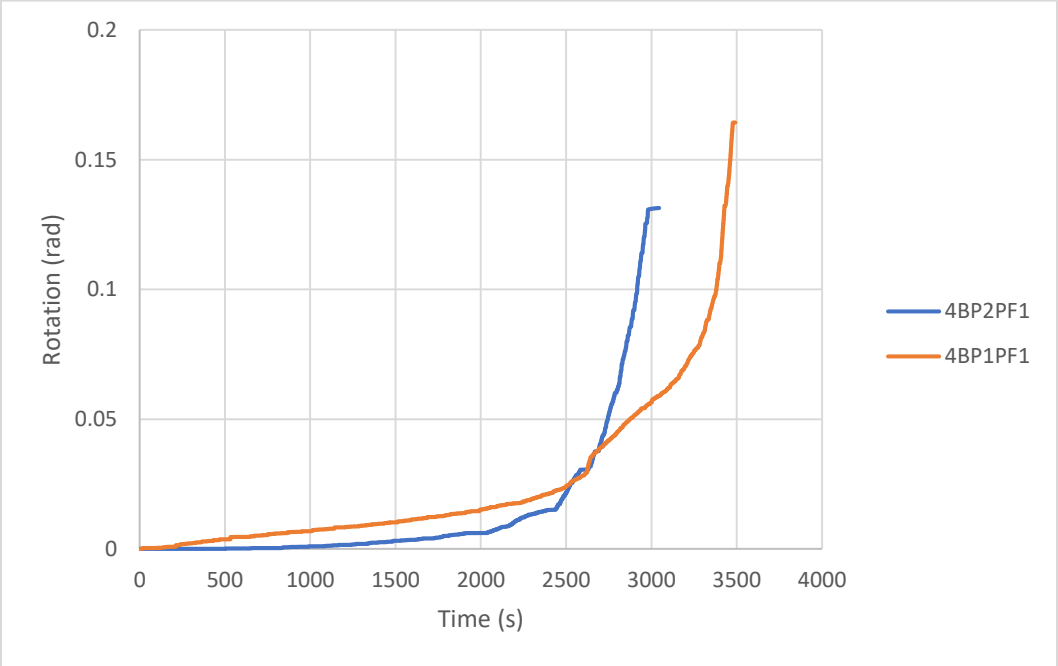

Figure 4.13. Time-rotation relationships of the beam connections $4BP1PF_1$ and $4BP2PF_1$ tested at elevated temperatures

(ii) Six bolts

From Figure 4.14, the rotation of beam configuration $6BP1PF_1$ and $6BP2PF_1$ underwent a linear increase for about 35 minutes, after which the rotation of connection configuration with pattern two ($6BP2PF_1$) experienced an extremely rapid increase. This rapid increase is a result of a sudden

split occurring along the whole beam length, at the second row of bolts which was also in line with a glue line plane. This led to a failure time for 6BP2PF$_1$ that is 6 minutes less than that of 6BP1PF$_1$.

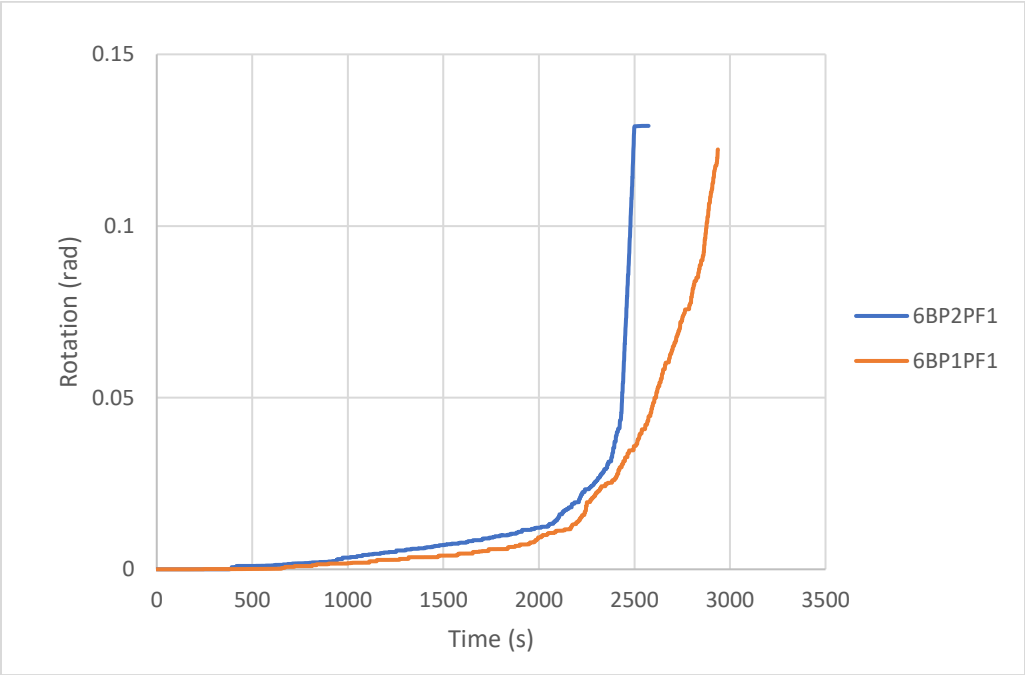

Figure 4.14. Time-rotation relationships of the beam connections 6BP1PF$_1$ and 6BP2PF$_1$ tested at elevated temperatures

(b) Effect of bolt number on the connection's rotational behavior

(i) Pattern one

When considering pattern one, the configuration with four bolts had a better failure time which was eight (8) minutes more than that of the 6 bolts. It was also observed that the connection with six (6) bolts failed by significant splitting along both the top and bottom row of bolts which resulted in an earlier exponential increase of rotation (Figure 4.15). However, the connection configuration of four (4) bolts failed by a minor splitting at the top of row bolt.

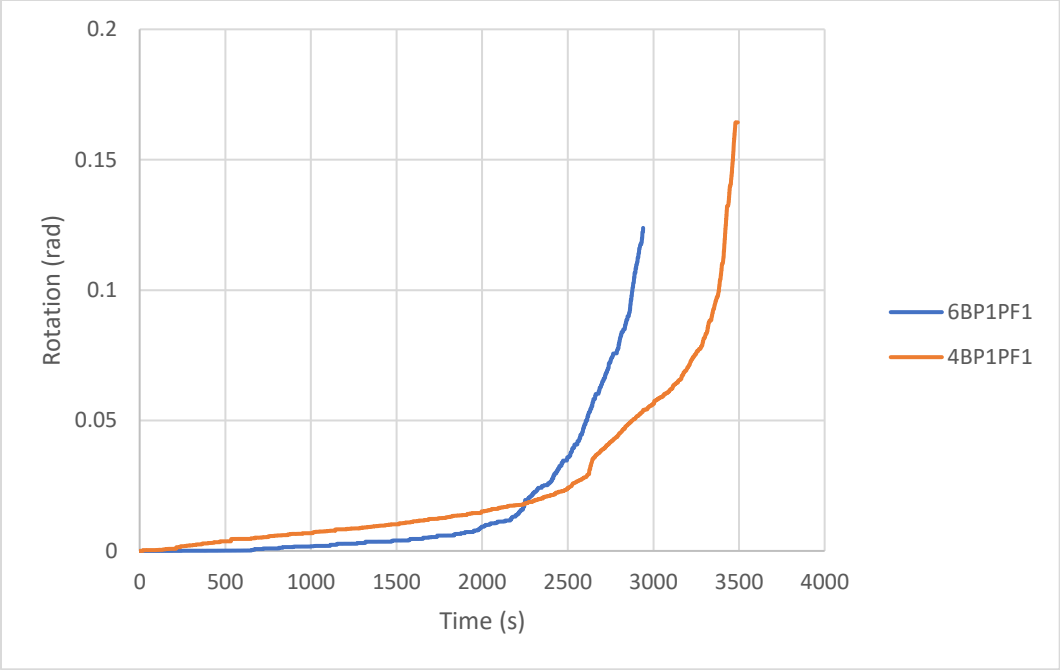

Figure 4.15. Time-rotation relationships of the beam connections 6BP1PF$_1$ and 4BP1PF$_1$ tested at elevated temperatures

(ii) Pattern two

Similar to pattern one, the configuration with four bolts had a higher failure time which was seven (7) minutes more than that of the 6 bolts. From Figure 4.16, it can be mentioned that the connection configuration of six bolt underwent a higher rate of rotation as compared to that of the connection configuration of four bolts. It was also observed that the connection with six (6) bolts failed by complete splitting at the second row of bolts along the beam length. However, the connection configuration with four (4) bolts failed by a splitting at the top row of bolts.

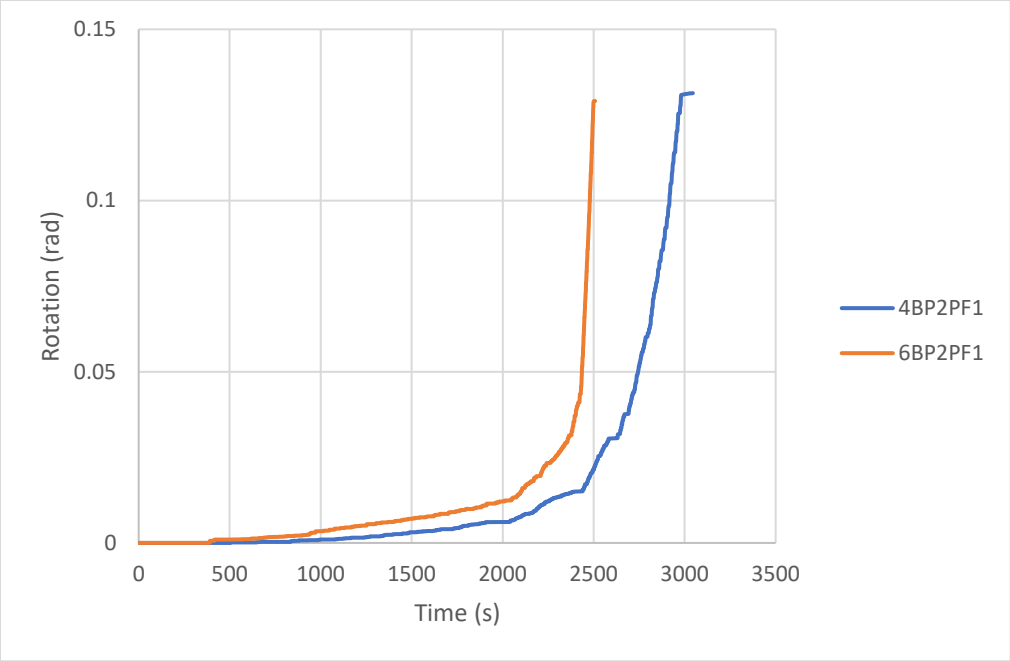

Figure 4.16. Time-rotation relationships of the beam connections 6BP2PF$_1$ and 4BP2PF$_1$ tested at elevated temperatures

- Comparison between protected and unprotected connections

(a) Four bolts arranged in pattern one

Figure 4.17 shows that all three tests conducted for position one with four bolts exhibited a similar linear rate of rotation for about 20 minutes, after which the unprotected connection (4BP1NF$_1$) experienced an exponential increase leading to a failure time that is about nine (9) and twenty three (23) shorter than that of the protected connections 4BP1PF$_2$ and 4BP1PF$_1$, respectively. This is attributed to the fact that, the protected bolts did not experience significant increase in temperature at the early stage of the fire test, hence there was no charring of the inner core of the wood section, which resulted in much less rotations of the protected connection configurations (4BP1PF$_1$ and 4BP2PF$_2$). This confirms that in the case of fire, the steel components of a connection heat up faster and cause char in the core of the wood section which increases to the rate of rotation and decreases the failure time. The two protected connections (4BP1PF$_1$ and 4BP1PF$_2$) continued to

have a similar linear increase for thirty minutes, after which the second test (4BP1PF$_2$) experienced a split at the glue line plane in line with the top row of bolts, leading to a time to failure that is fourteen minutes (14) less that that of 4BP1PF$_1$.

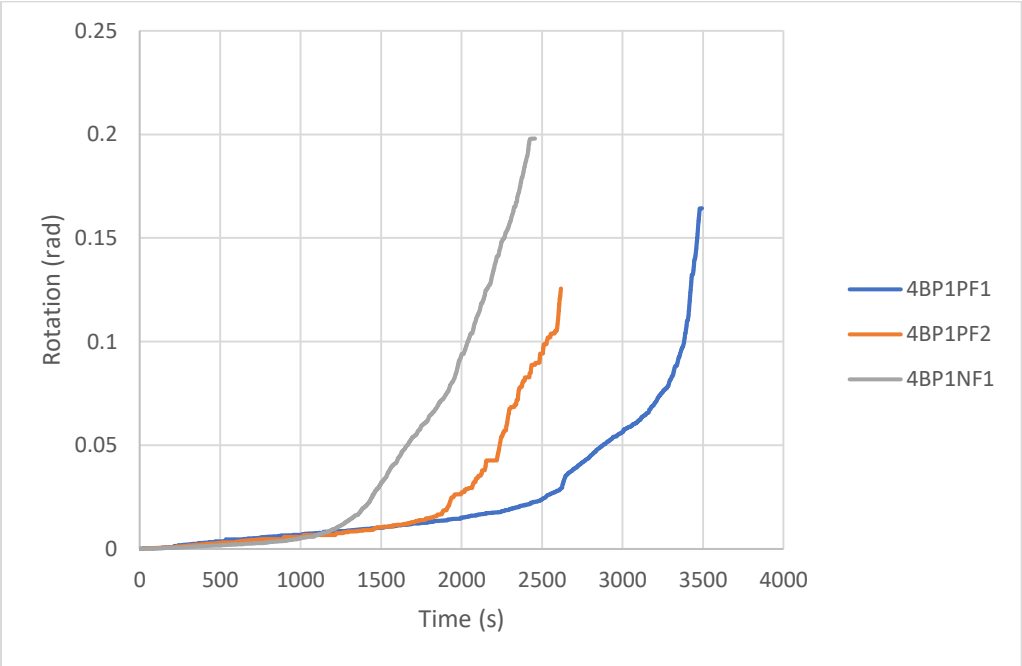

Figure 4.17. Time-rotation relationships of the beam connections 4BP1PF$_1$,4BP1PF$_2$ and 4BP1NF$_1$ tested at elevated temperatures

(b) Six bolts arranged in pattern one

Figure 4.18 shows that all six bolt connection experienced a linear increase in rotation for about sixteen (16) minutes, after which the unprotected connection experienced an exponential increase leading to a failure time that is about twenty six (26) minutes less than (6BP1PF$_2$) and forty (40) less than 6BP1PF$_1$. The earlier exponential increase of rotation of the unprotected connection is due to the increased heat transfer to the wood core caused by the bolts and steel plate. The two protected connections (6BP1PF$_1$ and 6BP1PF$_2$) experienced a similar linear increase for thirty seven (37) minutes, after which the first test (6BP1PF$_1$) experienced a split at the glue line plane

in line with the top row of bolts, leading to a time to failure that is fourteen minutes (14) less than that of 6BP1PF$_2$. Similar to the four bolts arranged in pattern one, it can also be mentioned from these results that the difference in failure time depends on the protection of the steel bolt and plates, and whether the bolts are aligned with the glued plane of the glulam.

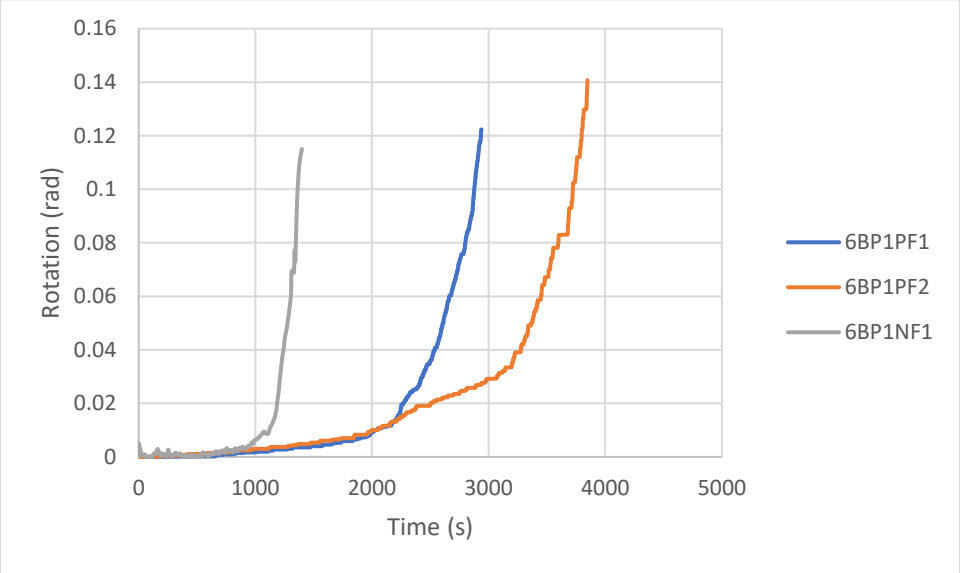

Figure 4.18. Time-rotation relationships of the beam connections 6BP1PF$_1$, 6BP1PF$_2$ and 6BP1NF$_1$ tested at elevated temperatures

(c) Four bolts arranged in pattern two

Figure 4.19 shows the time-rotation relationships of the two beam connection configurations of four bolts arranged in pattern two, during the fire tests. Both connection configurations had rotations that increased linearly during the first 14 minutes of the tests followed by an exponential rise that started in the connection configuration with no protection (4BP2NF$_1$). Similar to the pattern one connection configuration, the protected bolts did not experience significant increase in temperatures at the early stage of the fire test, hence there was no charring of the inner core of the wood section, which resulted in much less rotation of the connection configuration (4BP2PF$_1$)

leading to a longer failure time. The time to failure of the protected connection ($4BP2PF_1$) was about sixteen 16 minutes less than that of the unprotected connection ($4BP2NF_1$).

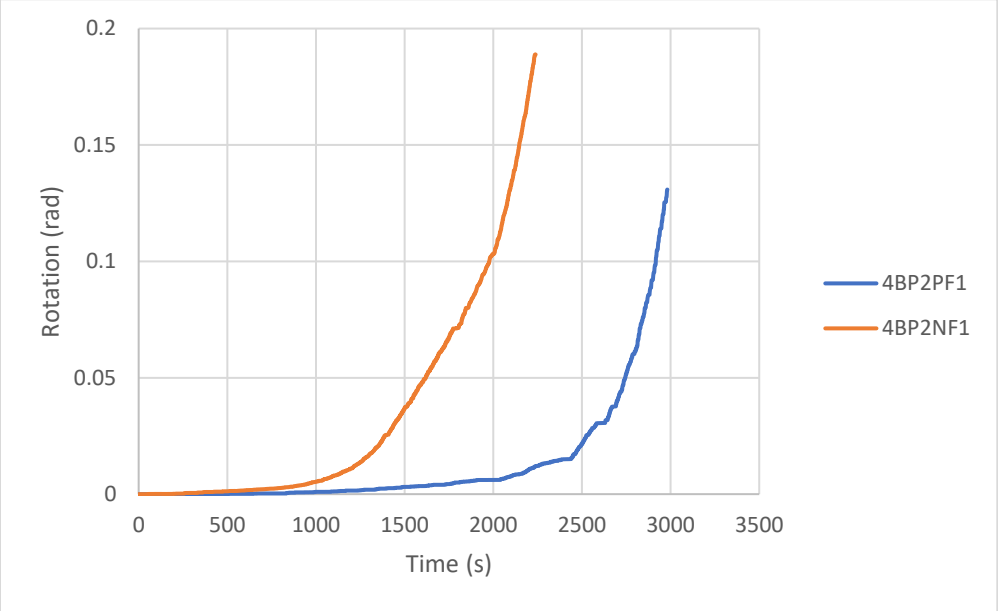

Figure 4.19. Time-rotation relationships of the beam connections $4BP2PF_1$ and $4BP2NF_1$ tested at elevated temperatures

(d) Six bolts arranged in pattern two

The time-rotation relationships of the two beam connection configurations of six bolts arranged in pattern two, during the fire tests is shown in Figure 4.20. Both protected and unprotected connection configuration had rotations that increased linearly during the first seventeen (17) minutes of the tests followed by an exponential rise that started in the connection configuration with no protection ($6BP2NF_1$). The time to failure of the protected connection ($6BP2PF_1$) was about fourteen (14) minutes less than that of the unprotected connection ($6BP2NF_1$).

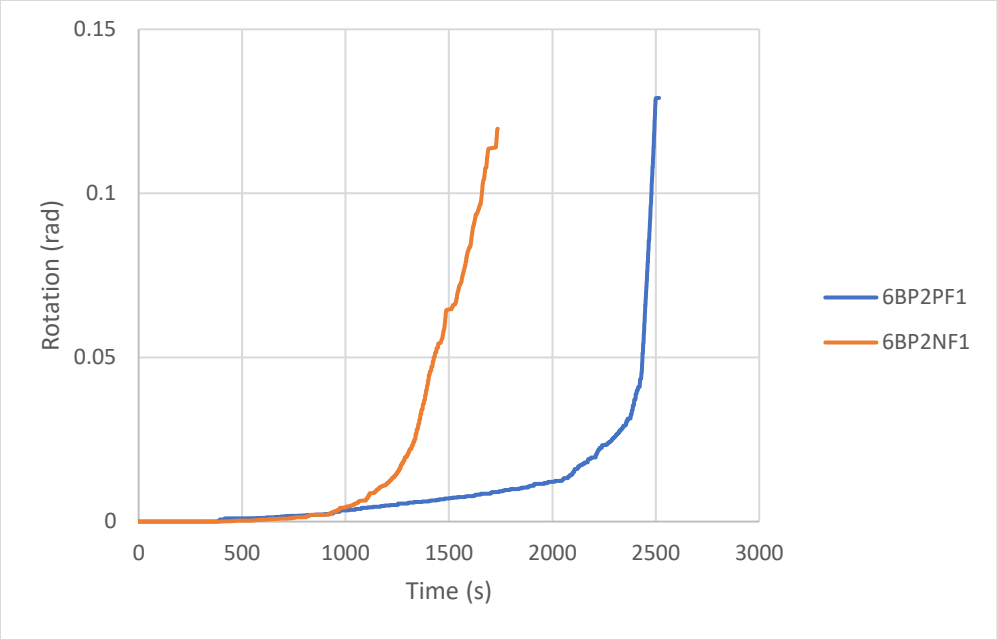

Figure 4.20. Time-rotation relationships of the beam connections 6BP2PF$_1$ and 6BP2NF$_1$ tested at elevated temperatures

4.2.4 Time-temperature curves

- Unprotected Connections

Figure 4.21 shows all the thermal measurements recorded during the fire resistance tests of the four unprotected beam connections (4BP1NF$_1$, 4BP2NF$_1$, 6BP1NF$_1$ and 6BP2NF$_1$). As shown in the figure, wood temperatures, at 20 mm depth from the beam front face (measured by TC3 and TC4), reached 100°C after about 5 minutes from the commencement of the test. At this stage, the moisture trapped in the wood section started to evaporate, and consequently the wood started to pyrolyze and eventually char when it reached a temperature of 300°C, at about 12 to 17 minutes. From the time-temperature curves shown in Figure 4.21, it can also be observed that, at the time of the connection's structural failure, the thermocouples at 20 mm depth from the beam face (TC3 and TC4) had recorded temperatures way beyond the wood charring temperature, above 800°C; and the thermocouples at 40 mm depth from the beam face (TC7 and TC8) recorded temperatures

around 200°C. The thermocouples embedded at 60 mm depth from the beam face (TC1 and TC2) recorded temperatures of around 100°C.

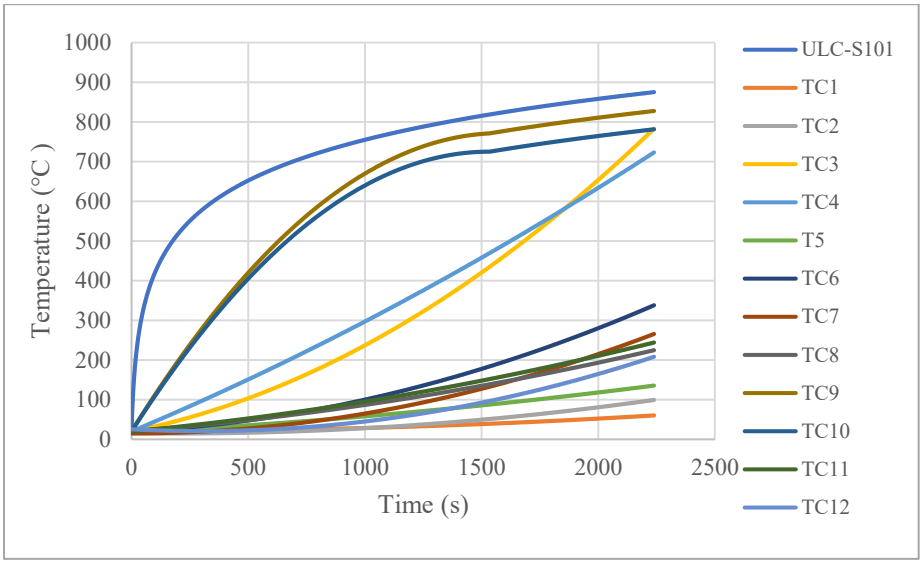

(a) Unprotected connection of 4 bolts arranged in pattern one (4BP1NF1)

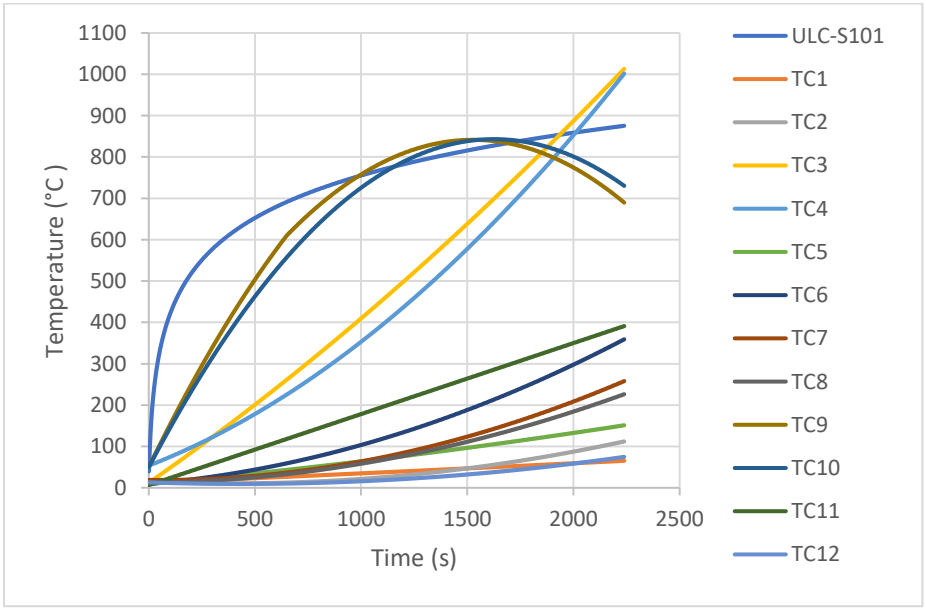

(b) Unprotected connection of 4 bolts arranged in pattern two (4BP2NF1)

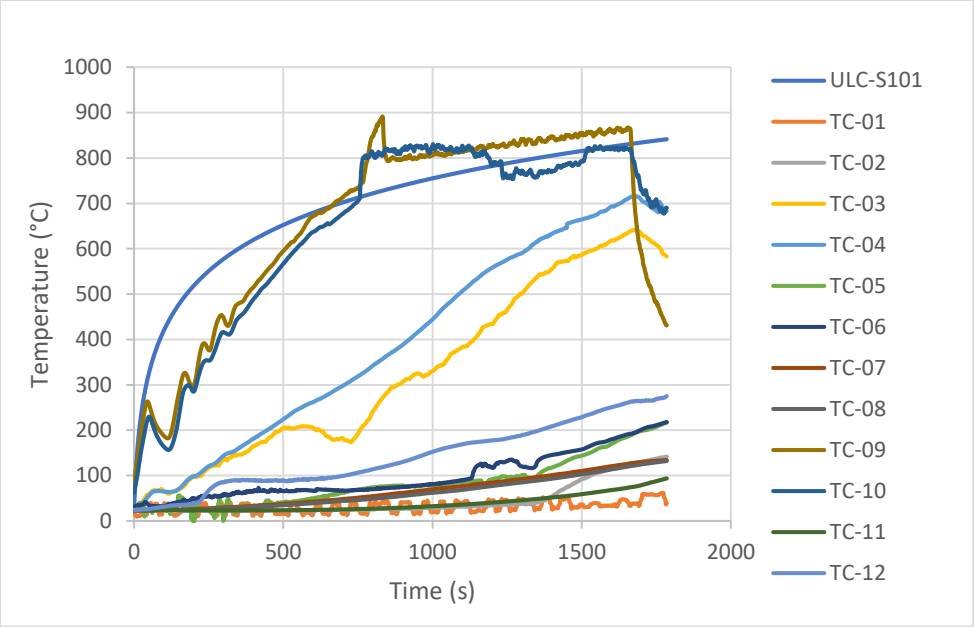

(c) Unprotected connection of 6 bolts arranged in pattern one ($6BP1NF_1$)

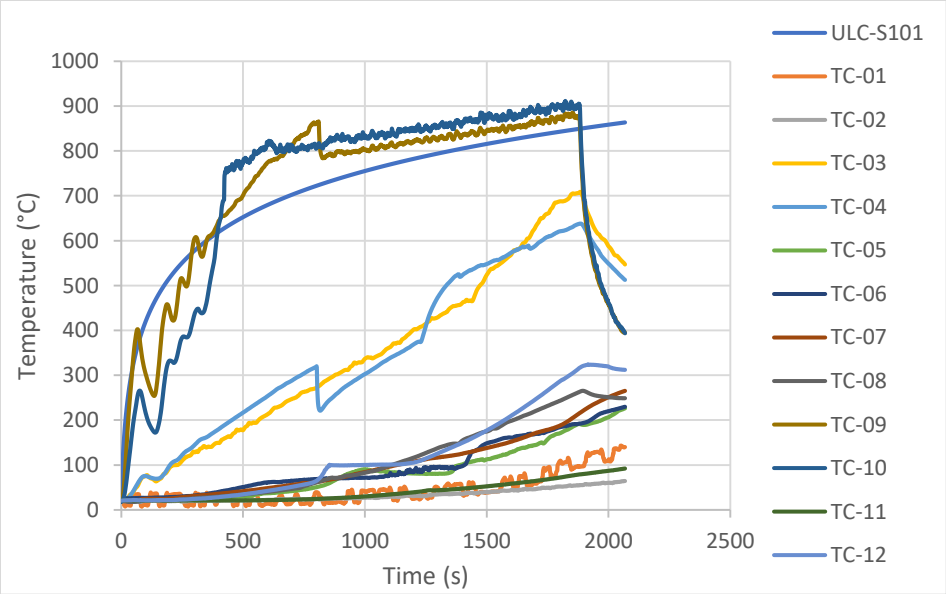

(d) Unprotected connection of 6 bolts arranged in pattern two ($6BP2NF_1$)

Figure 4.21. Time-temperature curves of unprotected connections

- Protected Connections

The thermocouples located at different depths of the protected glulam section ($4BP1PF_1$, $4BP1PF_2$, $4BP2PF_1$, $6BP1PF_1$, $6BP1PF_2$, $6BP2PF_1$) behaved very similar to that of the unprotected connections. However, the thermocouples TC-11 and TC-12 measuring the temperatures of the bolt nut (with 20 mm protection), and the thermocouples TC-13 and TC-14 measuring the temperatures of the bolt head, showed significant change in temperatures. The temperatures recorded by the thermocouple TC-11 and TC-12 about 20 minutes into the test. Whereas the thermocouples TC-13 and TC-14 exhibited an exponential increase about 30 minutes into the test. It is worth mentioning that the wood plug protection minimized the transfer of heat through the bolts and hence resulted in a failure time of the protected connections that is about an average of 20 minutes more than that of the unprotected connection (Figure 4.22).

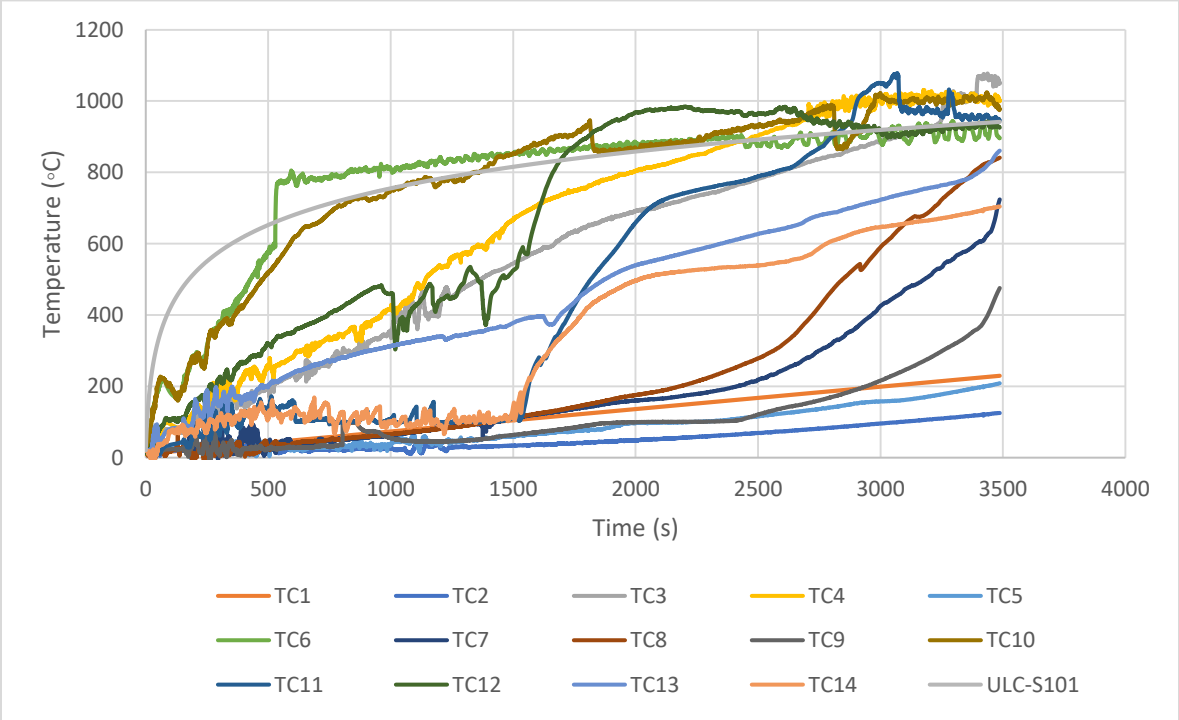

(a) First test of protected connection of 4 bolts arranged in pattern one ($4BP1PF_1$)

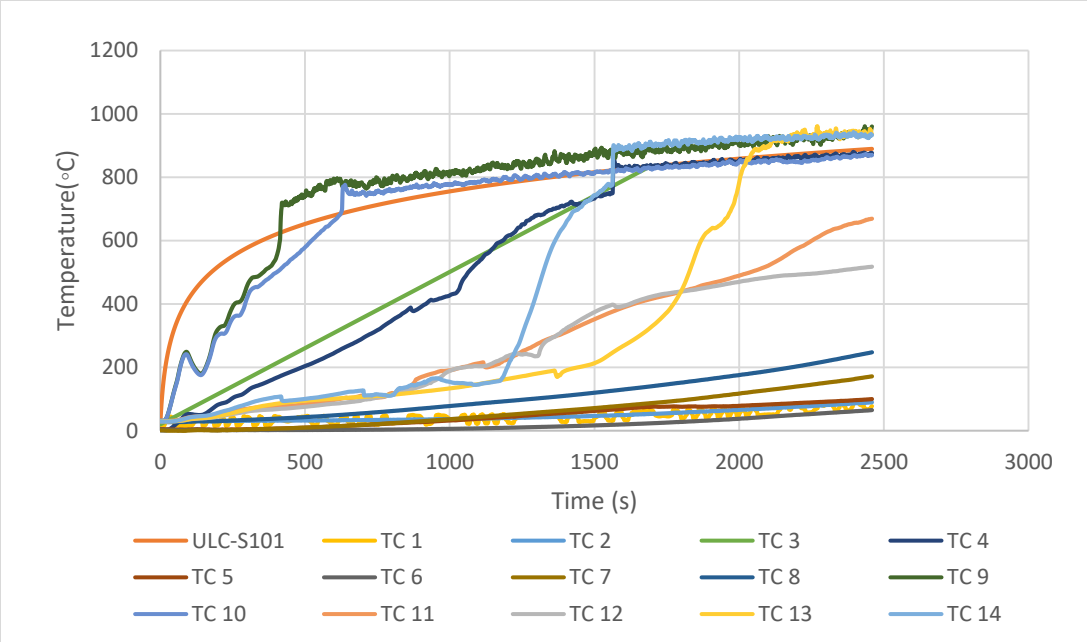

(b) Second test of Protected connection of 4 bolts arranged in pattern one (4BP1PF₂)

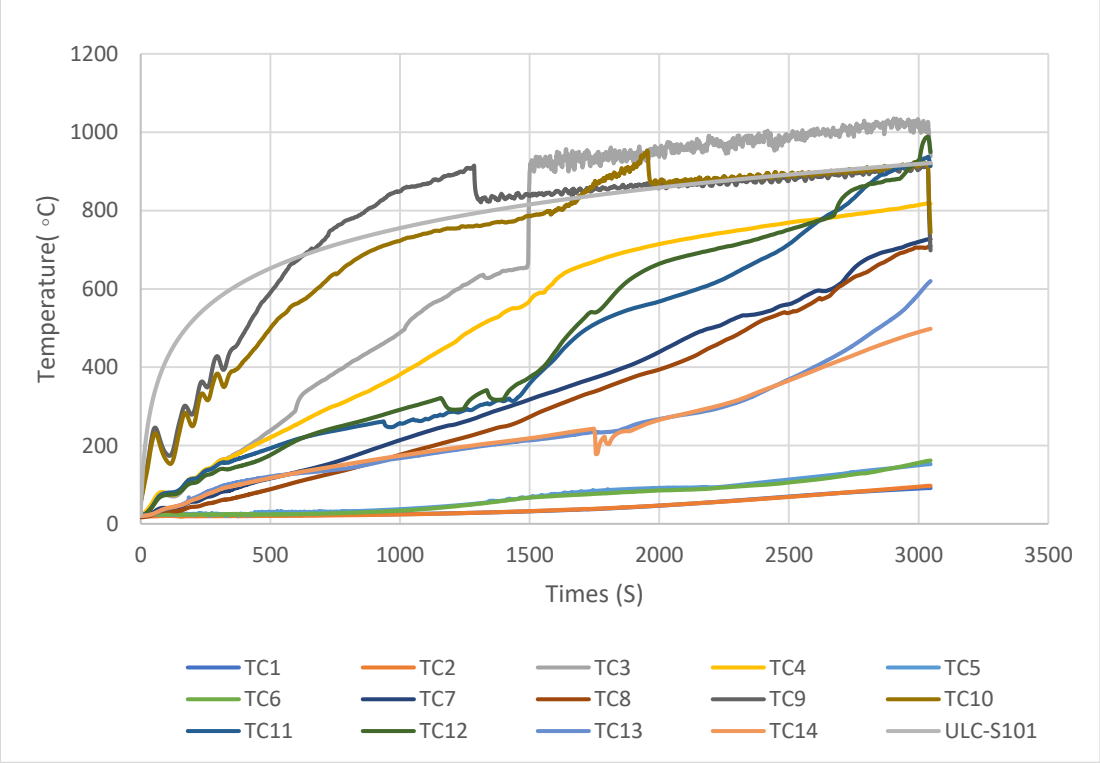

(c) Protected connection of 4 bolts arranged in pattern two (4BP2PF₁)

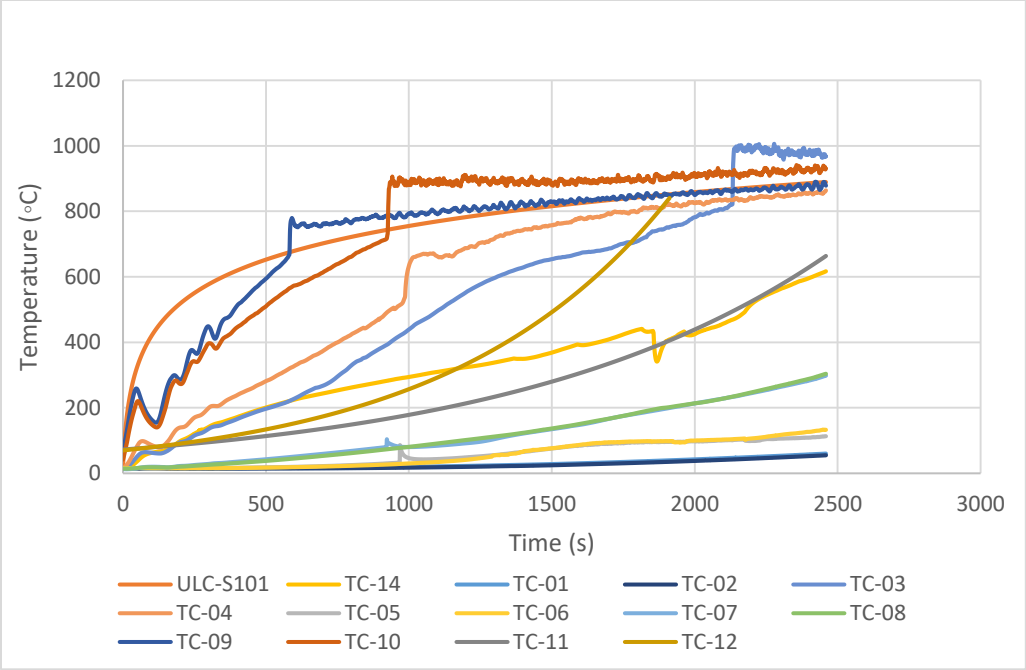

(d) First test of protected connection of 6 bolts arranged in pattern one (6BP1PF$_1$)

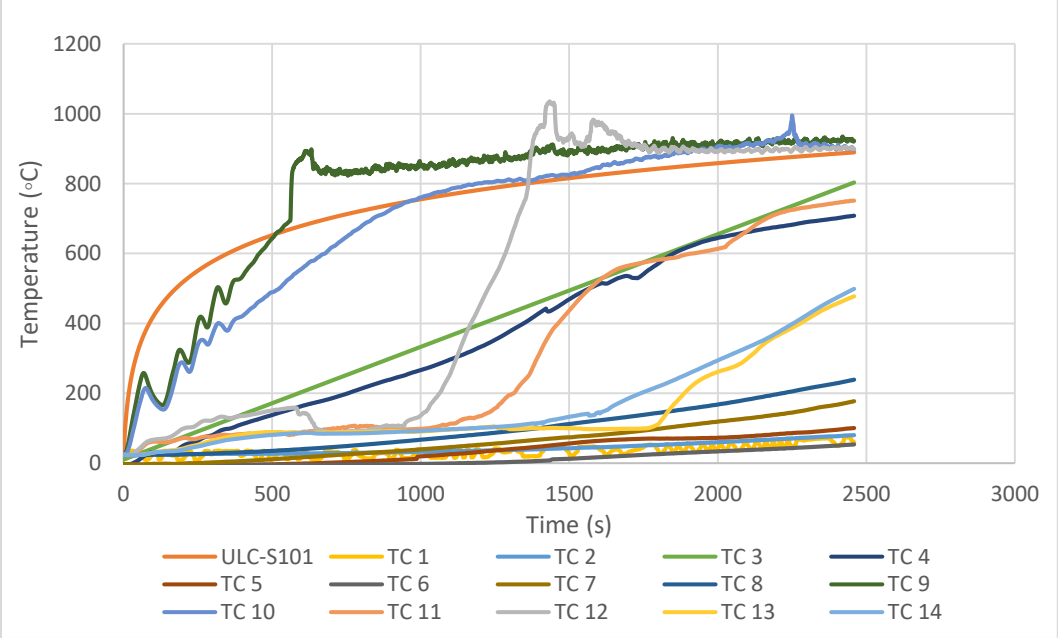

(e) Second test of protected connection of 6 bolts arranged in pattern one (6BP1PF$_2$)

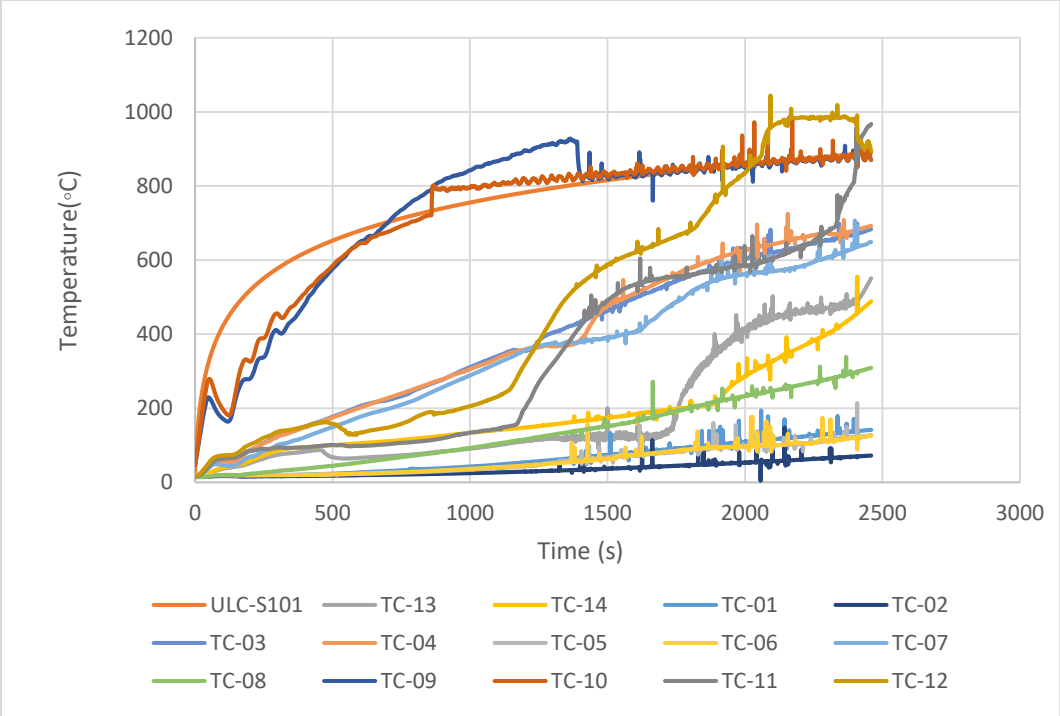

(f) Protected connection of 6 bolts arranged in pattern two ($6BP2PF_1$)

Figure 4.22. Time-temperature curves of unprotected connections

4.2.5 Summary

In summary it can be mention that the wood plugs contributed to the protected connections achieving an average failure time and linear rotation duration that is about 20 minutes more than that of the unprotected connections. Moreover, the protected connections experienced higher average charring rates as compare to that of the unprotected connections as shown in Table 4.3.

Table 4.3. Average fire performance results for protected and unprotected connection configurations

	Unprotected Connection	Protected Connection
Average failure time (mins)	28	49
Average charring rate (mm/mins)	0.79	0.91
Average linear rotation duration (mins)	18.5	38

Figure 4.23 clearly shows the influence of bolt number on the average failure time of the connections tested at elevated temperature. Figure 4.24 shows the effect of bolt and steel plate protection on the fire performance of the tested concealed glulam connections. Figure 4.25 also shows the effect of bolt pattern on the connections' failure time. The figures show that the protection of bolt and steel plate exhibited the most significant effect on the fire performance of concealed connection, as compared to the other factors (bolt pattern and bolt number) considered in this study.

- Effect of number of bolts on the connections' pattern and protection

Figure 4.23 shows that the connection configuration of four bolts performed better in all connection types except for the protected connection configuration of bolts arranged in pattern one. The average failure time of the protected connection of six bolts arranged on pattern one is higher than that of the four bolts because of the earlier splitting that occurred at the top row of bolts of the second tested connection of four bolts ($4BP1PF_2$), which was aligned with the glued line plane.

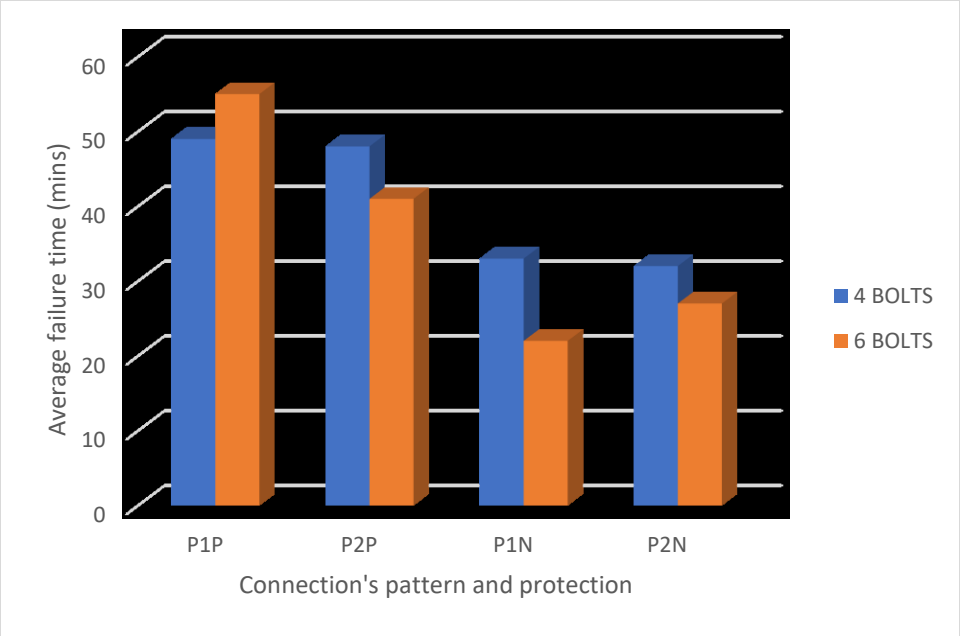

Figure 4.23. Summary of connections failure time; showing the effect of bolt number

- Effect of protection on the connections' bolt number and pattern

The protected connection exhibited significant difference in the average failure time as compared to unprotected connections. The protected connection of six bolts arranged in pattern one exhibited the maximum average failure time as compared with that of the other connections, Figure 4.24. This is because the second test performed for the connection configuration of six bolt arranged in pattern one (6BP1PF2) underwent gradual failure which led to a higher failure time. However, as shown in Figure 4.24, the unprotected connection of six bolts arranged in pattern one ($6BP1NF_1$) exhibited the minimum average failure time as a result of earlier wood split that occurred at top row of bolt that is aligned with glued line plane.

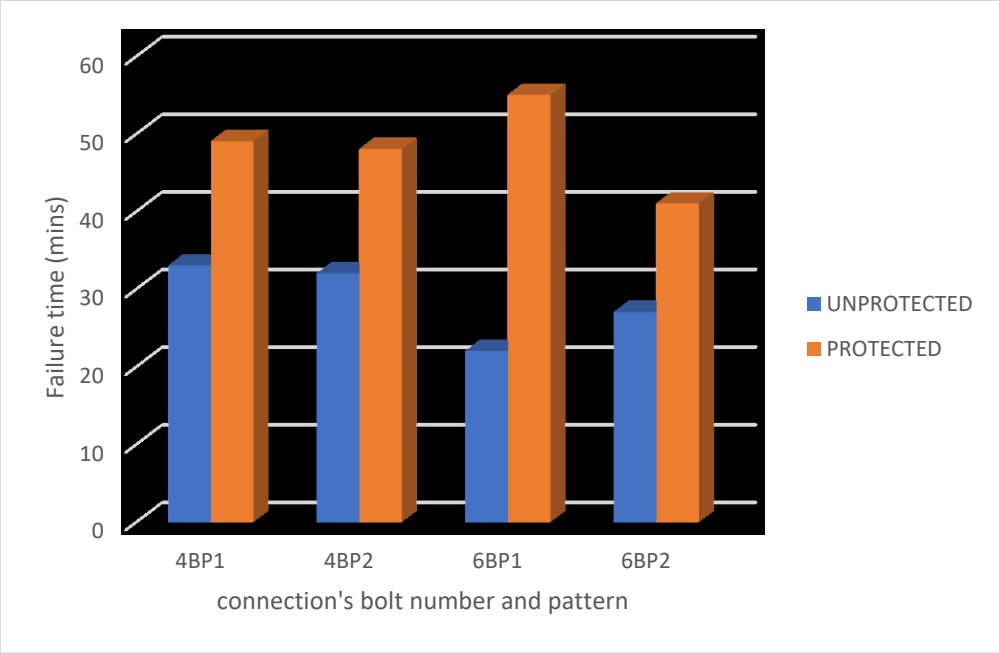

Figure 4.24. Summary of connections failure time; showing the effect of protection

- Effect of bolt pattern on the connections' bolt number and protection

As shown in Figure 4.25, bolt pattern had little effect on the protected connection configurations of four bolts, with the pattern one where the bolt rows are symmetrically place along the beam section, having a slightly higher average failure time than that of pattern two where the bottom row of bolts are located at mid-height of the beam section. When considering the connection configuration of six bolts, pattern one had a significant effect on the protected connection. However, the opposite occurred for the unprotected connection. This is due to an earlier split that occurred at the top row of bolts of the unprotected connection of six bolts arranged in pattern one ($6BP1NF_1$).

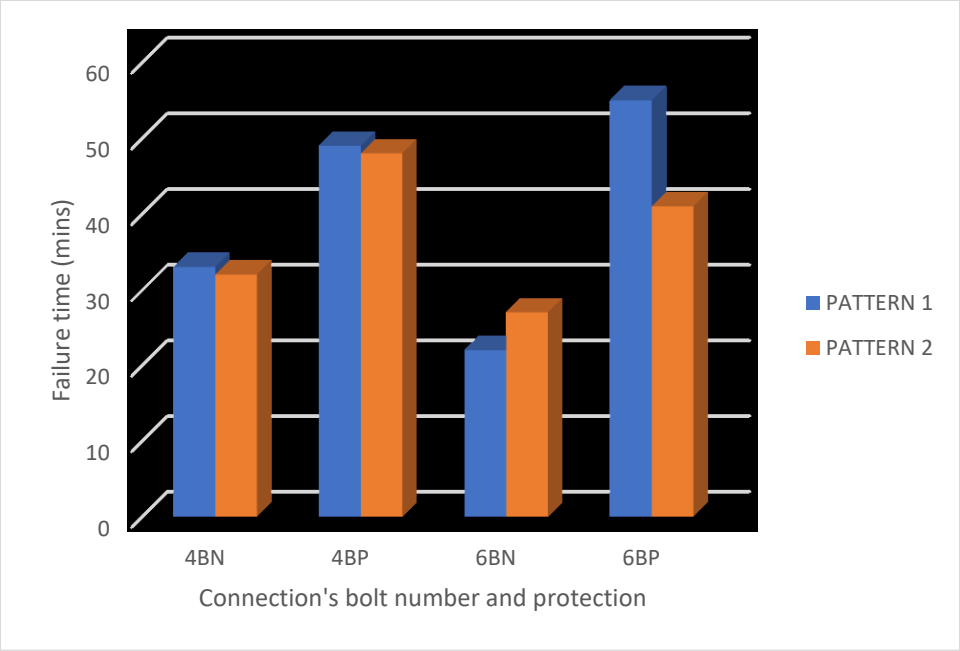

Figure 4.25. Summary of connections failure time; showing the effect of bolt pattern

5 CONCLUSIONS AND RECOMMENDATIONS

5.1 Conclusions

The experimental study presented in this thesis investigated the behavior of wood-steel-wood concealed connections, with two different bolt numbers and bolt patterns, at both, ambient and elevated temperatures. The study focused on the performance of the connections in terms of rotational behavior, moment-carrying capacity, failure modes and charring rates. The outcomes of this study helped in drawing the following conclusions;

- Ambient Temperature Tests

1) Raising the bottom row of bolts to the mid-height of the beam section increased the maximum moment capacity of the connections in ambient conditions;
2) The addition of protection slightly reduced the moment capacity of the connection in ambient condition due to the reduced beam cross section area;
3) Increasing the number of bolts from four (in two rows) to six (in two rows) increased the connections moment capacity;
4) All connection configurations exhibited initial failure of wood splitting at the top row of bolts subjected to tensile stresses, followed by splitting at the bottom row of bolts subjected to compressive stresses in the connection of the first bolt pattern; and row shear out at the bottom row of bolts in the connections of the second bolt pattern, after the steel bolts in the bottom row yielded.

- Elevated Temperatures Tests

1) The bolt pattern for the unprotected connections did not have considerable influence on the connection's failure time in fire;

2) Increasing the number of bolts from four to six, for the unprotected connections, reduced the connection's failure time in fire mainly due to the increased heat transferred to the wood section by the increased number of steel bolts.
3) The addition of wood plugs and strips to protect the steel bolts and plate edges, respectively, increased the connection's failure time in fire by about 20 minutes;
4) For both four- and six-bolt connections, the alignment of bolts with the glued line plane led to wood splitting in the connection and earlier failure time;
5) Failure time of the connections in fire did not depend on the connections' moment capacity.
6) The notional charring rate of glued-laminated timber with residual minimum dimension greater than 70 mm, employed in design of wood for fire safety is 0.7 mm/min (CSA-086-14, Table B.4.2). In this research, charring rate values exceeding 0.7 mm/min were recorded for all connections, due to the residual dimension of all test specimens being less than 70 mm. However, the protected connections experienced an average charring rate that is higher than that of the unprotected connections, this is because the protected connection lasted longer in fire and hence had a relative smaller residual section as compared to that of the unprotected connection.

5.2 Recommendations for Future Work

(1) Additional fire tests should be done applying transverse loads with less load ratios than 100% of the ultimate design capacity of the connections as per Eurocode recommendations;
(2) To better understand the effect of bolt number and bolt pattern on the fire performance of wood-steel-wood connections, research can be done to investigate methods to avoid early

splitting, like the use of self-tapping screws and the design of connections in a way that the bolt rows are not aligned with the glued line plane of glulam sections;

(3) To be able to use smaller glulam beam sections yet achieving reasonable failure times in fire as presented in this thesis, further research can be done using gypsum board protection with thickness that will provide similar protection duration as wood plug protection described in this research.

REFERENCES

[1] Buchanan, Structural Design for Fire Safety., John Wiley & Sons Ltd, Chichester, England, 2001.

[2] NBCC, National Building Code of Canada, Ottawa, ON, Canada: National Research Council of Canada, 2015.

[3] Sabah Ali, G. Hadjisophocleaus, Fire Performance of Hybrid Timber Connections. Faculty of Graduate Studies and Research, Ottawa, Ontario, Canada: Ottawa-Carleton Institute of Civil and Environmental Engineering Carleton University, 2016.

[4] Adam petrycki, Salem, structural fire performance of bolted glulam beam-to-column concealed connections. Department of Civil and Environmental Engineering Thunder Bay, Ontario, Canada, 2017.

[5] Racher P., Laplanche K., Dhima D., Bouchaïr A., Thermo-Mechanical Analysis of the Fire Performance of Dowelled Timber Connection. Engineering Structures, 32 (4), p. 1148-1157, 2010.

[6] L. Peng, Performance of Heavy Timber Connections in Fire, Ph D thesis submitted to the Faculty of Graduate Studies and Research, Ottawa, Ontario, Canada: Ottawa-Carleton Institute of Civil and Environmental Engineering Carleton University, 2010.

[7] Audebert, M., Dhima, D., Taazount, M., and Bouchaïr, A. Experimental and Numerical Analysis of Timber Connections in Tension Perpendicular to Grain in Fire. Fire Safety Journal volume 63 pages 125-137, 2014.

[8] Xu,B.H., Bouchaïr A., Racher P., Mechanical Behavior and Modelling of Dowelled Steel-to-Timber Moment-Resisting Connections. Journal of Structural Engineering, 141(6), 2015.

[9] Zarnani P., Quenneville P., Design Method for Coupled-Splice Timber Moment Connections. Proceedings of the 13th World Conference on Timber Engineering (WCTE2014), Quebec, Canada, 2014.

[10] ISO 834-1, Fire resistance tests - Elements of building construction, Part 1: General requirements., Switzerland.: International Organization for Standardization, 1999.

[11] BS 476 fire tests on building materials and structures, British Standards Institution, 1997.

[12] ASTM E119, Standard methods of fire tests of building constructions and materials. West Conshohochen, PA, USA: American Society for Testing and Materials, 2007.

[13] CAN/ULC-S101-14 Standard Methods of Fire Endurance Tests of Building Construction and Materials Fifth Edition, Canada, 2014.

[14] Slavid. R, Wood Architecture, London Laurence King Publishing Ltd pp 239, 2005.

[15] Canadian Wood Council, Introduction to Wood Design, Ontario, Canada, 2010.

[16] A. Jorissen, Double shear timber Double shear timber connections with dowel type fasteners. Ph.D Thesis, Delft University, Delft, Netherlands, 1998

[17] P. Rodd, The analysis of timber joints made with circular dowel connectors. Ph.D Thesis, University of Sussex, England, 1973.

[18] J. S. E. a. E. B. Sjodin, An experimental and numerical study of the effect of friction in single dowel joints, Holz Roh Werkst, 66: 363-372, 2008.

[19] P. Q. Ryan Habkirk, Bolted Wood Connections Loaded Perpendicular-to-Grain, Kingston, ON, Canada: Civil Engineering Department Royal Military College of Canada.

[20] Atreya, Arvind, 'Pyrolysis, Ignition and Flame Spread on Horizontal Surfaces of Wood.' Ph. D. diss, Harvard University, Cambridge, MA,1983.

[21] Fredlund, Bertil,'A model for Heat and Mass Transfer in Timber Structures during Fires' Institute of Science and Technology, Department of fire safety Engineering, Lund University, Lund, Sweden, 1988.

[22] Hadvig, Sven, 'Charring of wood in building Fires' Laboratory of heating and air-conditioning Technical university of Denmark, 1981.

[23] Parker, William J., 'prediction of the heat release rate of wood.' Ph.D. diss., George Washington university, Washington DC, 1988.

[24] White, Robert Hawthorne, 'Charring Rates of different wood species.' Ph.D. diss., University of Wisconsin, Madison, WI,1988.

[25] Truax, T. R .1959. Fire research and results at U.S. Forest Products Laboratory. U.S. Forest Serv., Forest Products Lab. Rep. No. 1999, Madison, Wis, 1959.

[26] Browne, F. L. Theories of the Combustion of Wood and Its Control, Forest Products Laboratory Report, Forest Service, U.S. Department of Agriculture, No.2136, 1958.

[27] Reszka P. In-Depth Temperature Profiles in Pyrolyzing Wood, Phd Thesis, University of Edinburgh, 2008.

[28] Erchinger C, Frangi A, Fontana M Fire design of steel-to-timber dowelled connections. Engineering Structures 32: 580-589. doi: 10.1016/j.engstruct.2009.11.004, 2010.

[29] MA Dietenberger and LE Hasburgh, Wood Products: Thermal Degradation and Fire, 2016.

[30] König, J. and Walleij, L. One-dimensional charring of timber exposed to standard and parametric fires in initially unprotected and post-protection fire situations,1999.

[31] R. White, Charring rate of composite timber products., The Proceedings of Wood and Fire Safety, Part1, 4th International Scientific Conference, Zvolen, Slovak Republic: 353-363, 2000.

[32] Lie, T.T. A method of assessing the fire resistance of laminated timber beams and columns. Canadian J. of Civil Eng., 4: 161-169, 1977.

[33] EN 1995-1-1 Eurocode 5 - Design of timber structures, Part 1-1: General rules and rules for buildings. CEN, Brussels, Belgium, 2004.

[34] R. Knudson, Performance of structural wood members exposed to fire. Ph.D Dissertation, University of California, Berkeley, USA, 1973.

[35] B. Fredlund, Modelling of Heat and Mass Transfer in Timber Structures During Fire., Fire Safety Journal, 20(39-69), 1993.

[36] J. R. C. P. a. C. G. Mehaffey, A model for predicting heat transfer through gypsum board/wood stud walls exposed to fire., Fire and materials, 18: 297-305, 1994.

[37] M. Janssens, A method for calculating the fire resistance of exposed timber decks., Proceedings of the Fifth International Symposium on Fire Safety Science ISFSS: Australia: 1189-1200, 1997.

[38] J. a. W. L. Konig, Timber frame assemblies exposed to standard and parametric fires, Part 2: a design model for standard fire exposure., Stockholm.: Rapport I 0001001, Swedish Institute for Wood Technology Research, 2000.

[39] Lie, T.T. Structural Fire Protection. American Society of Civil Engineers, New York, 1992.

[40] B. Gammon, Reliability analysis of wood-frame assemblies exposed to fire. Ph.D Dissertation, Berkeley, USA: University of California, 1987.

[41] H. a. M. J. Takeda, WALL2D: a model for predicting heat transfer through wood-stud walls exposed to fire., Fire and Materials, 22: 133-140, 1998.

[42] Preusser, R. Plastic and elastic behavior of wood affected by heat in open systems. Holztechnologie, 9(4): 229-231,1968.

[43] Schaffer, E.L. Elevated Temperature Effect on the Longitudinal Mechanical Properties of Wood. Ph.D. Thesis, Department of Mechanical Engineering, Univ. Wisconsin, Madison, WI, USA, 1970.

[44] Ostman, B.A. Wood tensile strength at temperatures and moisture contents simulating fire conditions. Wood Science and Technology, 19: 103-116,1985.

[45] Janssens, M.L. A method for calculating the fire resistance of exposed timber decks. Proceedings of the Fifth International Symposium on Fire Safety Science ISFSS, Australia: 1189-1200 ,1997.

[46] Thomas, G.C. Fire resistance of light timber framed walls and floors. Ph.D. Thesis, School of Engineering, University of Canterbury, New Zealand,1995.

[47] G. H. J. M. a. M. M. Lei Peng, Calculating Fire Resistance of Timber Connections, Fire and Materials – 12th International Conference San Francisco, USA. (Best Poster Award), 2011.

[48] EN 1993-1-2. Eurocode 3, Design of steel structures, Part1-2, CEN, Brussels, Belgium.: General rules - Structural fire design, 2005.

[49] Maik Gehloff, Maximilian Closen, Frank Lam, Reduced edge distances in bolted timber moment connections with perpendicular to grain reinforcements. World Conference on Timber Engineering, 2010.

[50] S. B. A. Boadi, G. Hadjisophocleaus, Full Scale Tests on the Performance of Hybrid Timber Connections in Real Fires. Faculty of Graduate Studies and Research, Ottawa, Ontario, Canada: Ottawa-Carleton Institute of Civil and Environmental Engineering Carleton University, 2015.

[51] Padro, P., Fire Behavior of Timber Connections. Dept. of Civil, Environmental and Geomatic Engineering (D-BAUG), Zurich, ETH Zurich, 2016.